# HYDRAULIC DESIGN OF TYROLEAN WEIRS IN HYDROPOWER PLANT PROJECTS

A THESIS SUBMITTED TO
THE GRADUATE SCHOOL OF NATURAL AND APPLIED SCIENCES
OF
MIDDLE EAST TECHNICAL UNIVERSITY

BY

CİHAN MARAŞ

IN PARTIAL FULLFILLMENT OF THE REQUIREMENTS
FOR
THE DEGREE OF MASTER OF SCIENCE
IN
CIVIL ENGINEERING

JANUARY 2014

Approval of the thesis:

**HYDRAULIC DESIGN OF TYROLEAN WEIRS IN HYDROPOWER PLANT PROJECTS**

submitted by **CİHAN MARAŞ** in partial fulfillment of the requirements for the degree of **Master of Science in Civil Engineering Department, Middle East Technical University** by,

Prof. Dr. Canan ÖZGEN
**Dean, Graduate School of Natural and Applied Sciences** _____

Prof. Dr. Ahmet Cevdet YALÇINER
**Head of Department, Civil Engineering** _____

Prof. Dr. Mustafa GÖĞÜŞ
**Supervisor, Civil Engineering Dept., METU** _____

**Examining Committee Members:**

Prof. Dr. Nevzat YILDIRIM
**Civil Engineering Dept., GAZİ University** _____

Prof. Dr. Mustafa GÖĞÜŞ
**Civil Engineering Dept., METU** _____

Assoc. Prof. Dr. A. Burcu ALTAN SAKARYA
**Civil Engineering Dept., METU** _____

Assoc. Prof. Dr. Mehmet Ali KÖKPINAR
**TAKK Dept., DSİ** _____

Assoc. Prof. Dr. Mete KÖKEN
**Civil Engineering Dept., METU** _____

**Date:** _____

**I hereby declare that all information in this document has been obtained and presented in accordance with academic rules and ethical conduct. I also declare that, as required by these rules and conduct, I have fully cited and referenced all material and results that are not original to this work.**

Name, Last name: Cihan MARAŞ

Signature:

## ABSTRACT

### HYDRAULIC DESIGN OF TYROLEAN WEIRS IN HYDROPOWER PLANT PROJECTS

MARAŞ, Cihan
M.Sc., Department of Civil Engineering
Supervisor: Prof. Dr. Mustafa GÖĞÜŞ

January 2014, 87 pages

Intake structures are defined as structures that divert water into a channel or tunnel leading to a powerhouse. A water intake structure must be able to divert the design discharge into the conveyance system with minimum head loss and negative impact on the local environment. Design and location of intakes are dependent on geological, hydraulic, structural and economic conditions.

Tyrolean type water-intake structures are commonly constructed on steeply sloped mountain rivers with reliable rock foundation to divert water. The amount of water to be diverted from the main channel is the major concern in these kind of structures. Incoming flow must satisfy the design discharge for an appropriate design. There are various parameters affecting the amount of diverted water and the present work does not fully clarify hydraulics of this structure. In this study, design methods of Tyrolean type water intake structures are researched. The researches are made in two perspectives named as constant energy level and constant energy head hypothesis. In the first stage of this study, the theoretical methods related to the design of Tyrolean weirs are presented. In the second stage experimental solutions obtained as a result of hydraulic studies are discussed. In the third stage outcome of the theoretical methods

are compared with the experimental methods. It was shown that the Tyrolean weir designed with the method based on experimental results provides more diverted discharge from the main channel with a trash rack of shorter length than those of the other methods. Finally, the situations of some of the currently operating facilities are examined.

**Keywords:** Keywords: Tyrolean weirs, hydraulics, open channel flow, water capture efficiency, discharge coefficient, intake racks.

# ÖZ

## HİDROELEKTRİK SANTRAL PROJELERİNDE KULLANILAN TİROL TİPİ SAVAKLARIN HİDROLİK PROJELENDİRİLMESİ

MARAŞ, Cihan
Yüksek Lisans, İnşaat Mühendisliği Bölümü
Tez Yöneticisi: Prof. Dr. Mustafa GÖĞÜŞ

Ocak 2014, 87 sayfa

Su alma yapıları, suyu santrale giden bir kanal veya tünele yönlendiren yapılar olarak tanımlanır. Bir su alma yapısı, suyu iletim sistemine en düşük enerji kaybıyla ve çevreye herhangi bir olumsuz etki yaratmadan iletmelidir. Su alma yapılarının tasarımı ve yeri; jeolojik, hidrolojik, yapısal ve ekonomik koşullara bağlıdır.

Tirol tipi regülatörler genel olarak yüksek eğimli nehirlerde güvenilir zeminler üzerinde suyu yönlendirmek için inşa edilirler. Ana kanaldan yönlendirelecek olan suyun miktarı bu tür yapılarda büyük önem taşır. Uygun bir tasarımda yönlendirilen debi tasarım debisini karşılayabilir olmalıdır. Yönlendirilen suyun miktarını etkileyen çeşitli parametreler vardır ve günümüz çalışmaları bu yapıların hidroliğini tam olarak aydınlatmamaktadır. Bu çalışmada, Tirol tipi su alma yapılarının tasarım metodları araştırılmıştır. Araştırmalar sabit enerji yüksekliği ve sabit enerji seviyesi olarak adlandırılan iki bakış açısıyla yapılmıştır. Çalışmanın ilk aşamasında, tirol tipi savakların tasarımıyla alakalı teorik çalışmalar sunulmuştur. İkinci aşamada ise hidrolik çalışmalar sonucu elde edilen deneysel yöntemler verilmiştir. Üçüncü aşamada, teorik yöntemlerden elde edilen sonuçlar, deneysel yöntemlerden elde edilen sonuçlar ile karşılaştırılmıştır. Deneysel yöntemlere göre tasarlanmış tirol tipi

savağın diğer yöntemlere göre daha kısa ızgara ile ana kanaldan daha çok debi aldığı gösterilmiştir. Son olarak, şu an güncel olarak işletmede olan tesisler incelenmiştir.

**Anahtar Kelimeler:** Tirol tipi savaklar, hidrolik, açık kanal akımı, su alma verimliliği, debi katsayısı, su alma ızgaraları.

**To my precious family and my lovely wife**

## ACKNOWLEDGEMENTS

First of all, I would like to express my sincere gratitude to Prof. Dr. Mustafa Göğüş, for his support, patience, encouragement and confidence on me from the very first day.

I would also like to express my sincere appreciation for my lovely wife Güliz MARAŞ for her valuable love, friendship, support and help.

For their understanding, endless patience and encouragement throughout my study, my sincere thanks go to my parents, Ali MARAŞ and Kadriye MARAŞ, and my brothers, Çağrı and Hakan MARAŞ.

I am also grateful to Besim GÜLCÜ for providing unique data for my study and my coworkers Atınç YENİ, Cevahir ALTIN, Melek GÜNER and Mustafa "Uruş" ÖNEN for their encouragement and support during my thesis study.

I want to thank to Mehmet Tarık SAĞCAN, İrem SAĞCAN, Koray TAŞTANKAYA, Burak AYCAN, Başak BİNGÖL, Erdem SARIGİL, Ersen TORAMAN, Nihan UZUNOĞLU, Gökhan TEZCAN, Selçuk ÖKSÜZ, Taylan ÇAKIROĞLU and Ufuk YİĞİT for being great friends to me.

## TABLE OF CONTENTS

# LIST OF TABLES

TABLES

# LIST OF FIGURES

FIGURES

SYMBOLS

| | | |
|---|---|---|
| $a$ | : | Center distance between two adjacent bars of the Tyrolean screen |
| $C_d$ | : | Discharge coefficient for an inclined Tyrolean screen |
| $C_c$ | | A coefficient introduced in Equation 2.21 |
| $D$ | | Diameter of the rack bars |
| $e$ | : | Clearance distance between bars of the Tyrolean screen |
| $(F_r)_e$ | : | Froude number based on bar spacing |
| $g$ | : | Gravitational acceleration |
| $h_0$ | : | Flow depth at just upstream of the screen |
| $h_c$ | : | Critical flow depth |
| $H_0$ | : | The energy head of the flow at upstream of the screen |
| $H_c$ | : | Critical energy head |
| $\ell$ | | The required rack length to divert all incoming discharge |
| $L$ | : | Length of the Tyrolean screen |
| $L_1$ | : | The distance of the point where the flow nappe crosses the axis of the Tyrolean screen |
| $L_2$ | : | Total wetted rack length |
| $q_{max}$ | | Maximum discharge for the energy head |
| $(q_w)_i$ | : | Diverted unit discharge by the Tyrolean screen |
| $(q_w)_T$ | : | Total unit discharge in the main channel |
| $(q_w)_{out}$ | : | The discharge that passes over the trash rack |
| $s$ | | Distance of any point away from the origin of ellipse |
| $t$ | | Thickness of the bar |
| ***WCE*** | : | **W**ater **C**apture **E**fficiency |
| $\chi$ | | Reduction factor used in calculation of the flow depth |
| $\alpha$ | : | Angle between the velocity vector $V_B$ and the axis of the rack |
| $\beta$ | | A function in Table 1 |
| $\theta$ | : | Angle of inclination of the screen |
| $\lambda$ | | Discharge coefficient parameter used in Equation 1.1 |
| $\mu_s$ | : | Contraction coefficient |
| $\mu_m$ | | A parameter introduced in Equation 1.2 |
| $\varphi$ | | A parameter which depends on maximum discharge |
| $\phi$ | | A function in Table 1 |
| $\psi$ | : | The net rack opening area per unit width of the rack |
| $\omega$ | : | Rack porosity |

# CHAPTER 1

## INTRODUCTION

### 1.1 General

Hydropower is the most common renewable energy source in the world. According to, Turkish Electricity Transmission Company (TEİAŞ), %24.5 of energy generation are procured by hydropower plants and only %38 of hydraulic potential of Turkey is used for that amount. It is known that, shortage in energy will become a serious problem in the next 15 years due to the growing industry level and growth in population. Construction of hydroelectric power plants by considering full hydraulic potential of Turkey is one of the best solution to overcome energy problem. Except a few problematic projects, all possible large dams are in construction or operation in Turkey. Remaining part of the hydraulic potential are thought to be generated by small hydropower plants mainly run-off river power plants.

The most important problem of run-off river system is sediment that is carried along water. Since sediment cause damages on turbines, even intrusion of the smallest particle is not tolerated. Especially in steep rivers this situation needs high attention.

A water intake structure must be able to divert the design discharge into the conveyance system with minimum head loss and negative impact on the local environment.

Tyrolean weirs are known to be very convenient water intake structures to divert desirable amount of water to the system with minimum amount of sediment carried by the flow. Figure 1 shows a typical Tyrolean weir and its screen.

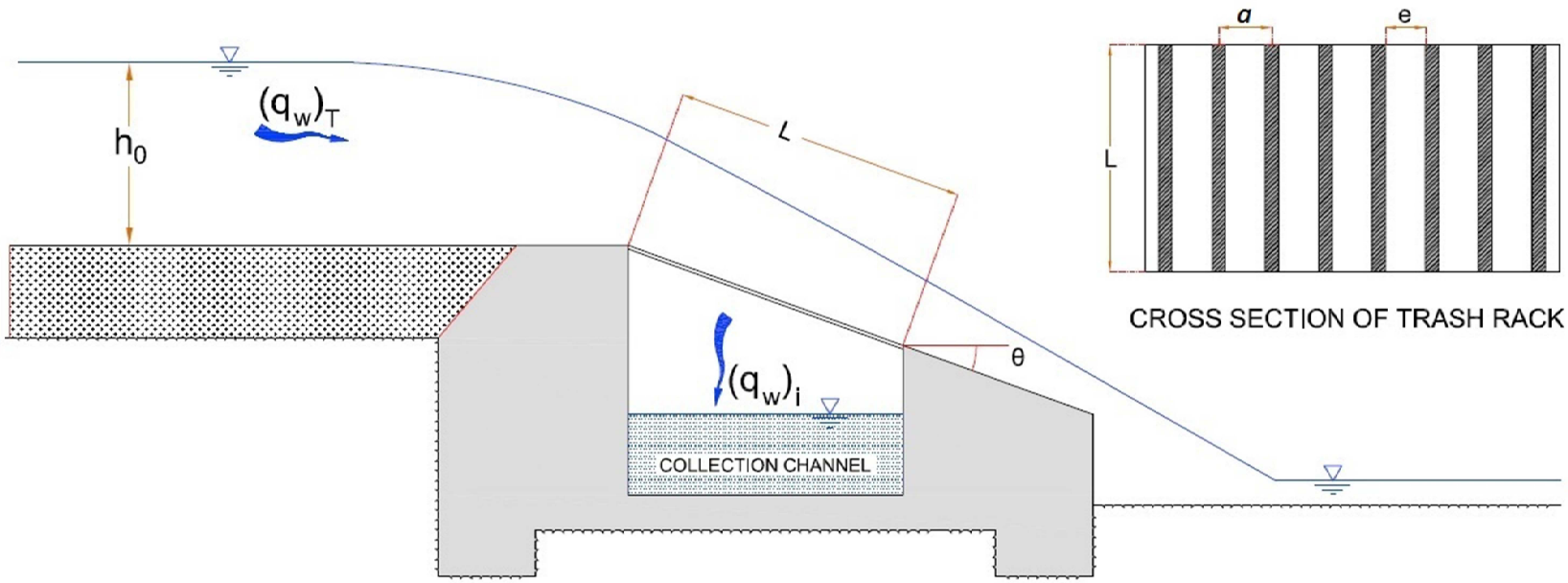


Figure 1 A Tyrolean weir and its screen (Yılmaz, 2010)

Tyrolean weir is a water intake structure which diverts water and some of the sediment carried by the river to a collection channel through a screen. The depth of the collection channel must be designed in such a way that the recirculation of the discharge back on the rack should be prevented. Water and sediment are leaded to a sedimentation tank or settling basin through the collection channel by gravity, where water is separated from undesired sediment and transferred to the system.

The trash rack functions as a filter to remove the material and stones from entering to the intake. The trash rack or bars of the screen are placed over the collection channel in the direction of flow. Also, to obtain a minimum risk of clogging and to prevent intrusion of coarse material to the collection channel, the bars must be placed with a certain bottom slope. Sediment, which have smaller sizes than the rack openings, enter the collection channel and are separated from the system by suitable ejection systems.

The screen should be sized so that the riverbed sediment should not enter the channel, and at the same time, to be large enough to let enough water to be diverted. The basic design variables for trash racks are the openings between the adjacent bars , "*e*", and their center spacings "*a*" (Fig. 1). Characteristics of the sediment, allowed to pass through the bars, define these values. Types of rack bars with different profiles are shown in Figure 2. The rectangular racks are rapidly jammed by particles, because of this reason they are not suggested to be used for intakes (Fig 2a). The bulb-ended bars are more rigid and have better performance (Fig 2b). Eventually, the best shape is the round-head bars that prevent sediments from clogging and due to their higher moment of inertia, they are more resistant against impact of particles when compared to other profiles (Fig. 2c).

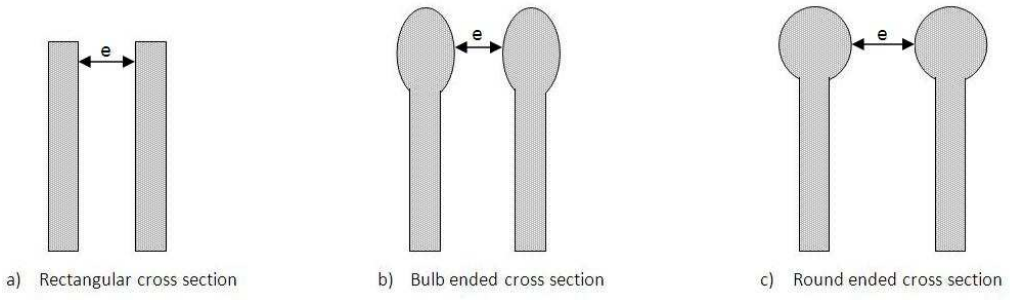


Figure 2 : Types of rack bars with different profiles (Andaroodi M. 2005)

For a detailed design, there are several hydraulic parameters that needed to be analyzed. Design of a Tyrolean weir mainly depends on discharge of the river, the design discharge, the characteristics of suspended and bed load and physical characteristic of the project area.

The purpose of this thesis is to present a Tyrolean weir design manual for engineers. For this reason a series of theoretical and experimental methods are presented and current situation of Tyrolean weirs are discussed by giving some examples from some of the projects which are in operation.

In the next section, the literature review is given. The theoretical methods are presented in Chapter II. The experimental methods are explained in Chapter III. Comparison of theoretical methods and experimental method is given in Chapter IV. Discussion of current situation of Tyrolean weirs and some related projects are examined in Chapter IV. Conclusions and the further recommendations are presented in Chapter V.

## 1.2 Literature Review

By assuming constant energy head and conventional orifice equation, Kuntzmann and Bouvard defined a computational approach for the free-surface profile over the bottom racks (as cited in Brunella et al., 2003).

Frank derived an equation to calculate the trash rack length for the selected unit discharge of $(q_w)_T$ , by assuming no head loss over the racks (as cited in Drobir et al., 1999).

$$L = 2.561\frac{(q_w)_T}{\lambda\sqrt{h}_0} \quad \text{.....(1.1)}$$

where $\lambda = \psi\mu_s\sqrt{2g\cos\theta}$ ; discharge coefficient, $\psi = e/a$ ; $e$ is the clearance distance and $a$ is the center distance between two adjacent bars of the Tyrolean screen.

$\mu_s = 0.8052\psi^{-0.16}(a/h_0)^{0.13}$; contraction coefficient, which depends on the characteristics of the trash rack and the flow depth over the trash rack; $g$ is the gravitational acceleration, $h_0$ is the flow depth at just upstream section of the trash rack and given as $h_0 = \chi h_c$ ; $\chi$ is the reduction factor which is calculated from $(2\cos\theta)\chi^3 - \chi^2 + 1 = 0$ , and $\theta$ is the angle of the inclination of the trash rack.

$h_c = \sqrt[3]{(q_w)_T^2/g}$ ; critical flow depth and $(q_w)_T$ is the total incoming discharge.

By assuming that the energy line over the trash rack is parallel to the screen, Noseda (1956) derived an equation valid only for horizontal racks, to calculate the wetted rack length.

$$L = 1.185\frac{H_c}{\mu_m\psi} \quad \text{.....(1.2)}$$

where $H_c$ is the specific energy head of the flow over the trash rack and $\mu_m = 1.22.\mu_s$ is recommended.

Bianco and Ripellino verified Noseda's (1956) observations with a larger model and found no essential scale effects (as cited in Brunella et al., 2003). Their bar profiles were semicircular at the top with a rectangular bottom reinforcement.

Özcan (1999) presented the theoretical solutions based on constant energy level and constant energy head hypothesis.

A Tyrolean weir model with a scale of 1:10 was built by Drobir (1999) in the hydraulic laboratory of University of Technology, Vienna. A series of experiments were conducted to measure the wetted rack length for four different rack inclinations varying from 0% to 30%, with five different discharges [$(q_w)_T$= 0.25, 0.50, 1.00, 1.50, 2.00 $m^2/s$]. Also to determine the effect of bar spacing two different clearance distances (10.0 and 15.0 cm) were examined. According to the results of the experiments two different wetted rack lengths were observed; $L_1$, the distance where the axis of the trash rack crossed with the flow and, $L_2$, the total wetted length over the trash rack (Figure 3).

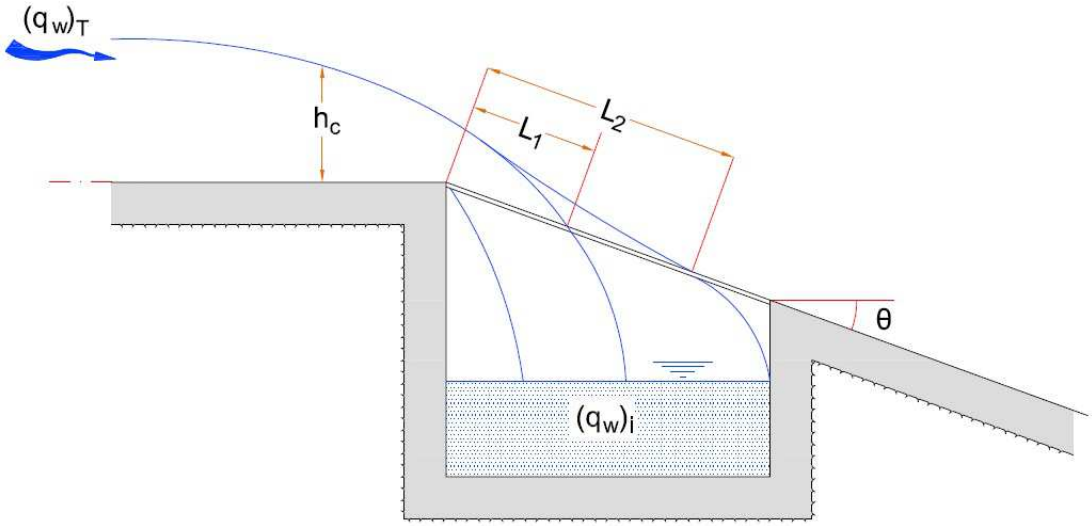


Figure 3 : Sketch of rack lengths $L_1$ and $L_2$ of a Tyrolean screen

In order to determine the effect of porosity, slope and geometry of the trash rack on hydraulics of incoming flow that passes through the openings between the rack bars, Brunella et al. (2003) conducted a series of experiments. A rectangular channel with 0.5 m width and 7.0 m length was used. Experiments were repeated for each rack geometry having various properties. The bars of the bottom intake had 12 mm and 6 mm diameters with lengths of 0.60 m and 0.45 m, and bars were placed with 6 mm and 3 mm clearance spacings with respect to each other. Eight different angles of inclinations were used to observe the effect of the bottom slope [ $\theta$ = 0, 7, 19, 28, 35, 39, 44 and 51°]. According to the results of the experiments water surface profiles and velocity distributions were gauged and it was seen that surface profiles of the systems with large and small bottom slopes were almost identical. By using the results of the experiments and other data obtained from literature Brunella et al. (2003) derived an equation (Eq. 1.3) for the relative rack length, ($L_2/H_c$), as a function of the main channel discharge. The wetted rack length $L_2$ implies that all the incoming discharge is diverted by the rack. [$(q_w)_i = (q_w)_T$].

$$C_d \omega \left( \frac{L_2}{H_c} \right) = 0.83 \quad \text{.....(1.3)}$$

where $C_d$ is the discharge coefficient, $H_c$ is the critic energy head, and $\omega$ is the rack porosity which corresponds to the ratio of the total net spacing between the rack bars to the main channel width.

It was found that as a function of rack porosity ($\omega$), the discharge coefficient ($C_d$) was varying between 0.87 and 1.10

The following expression about *Cd* is given by Subramanya (as cited in Şahiner, 2012) for subcritical approach flow and supercritical flow over the racks of rounded bars.

$$C_d = 0.53 + 0.4 \log\left( \frac{D}{e} \right) - 0.61 \tan\theta \quad \text{.....(1.4)}$$

where; $D$ is the diameter of the rack bars, $e$ is the spacing of the rack bars, $\theta$ is the inclination angle of the rack bars.

The discharge characteristics of flat bars were studied by Ghosh and Ahmad with a series of experiment. As a result of the study, it was seen that the specific energy over the racks was nearly constant. In another stage of their study $C_d$ values for flat bars were also compared with $C_d$ values calculated by Subramanya's relationship, i.e, Eq.(1.4). It was observed that $C_d$ values obtained by Subramanya's relationship overrated. Equation of $C_d$ for flat bars was derived by Ghosh and Ahmad as follows (Ahmad and Mittal, 2006);

$$C_d = 0.1296\left(\frac{t}{e}\right) + 0.4284(\tan\theta)^2 + 0.1764 \quad \text{.....(1.5)}$$

where $t$ is the thickness of the bars.

It is concluded that in case of limited data range in order to design flat bars Eq. 1.5 should be used. To derive a better equation in terms of certainty, more experimental and field data are required (Ahmad and Mittal, 2006).

In order to find the effects of screen slope and area opening of the screen on the diverted discharge, a series of experiments conducted by Kamanbedast and Bejestan (2008). A conduit with 60 cm width, 8 m length and 60 cm height was used. Six models of bottom racks with three different area openings equal to 30, 35 and 40 % using two different bars of 6 and 8 mm diameter were tested. Four different slopes; 10, 20, 30 and 40% and five different flow discharges were applied on each model. It was observed the area spacing of the bars and the rack slope is the only variable that affect the ratio of the diverted discharge to the total incoming discharge. As a result of the experiments it was indicated the discharge ratio increases as the slope of the rack increases. When the rack area opening is 40% and the slope is 30 % the discharge ratio reaches to a maximum value of 0.8. On the other hand, when the effect of sedimentation is considered those values become smaller. When sediment

was used in experiments, it was seen that the discharge ratio dropped 10 % because of the clogging of spacings between trash rack bars.

Yılmaz (2010) conducted a series of experiments in order to investigate the hydraulic characteristics of Tyrolean weirs. Metal bars which had circular cross section and 1 cm diameter were used for bottom intake racks. The experiments were repeated for three clearance distances between bars; 3 mm, 6 mm and 10 mm, and three angles of rack inclination; 14.5°, 9.6° and 4.8°.

Şahiner (2012) performed a series of experiments in the same setup used by Yılmaz (2010) with the same racks having three different screen slopes ($\theta_1$ = 37.0°, $\theta_2$ = 32.8° and $\theta_3$ = 27.8°). Şahiner (2012) also conducted similar experiments with perforated metal panels having circular openings with three different diameters ($d_1$ = 3 mm, $d_2$ = 6 mm and $d_3$ = 10 mm).

As a result of both experiments conducted by Yılmaz and Şahiner the graphs of variations of; the discharge coefficient $C_d$, the ratio of the diverted discharge to the total water discharge, $[(q_w)_i/(q_w)_T]$, and the dimensionless wetted rack length , $L_2/e$, with the relevant dimensionless parameters were drawn. By using the charts the diverted discharge can be calculated provided that the design parameters are determined.

# CHAPTER 2

## THEORETICAL METHODS

### 2.1 Introduction

The theoretical studies related to the performance of the trash rack of a Tyrolean weir were presented in this chapter. These methods are used to determine the bars' length and spacing according to the desired discharge. To calculate the trash rack length, the unit discharge that passes over the weir is needed to be known.

For the sake of construction the upstream side of the trash rack can be considered horizontal or inclined as seen in Figure 4. In Figure 4.a the critical depth and minimum energy is observed somewhere close to point A. However, in Figure 4.b, the critical depth is reached much earlier from point A and in this spot the flow has smaller depth. These two conditions must be separated from each other in hydraulic calculations.

Calculation of the discharge that passes through the trash rack depends on the water surface profile over the weir. The discharge that passes from point A starts to drop into the collection channel and the discharge over the weir reduces along the trash rack. Flow over the trash rack is affected by friction of the bars and surface tension.

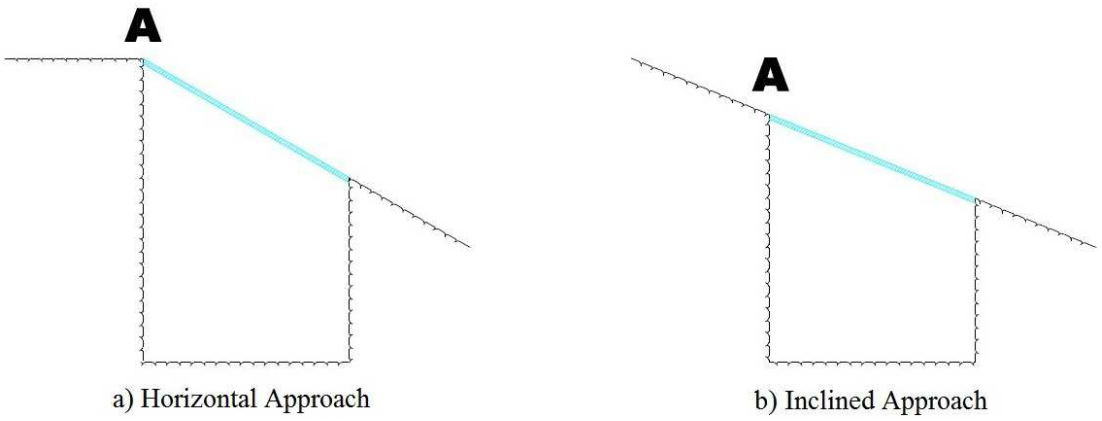


Figure 4 : Tyrolean weirs with horizontal and inclined approaches

Eventually, when all these factors are considered, hydraulic calculation of the discharge through the trash rack becomes notably harder. Therefore, researchers, who work in this subject, made some assumptions. For example, friction effects are ignored due to small friction length over the trash rack. Surface tension of water between bars is also ignored. And fluctuations in the flow depths over the rack bars are not considered in calculations. Accordingly, two hypothesis are propounded.

1. Constant Energy Level (Energy Grade Line is horizontal)

2. Constant Energy Head (Energy Grade Line is parallel to the trash rack)

If the trash rack is placed horizontally, both hypothesis become equal. But, the trash racks are designed inclined in projects. When the trash rack is arranged inclined, both hypothesis appear as boundary conditions. However, neither represents the exact solution.

## 2.2 Constant Energy Level Hypothesis

There are two solution methods that can be applied to constant energy level hypothesis.

### 2.2.1 Iterative Method

As seen in Figure 5, the depth $h_1$ which occurs at the head of the trash rack is lower than $h_0$ which is the flow depth at approach. Firstly, the flow depth $h_0$ and the energy head $H_0$ must be calculated according to the unit discharge $(q_w)_T$. The energy level is assumed to be constant along the trash rack and the calculations start from the location where the flow depth is $h_1$.

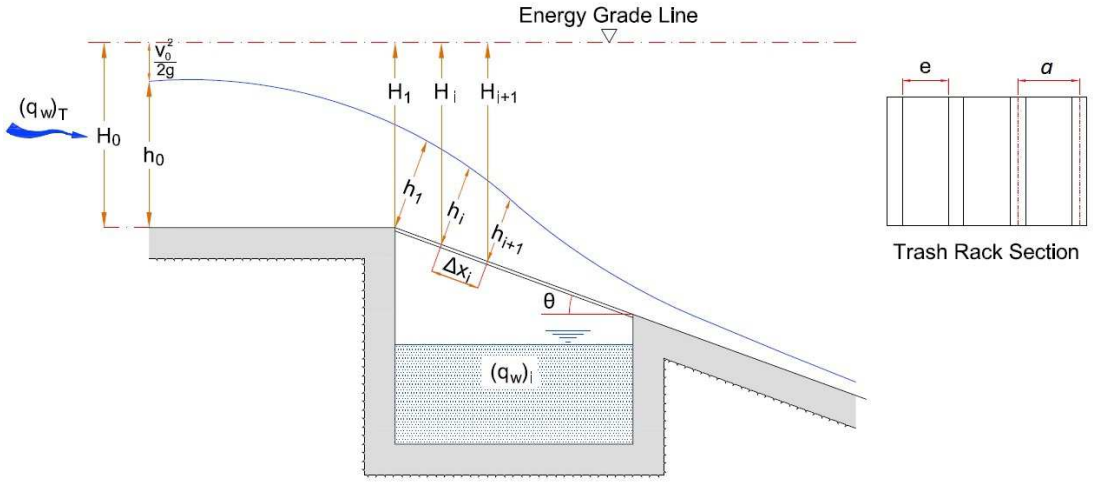


Figure 5 : Calculation system of trash rack with constant energy level

Eq. 2.1 can be written with the help of energy equation by considering a unit width with length $x_i$, depth $h_i$ and unit discharge $q_i$ over the trash rack.

$$q_i = h_i\sqrt{2g(H_i - h_i\cos\theta)} \quad \text{.....(2.1)}$$

In Eq. 2.1, ($\theta$) is the angle of the trash rack with respect to horizontal surface. To find the energy head $H_i$, elevation difference $x_i.sin(\theta)$ must be added to the energy head $H_0$. After that, for depth $h_{i+1}$, which is searched for, another value is assumed. For calculation of $(q_w)_i$ that passes through $\Delta x_i$, flow is identified with an orifice flow, and the following equation is given by using the flow depth at that section.

$$(q_w)_i = \lambda\sqrt{h}(\Delta x_i) \quad \text{.....(2.2)}$$

where $\lambda = \psi\mu_s\sqrt{2g\cos\theta}$ ; $\psi = e/a$ , $e$ and $a$ are net and gross spacings between bars, respectively. $\mu_s$ is a contraction coefficient which depends on the type of the trash rack.

For $0.2 < \frac{h}{a} < 3.5$ , Noseda defines $\mu_s$ as follows (Çeçen, 1962);

$$\mu_s = 0.66\psi^{-0.16}\left(\frac{a}{h}\right)^{0.13} \quad \text{……..……(2.3)}$$

In Eq. 2.2 and Eq. 2.3 the flow depth ($h$) is accepted as the average depth of $h_i$ and $h_{i+1}$ for $\Delta x_i$ interval. Afterwards, $(q_w)_i$ discharge that passed through bars between $h_i$ and $h_{i+1}$, is determined, it is subtracted from $q_i$ to calculate $q_{i+1}$. By using this discharge, $h_{i+1}$ is controlled with the help of Eq 2.1. Water surface profile and discharge distribution over the trash rack must be defined by iterating for each interval.

### 2.2.2 Closed Form Solution Method

Iterative method needs much amount of time and effort to solve. Frank (1956) developed a closed solution with some approaches (Çeçen, 1962). In this approach, the change in the flow depth is accepted as elliptic. As seen in Figure 6, when all the incoming discharge is diverted, ($(q_w)_T=(q_w)_i$), and $h_1$ and axis of the ellipse are defined, it is possible to write Eq. 2.4.

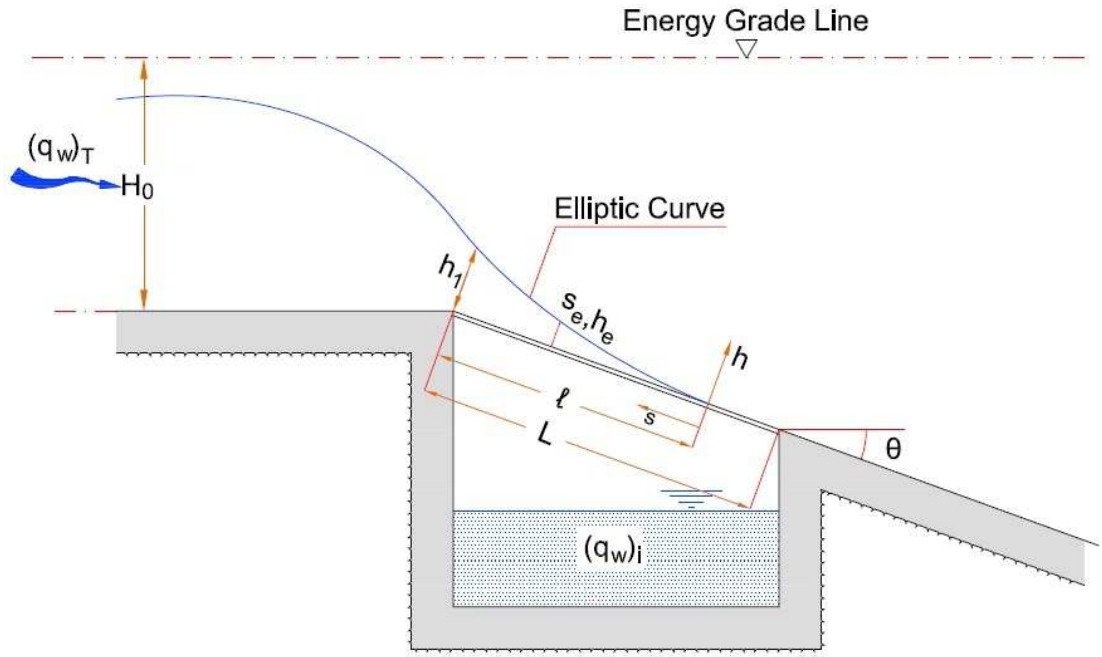


Figure 6 : Hydraulic system of trash rack in closed form solution

$$\frac{s^2}{l^2} = 2\frac{h}{h_1} - \frac{h^2}{h_1^2} \quad \text{.....(2.4)}$$

For $(q_w)_T=(q_w)_i$, the length "$\ell$" is calculated as follows;

Any distance $s_e$ away from the origin of the ellipse can be computed by using Eq. 2.4.

$$s_e = \sqrt{2\frac{l^2}{h_1}h_e - \frac{l^2}{h_1^2}h_e^2} \quad \text{.....(2.5)}$$

where $h_e$ is the flow depth at distance $s_e$. The amount of water entered the collection channel through the distance $ds_e$ can be found with the help of Eq 2.5.

$$ds_e = \frac{l}{h_1}\frac{(h_1 - h_e)}{\sqrt{2h_1h_e - h_e^2}}dh_e \quad \text{.....(2.6)}$$

The discharge diverted to the collection channel is given in Eq 2.10. by using Eq 2.2. and 2.6.

$$dq = \lambda\sqrt{h_0}\,ds_e = \lambda\frac{l}{h_1}\frac{\sqrt{h_e}\left(h_1 - h_e\right)}{\sqrt{2h_1h_e - h_e^{\,2}}}dh_e \quad \text{.....(2.7)}$$

$$(q_w)_i = \int dq = \lambda\frac{l}{h_1}\int_{h_e=0}^{h_e=h_1}\frac{\sqrt{h_e}\left(h_1 - h_e\right)}{\sqrt{2h_1h_e - h_e^{\,2}}}dh_e \quad \text{.....(2.8)}$$

$$(q_w)_i = \frac{2}{3}\lambda\sqrt{h_1}\,l\left(1+\frac{h_e}{h_1}\right)\sqrt{2-\frac{h_e}{h_1}}\;\Bigg|_{h_e=0}^{h_e=h_1} \quad \text{.....(2.9)}$$

$$(q_w)_i = \frac{2}{3}\lambda\sqrt{h_1}\,l\left(2-\sqrt{2}\right) = 0.391\lambda\sqrt{h_1}\,l \quad \text{.....(2.10)}$$

For $(q_w)_i = (q_w)_T$, the wetted length can be computed as;

$$l = 2.561\frac{(q_w)_T}{\lambda\sqrt{h_1}} \quad \text{.....(2.11)}$$

As seen in Figure 7, in some cases, the incoming total discharge $(q_w)_T$ may not be diverted into the collection channel. According to Frank (1956), elliptic approach can be used to calculate the design parameters. In these cases, the length of the elliptic curve is computed by using the incoming discharge, $(q_w)_T$ and energy head $H_0$. The length between where the flow depth is zero and the end of trash rack is $s = \ell - L$.

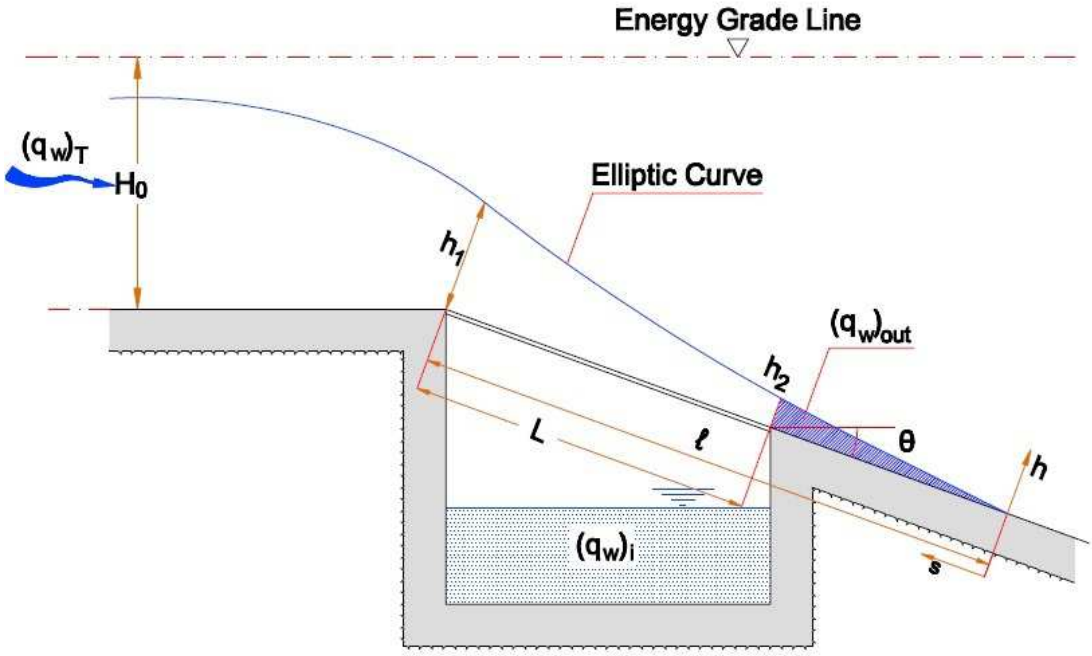


Figure 7 : Elliptic curve approach, in cases where the total flow can not be diverted

The diverted discharge $(q_w)_i$ can be calculated by making the following assumptions about elliptic curve approach.

1. The hatched area under the elliptic curve after the depth $h_2$ is accepted as the total discharge that goes to downstream.

2. The area under the elliptic curve between the depth $h_1$ and $h_2$ is accepted as the discharge diverted into the collection channel.

By modifying Eq. 2.9 considering the 2nd item given above this case Eq. 2.13 is obtained.

$$(q_w)_i = \frac{2}{3}\lambda\sqrt{h_1}\,l\left(1+\frac{h_e}{h_1}\right)\sqrt{2-\frac{h_e}{h_1}}\;\Bigg|_{h_e=h_2}^{h_e=h_1} \qquad \text{.....(2.12)}$$

$$(q_w)_i = \frac{2}{3}\lambda\sqrt{h_1}l\left[2-\left(1+\frac{h_2}{h_1}\right)\left(\sqrt{2-\frac{h_2}{h_1}}\right)\right] \quad \text{.....(2.13)}$$

Eq. 2.11 can be integrated into Eq. 2.13 and the final form of the closed form solution formula is obtained as follows in Eq. 2.14.

$$(q_w)_i = 1.707(q_w)_T\left[2-\left(1+\frac{h_2}{h_1}\right)\left(\sqrt{2-\frac{h_2}{h_1}}\right)\right] \quad \text{.....(2.14)}$$

## 2.3 Constant Energy Head Hypothesis

In this approach, the energy head is accepted as constant and because of this reason, slope of the energy grade line is equal to the inclination angle of the trash rack. Figure 8 shows the constant energy head approach scheme.

### 2.3.1 Iterative Method

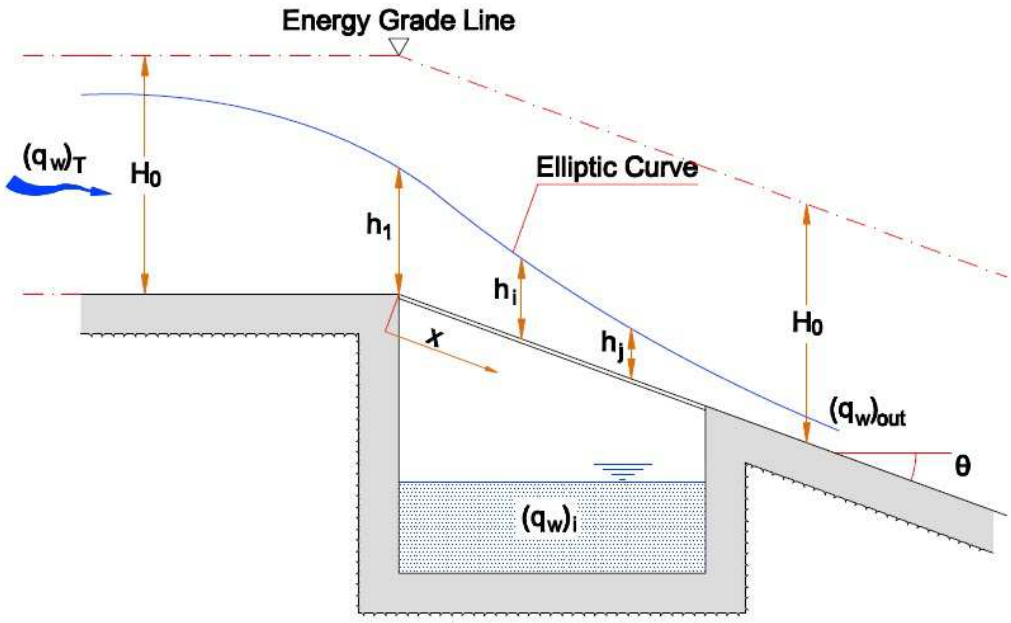


Figure 8 : Constant energy head approach scheme

Noseda defined the differential equation of the water surface as in Eq. 2.15, when inclination angle of the trash rack $\theta$ is sufficiently small ($h \approx h\cos\theta$) (Çeçen, 1962).

$$\frac{dh}{dx} = -\frac{2\mu_s \psi \sqrt{H_0(H_0 - h)}}{2H_0 - 3h} \quad \text{.....(2.15)}$$

Eq. 2.15 can be integrated directly between $i$ and $j$ points by assuming $\mu_s$ has a constant value. This integration has a closed form solution.

$$x_j - x_i = \frac{H_0}{\mu_s \psi}\left[\phi\left(\frac{h_j}{H_0}\right) - \phi\left(\frac{h_i}{H_0}\right)\right] \quad \text{.....(2.16)}$$

$$\phi\left(\frac{h}{H_0}\right) = \frac{1}{2}\arccos\left(\sqrt{\frac{h}{H_0}}\right) - \frac{3}{2}\sqrt{\frac{h}{H_0} - \left(1 - \frac{h}{H_0}\right)} \quad \text{.....(2.17)}$$

The solutions of the function in terms of $\phi\left(\frac{h}{H_0}\right)$ and $\left(\frac{h}{H_0}\right)$ is given in Table 1.

In this approach, it is recommended that the calculations must be completed step by step. Not only the flow depth, but also the discharges at selected points can be calculated by determining the maximum discharge ($q_{max}$) for energy head $H_0$.

$$q_{\max} = h_c V_c = \frac{2}{3} H_0 \sqrt{2g\left(H_0 - \frac{2}{3}H_0\right)} = \frac{2\sqrt{2g}}{3\sqrt{3}} H_0^{3/2} = 1.705 H_0^{3/2} \quad \text{.....(2.18)}$$

When Eq. 2.16 is modified for $q_{max}$, Eq. 2.19 is obtained.

$$x_j - x_i = \frac{H_0}{\mu_s \psi}\left[\beta\left(\frac{q_j}{q_{\max}}\right) - \beta\left(\frac{q_i}{q_{\max}}\right)\right] \quad \text{.....(2.19)}$$

The closed form of Eq. 2.19 can be written as;

$$\beta\left(\frac{q}{q_{\max}}\right)=\frac{1}{2}\arccos\left(\frac{1}{\sqrt{3}}\sqrt{2\cos\varphi+1}\right)-\frac{\sqrt{2}}{2}\sqrt{(2\cos\varphi+1)(1-\cos\varphi)} \quad \text{……..(2.20)}$$

Solutions of $\beta$ function in terms of $\beta\left(\frac{q}{q_{\max}}\right)$ is given in Table 1.

$\varphi$ is calculated separately for subcritical and supercritical flow cases.

For subcritical flow case $$\varphi=\frac{1}{3}\arccos\left[1-2\left(\frac{q}{q_{\max}}\right)^2\right]$$

For supercritical flow case $$\varphi=\frac{1}{3}\arccos\left[1-2\left(\frac{q}{q_{\max}}\right)^2\right]+240^{o}$$

Table 1: Solutions of functions $\varphi$ and $\beta$

| $\left(\frac{h}{H_0}\right)$ | $\phi\left(\frac{h}{H_0}\right)$ | $\left(\frac{q}{q_{\max}}\right)$ | $\beta\left(\frac{q}{q_{\max}}\right)$ | |
|---|---|---|---|---|
| | | | Subcritical | Supercritical |
| 0 | 0.7854 | 0 | 0 | 0.7854 |
| 0.05 | 0.3457 | 0.05 | -0.0192 | 0.5084 |
| 0.10 | 0.1745 | 0.10 | -0.0385 | 0.3937 |
| 0.15 | 0.0510 | 0.15 | -0.0578 | 0.3072 |
| 0.20 | -0.0464 | 0.20 | -0.0771 | 0.2342 |
| 0.25 | -0.1259 | 0.25 | -0.0965 | 0.1702 |
| 0.30 | -0.1921 | 0.30 | -0.1158 | 0.1127 |
| 0.35 | -0.2466 | 0.35 | -0.1352 | 0.0617 |
| 0.40 | -0.2918 | 0.40 | -0.1546 | 0.0117 |
| 0.45 | -0.3290 | 0.45 | -0.1742 | -0.0337 |
| 0.50 | -0.3573 | 0.50 | -0.1938 | -0.0762 |
| 0.55 | -0.3791 | 0.55 | -0.2134 | -0.1162 |
| 0.60 | -0.3925 | 0.60 | -0.2332 | -0.1543 |
| 0.65 | -0.3989 | 0.65 | -0.2532 | -0.1904 |
| 0.70 | -0.3976 | 0.70 | -0.2732 | -0.2247 |
| 0.75 | -0.3877 | 0.75 | -0.2934 | -0.2575 |
| 0.80 | -0.3682 | 0.80 | -0.3139 | -0.2887 |
| 0.85 | -0.3367 | 0.85 | -0.3346 | -0.3187 |
| 0.90 | -0.2891 | 0.90 | -0.3556 | -0.3471 |
| 0.95 | -0.2142 | 0.95 | -0.3771 | -0.3743 |
| 1.00 | 0 | 1.00 | -0.3994 | -0.3994 |

### 2.3.2 Closed Form Solution Method

The closed form solution of constant energy head method is produced by ignoring head loss and recommended for the horizontal trash racks. Slope of the energy grade line becomes equal to the slope of the trash rack.

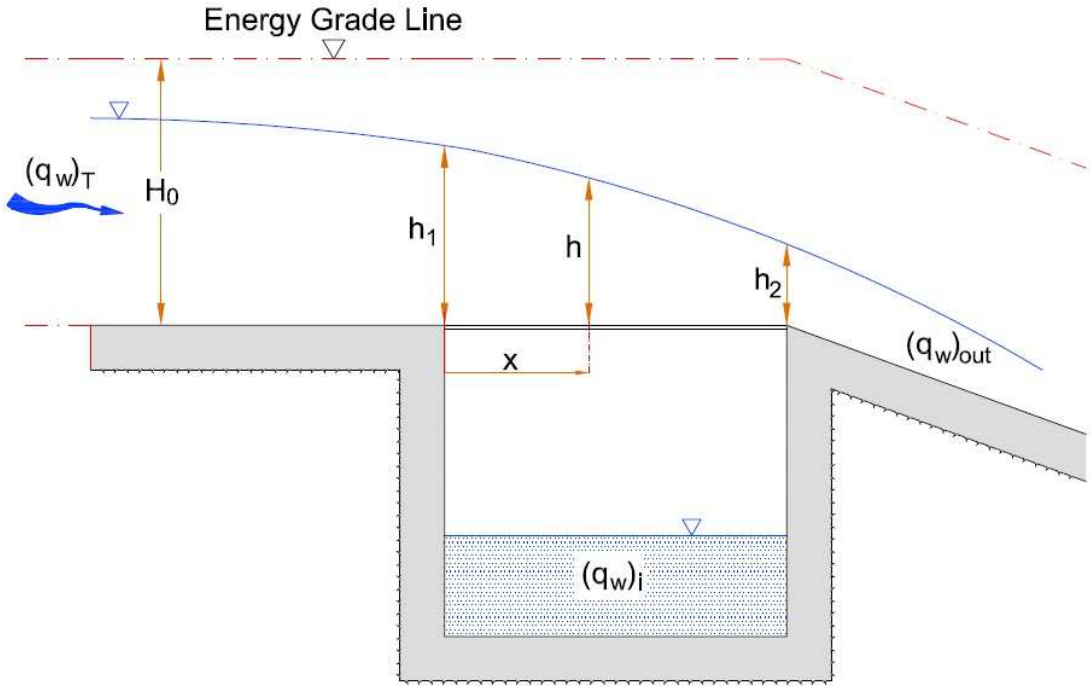


Figure 9 : Constant energy head approach closed form solution scheme

For a given x interval, to determine the amount of water that passes through the trash rack, $(q_w)_i$, can be calculated by the following formula;

$$(q_w)_i = C_c \mu_s \sqrt{2gH_0}\, x \qquad \text{.....(2.21)}$$

$(q_w)_T$ can be written as follows with the help of Eq. 2.1 for $\theta$=0$^o$.

$$(q_w)_T = h\sqrt{2g(H_0 - h)} \qquad \text{.....(2.22)}$$

For an interval dx, the reduction in amount of water that passes over the trash rack equals to the amount of diverted water through the trash rack.

$$\frac{d(q_w)_i}{dx} = -\frac{d(q_w)_T}{dx} = C_c \mu_s \sqrt{2gH_0} \quad \text{.....(2.23)}$$

$$\frac{d(q_w)_T}{dh} = \frac{2gH_0 - 3gh}{\sqrt{2gH_0 - 2gh}} \quad \text{.....(2.24)}$$

By integrating Eq. 2.23 into Eq. 2.24, Eq. 2.25 is obtained.

$$\frac{3gh - 2gH_0}{\sqrt{2gH_0 - 2gh}} dh = C_c \mu_s \sqrt{2gH_0}\, dx \quad \text{.....(2.25)}$$

By using Eq. 2.25, the relation between the head of the trash rack ($h$=$h_1$ and $x$=0) and any point on the trash rack at distance $x$ from the head with the flow depth $h$ can be written as follows;

$$\int_{h=h_1}^{h=h} \frac{3h - 2H_0}{\sqrt{(H_0 - h)}} dh = 2C_c \mu_s \sqrt{H_0} \int_{x=0}^{x=x} dx \quad \text{.....(2.26)}$$

$$-2h\left(\sqrt{H_0 - h}\right)\Big|_{h=h_1}^{h=h} = 2C_c \mu_s \sqrt{H_0}\, x \quad \text{.....(2.27)}$$

$$h_1\sqrt{1 - \frac{h_1}{H_0}} - h\sqrt{1 - \frac{h}{H_0}} = C_c \mu_s x \quad \text{.....(2.28)}$$

By multiplying each side of the equation with $\frac{1}{H_0}$, the expression of $\frac{x}{H_0}$ can be obtained as follows.

$$\frac{x}{H_0} = \frac{1}{C_c \mu_s}\left(\frac{h_1}{H_0}\sqrt{1-\frac{h_1}{H_0}} - \frac{h}{H_0}\sqrt{1-\frac{h}{H_0}}\right) \text{……...……..(2.29)}$$

By using Eq. 2.29 water surface profile of the flow can be calculated. When $x$ is selected as the full length of the trash rack, ($L$), the flow depth $h_2$ is can also be computed. Furthermore, the discharge that passes over the trash rack, $(q_w)_{out}$, is obtained by using Eq. 2.22.

$$(q_w)_{out} = h_2\sqrt{2g(H_0 - h_2)} \text{ ……...……...……..(2.30)}$$

So the discharge that is diverted into the collection channel can be calculated by

$$(q_w)_i = (q_w)_T - (q_w)_{out} \text{……..(2.31)}$$

The coefficient $C_c$ is selected as 0.497 for horizontal trash rack, and 0.435 for trash rack inclination of 0.2 (Özcan, 1999).

# CHAPTER 3

## EXPERIMENTAL METHODS

### 3.1 Introduction

A Tyrolean weir model was constructed in Hydromechanics Laboratory of Middle East Technical University to investigate the hydraulic characteristics of Tyrolean weirs. Yılmaz (2010) and Şahiner (2012) conducted a series of experiments by considering different variations on the same physical model to discover the performances of the trash racks.

### 3.2 Experimental Setup

Tyrolean weir model included a reservoir, a main channel, a water intake pipe, a water intake screen and a side channel (Figure 10). The water intake pipe of 30 cm diameter directed water from reservoir to main channel. The flow rate of system was measured by an ultrasonic flow meter placed on the water intake pipe. The main channel used in the experiments was 7.0 m in length, 1.98 m in width and had a slope of $S_0$=0.001. For Tyrolean screen metal bars having 10 mm diameter were used. Three different clearance distances were analyzed ($e_1$ = 3 mm, $e_2$ = 6 mm, $e_3$ = 10 mm). The model was tested at six different angle of inclinations; $\theta_1 = 14.477^o$, $\theta_2 = 9.594^o$, $\theta_3 = 4.780^o$ (Yılmaz, 2010), $\theta_4 = 37.000^o$, $\theta_5 = 32.800^o$, $\theta_6 = 27.800^o$ (Şahiner, 2012). A collection channel was built under the Tyrolean screen, which was 1.98 m length and 0.60 m width with 0.1 bottom slope. The water in the collection channel was diverted to the side channel 6.5 m in length and 0.70 m in width.

Figure 10 : Picture of the Tyrolean weir model used by Yılmaz (2010) and Şahiner (2012)

### 3.3 The Formulas Used in the Analysis of Experimental Results

In order to analyze the outcome of the experiments and provide a solution method, formulas for the discharge coefficient $C_d$, water capture efficiency $(q_w)_i/(q_w)_T$ ($WCE$) and wetted rack length $L_2/e$ were derived referring to the definition sketch presented in Figure 11 (Yılmaz 2010; Şahiner 2012).

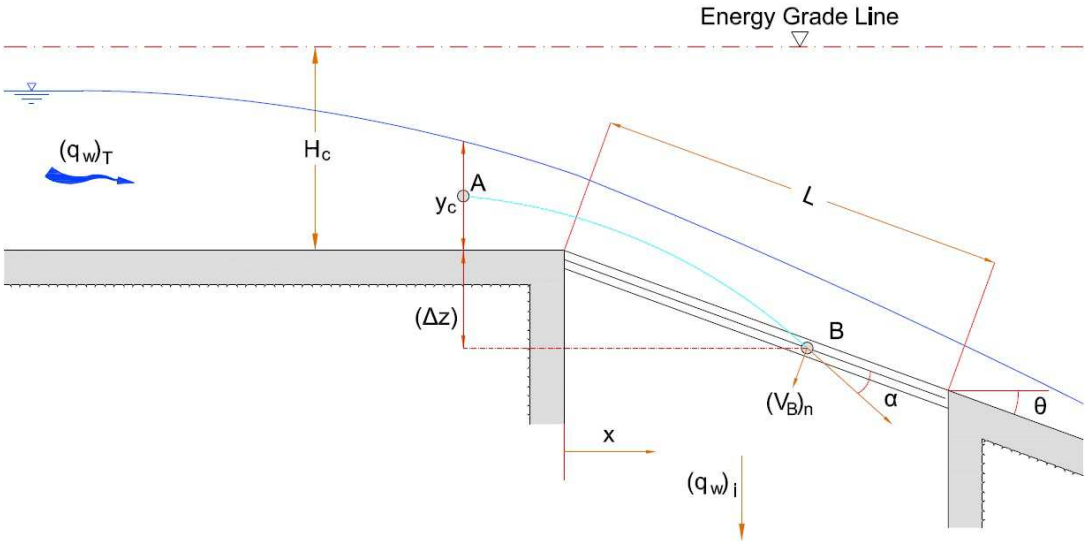


Figure 11 : Definition sketch for a Tyrolean weir (Yılmaz, 2010)

$$(q_w)_i = C_d \psi \sqrt{2gH_c} \quad \text{.....(3.1)}$$

where $C_d$ is the overall discharge coefficient and covers all assumptions made in the derivation of $(q_w)_i$ and $e/a$ $(\psi)$ is the net rack opening area per unit width of the rack.

$$C_d = f_1\left[(F_r)_e, \frac{L}{e}, \frac{e}{a}, \theta\right] \quad \text{.....(3.2)}$$

$$\frac{(q_w)_i}{(q_w)_T} = f_2\left[(F_r)_e, \frac{L}{e}, \frac{e}{a}, \theta\right] \quad \text{.....(3.3)}$$

and

$$\frac{L_2}{e} = f_3\left[(F_r)_e, \frac{e}{a}, \theta\right] \quad \text{.....(3.4)}$$

where $(Fr)_e^{\,2} = \dfrac{(q_w)_T^{\,2}}{(e^3 g)}$ , square of the Froude number based on bar opening.

The variation of $C_d$, $\frac{(q_w)_i}{(q_w)_T}$ and $\frac{L_2}{e}$ with the related dimensionless terms presented in Equations 3.2, 3.3 and 3.4 were used to the prepare the design charts shown in Figures 12-47. From these figures the following conclusions were made;

- For a screen of given *L/e*, as $(Fr)_e$ increases, $C_d$ value increases and reaches to maximum value.
- The screen of the lowest *L/e* has the largest $C_d$ value.
- When $(Fr)_e$ is constant, $C_d$ values increase as *L/e* decreases.
- For a given angle of inclination ($\theta$), as the bar spacing increases, $C_d$ values decrease for constant $(Fr)_e$ and *L/e*.

When the angle of inclination $(\theta)$ , rack opening *(e)*, rack length *(L)* and total discharge $(q_w)_T$ are given for a Tyrolean weir, the diverted discharge $(q_w)_i$ can be calculated by following the steps given in the chart below.

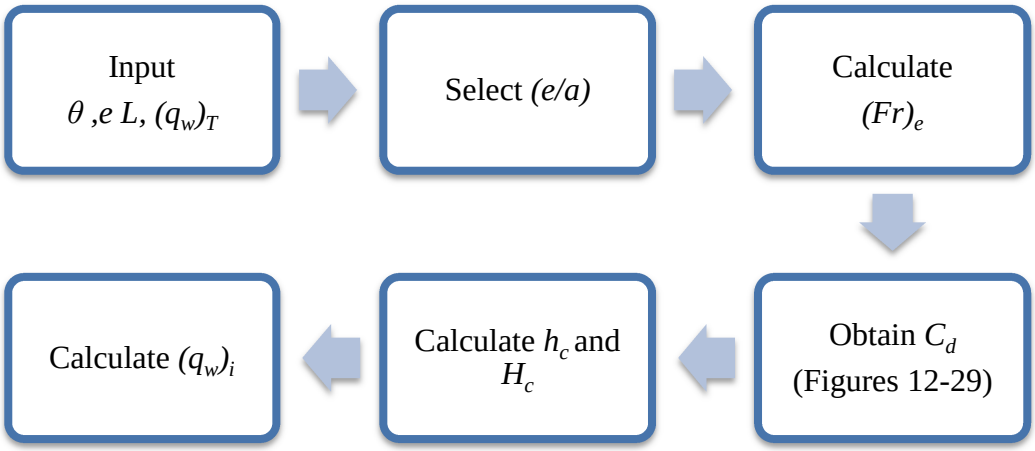

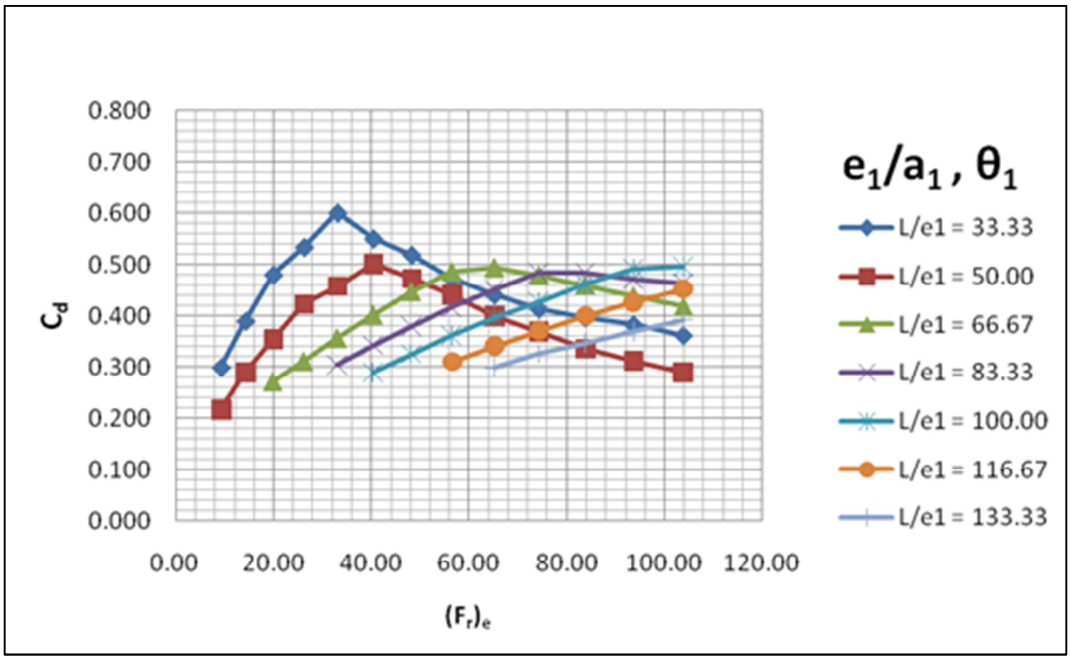


Figure 12 : $C_d$ vs $(Fr)_e$ for $e_1/a_1$ = 0.23 and $\theta_1$ = 14.477° (Yılmaz,2010)

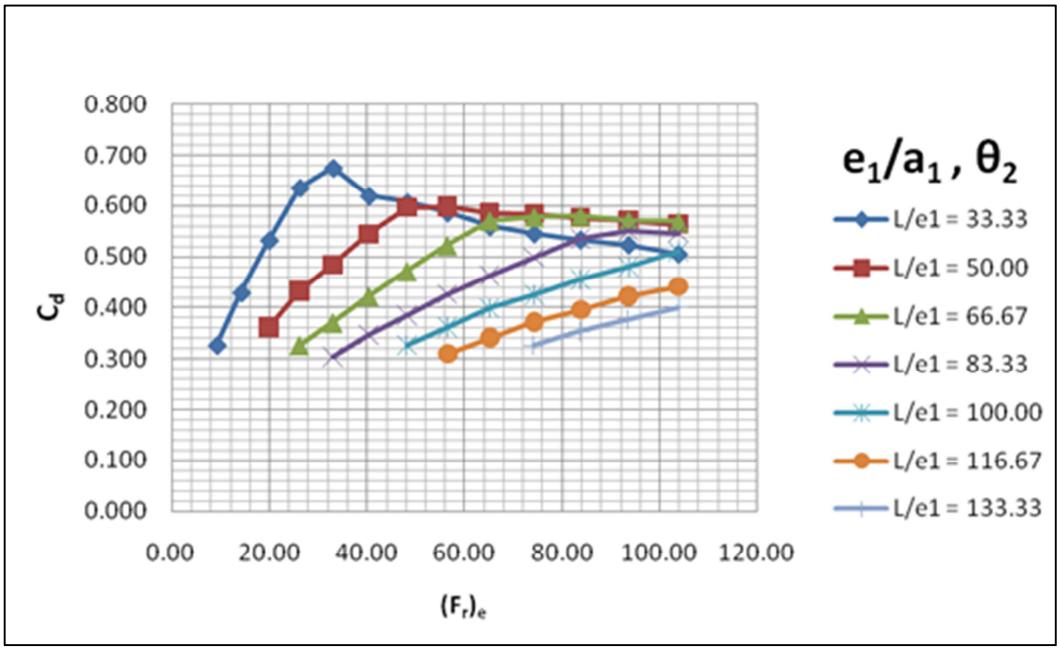


Figure 13 : $C_d$ vs $(Fr)_e$ for $e_1/a_1$ = 0.23 and $\theta_2$ = 9.594° (Yılmaz,2010)

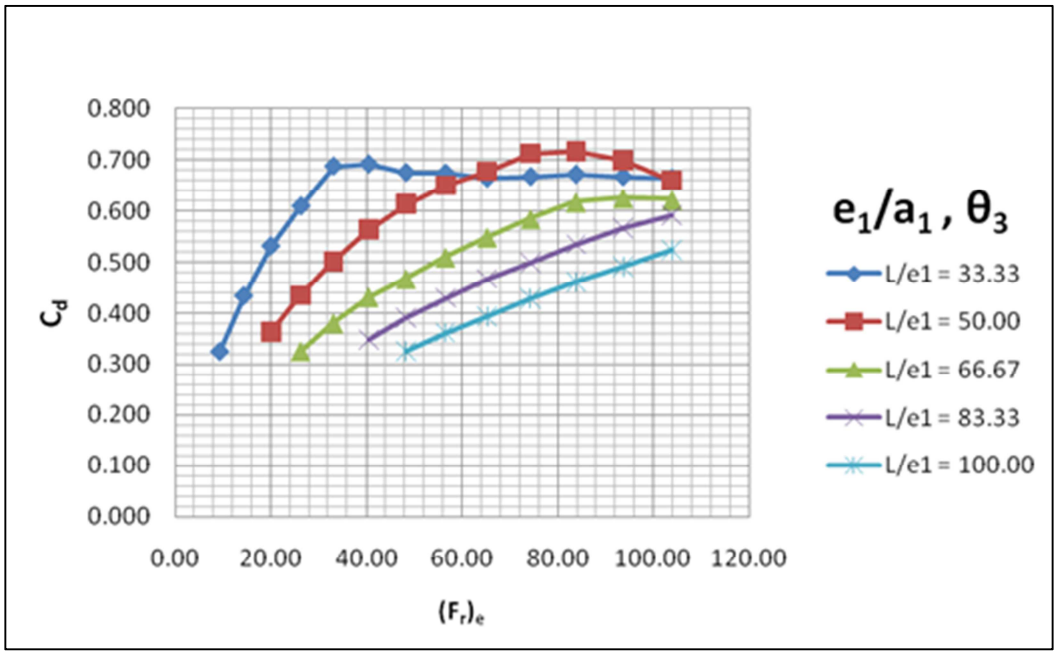


Figure 14 : $C_d$ vs $(Fr)_e$ for $e_1/a_1$ = 0.23 and $\theta_3$ = 4.780° (Yılmaz,2010)

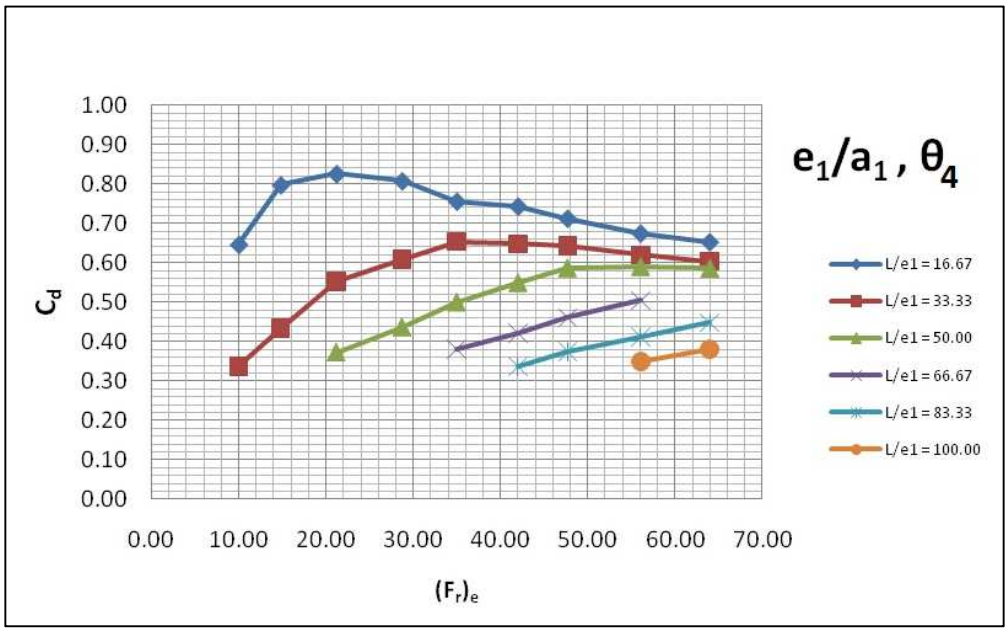


Figure 15 : $C_d$ vs $(Fr)_e$ for $e_1/a_1$ = 0.23 and $\theta_4$ = 37.000° (Şahiner,2012)

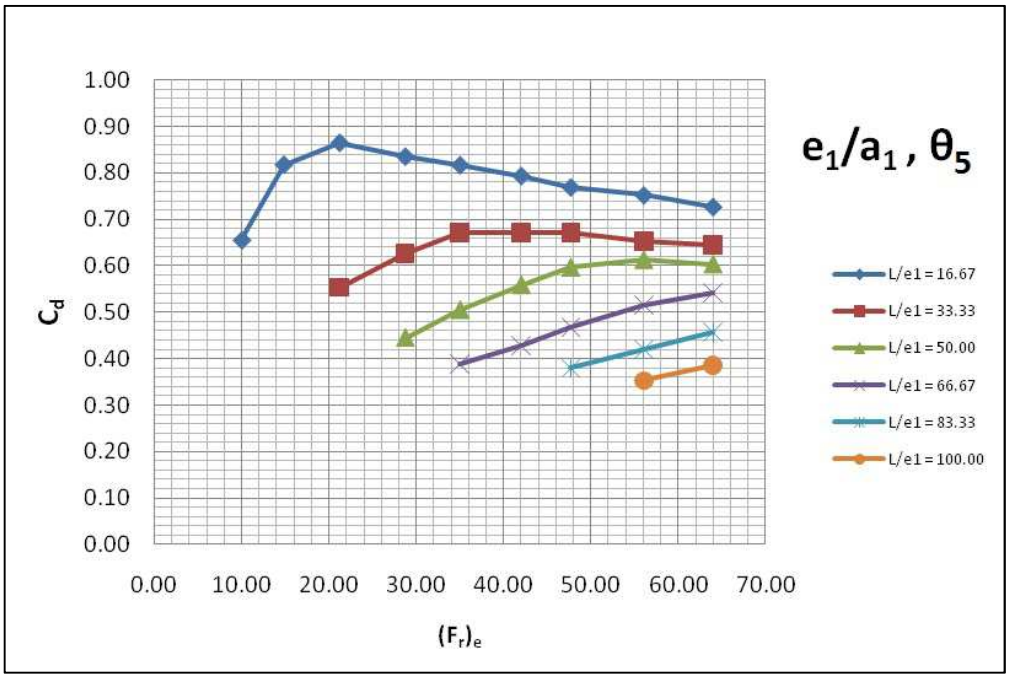


Figure 16 : $C_d$ vs $(Fr)_e$ for $e_1/a_1$ = 0.23 and $\theta_5$ = 32.800° (Şahiner,2012)

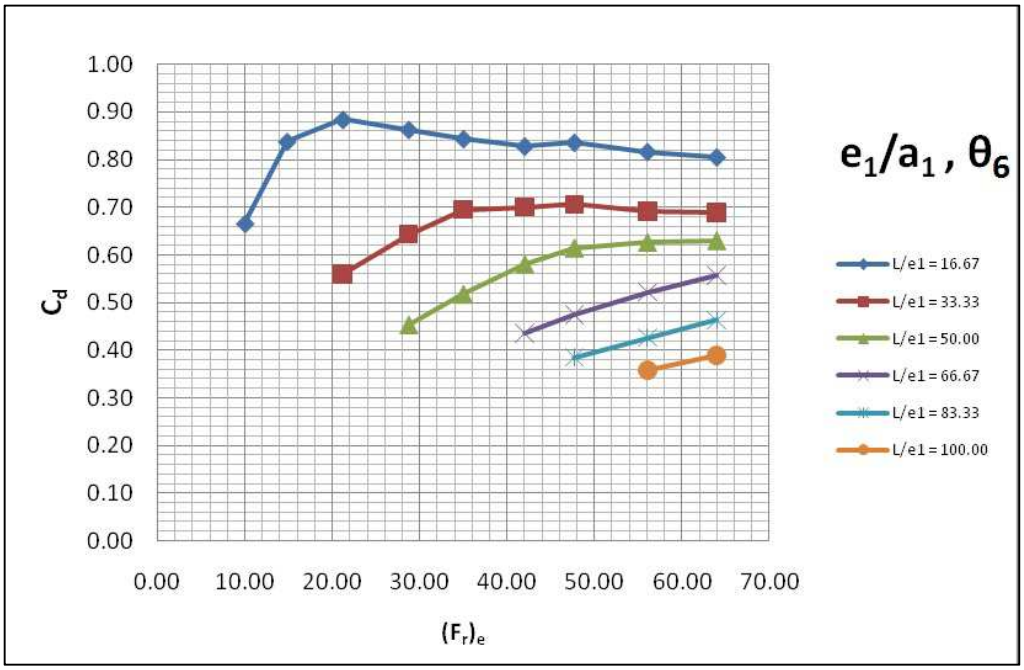


Figure 17 : $C_d$ vs $(Fr)_e$ for $e_1/a_1$ = 0.23 and $\theta_6$ = 27.800° (Şahiner,2012)

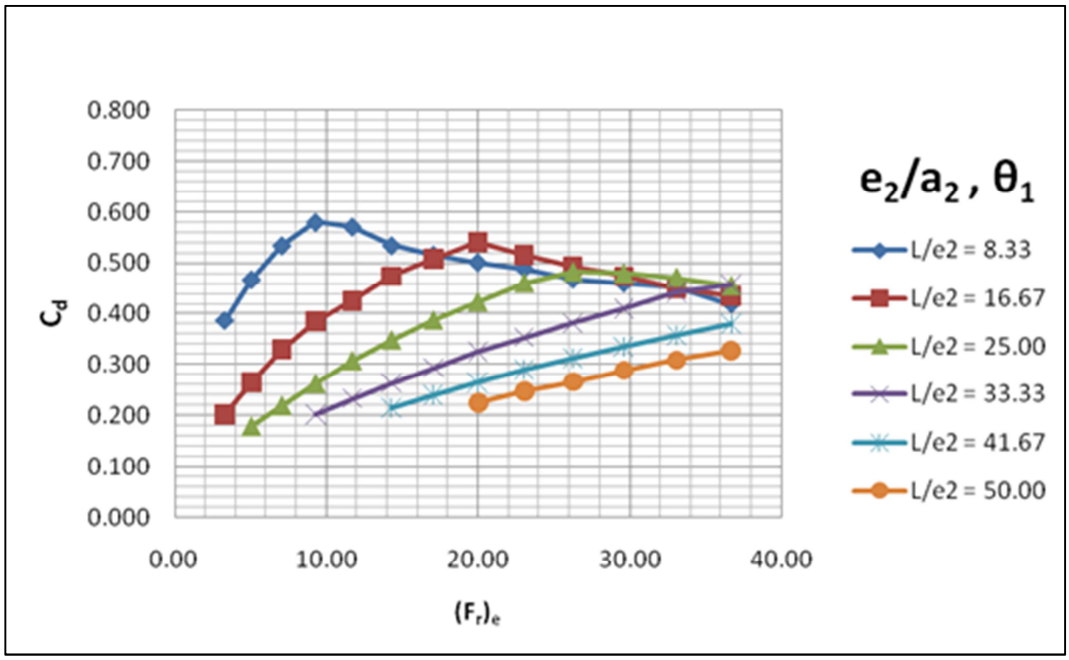


Figure 18 : $C_d$ vs $(Fr)_e$ for $e_2/a_2$ = 0.375 and $\theta_1$ = 14.477° (Yılmaz,2010)

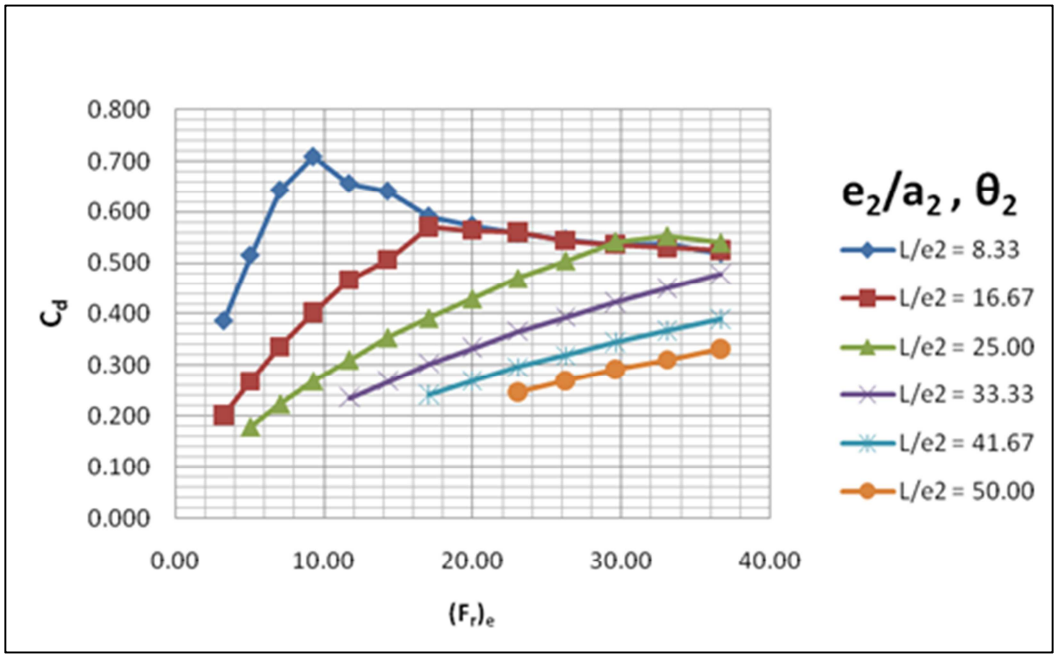


Figure 19 : $C_d$ vs $(Fr)_e$ for $e_2/a_2$ = 0.375 and $\theta_2$ = 9.594° (Yılmaz,2010)

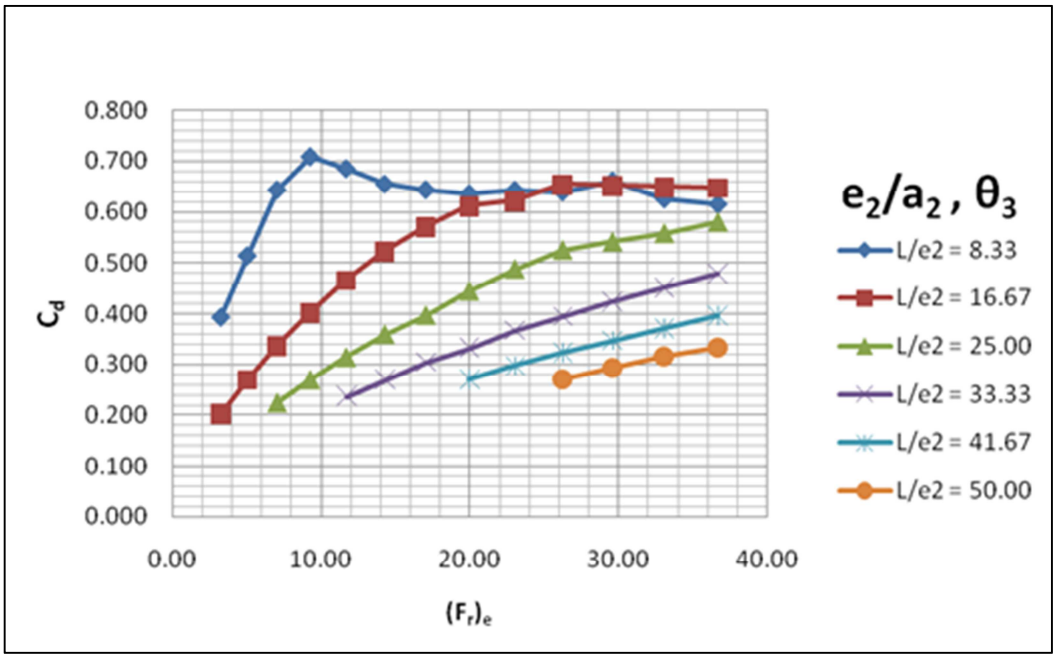


Figure 20 : $C_d$ vs $(Fr)_e$ for $e_2/a_2$ = 0.375 and $\theta_3$ = 4.780° (Yılmaz,2010)

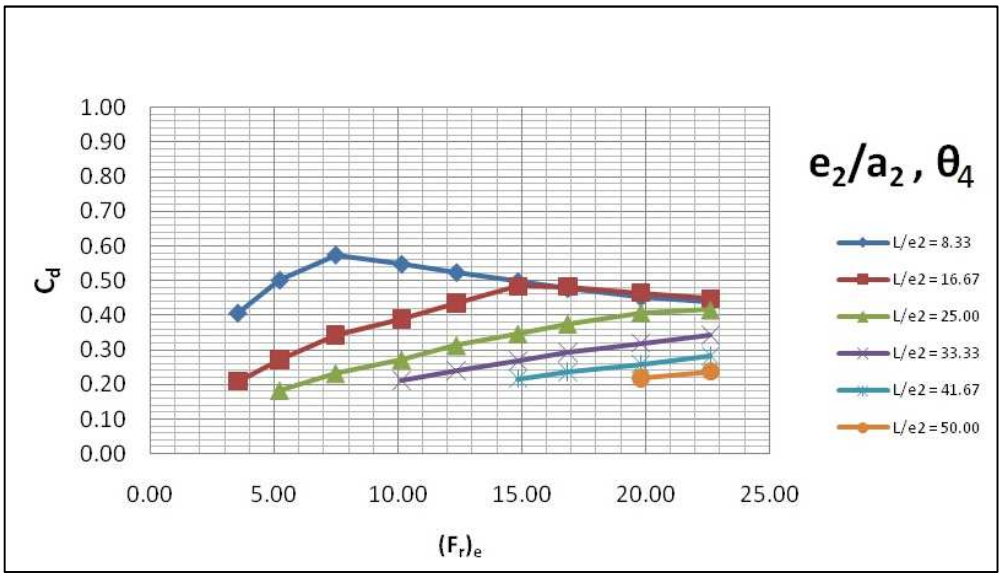


Figure 21 : $C_d$ vs $(Fr)_e$ for $e_2/a_2$ = 0.375 and $\theta_4$ = 37.000° (Şahiner,2012)

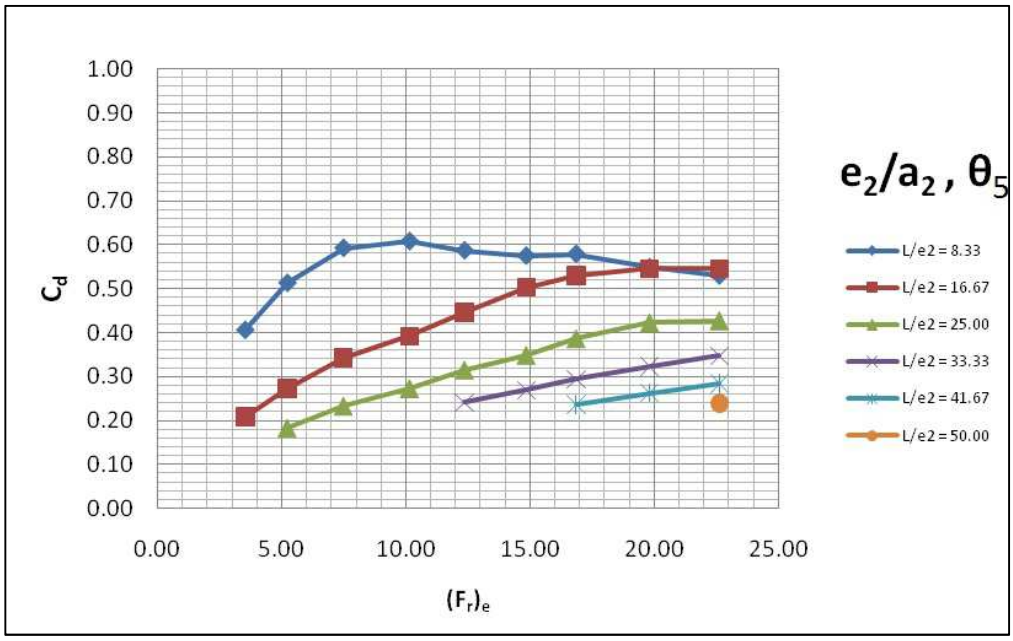


Figure 22 : $C_d$ vs $(Fr)_e$ for $e_2/a_2$ = 0.375 and $\theta_5$ = 32.800° (Şahiner,2012)

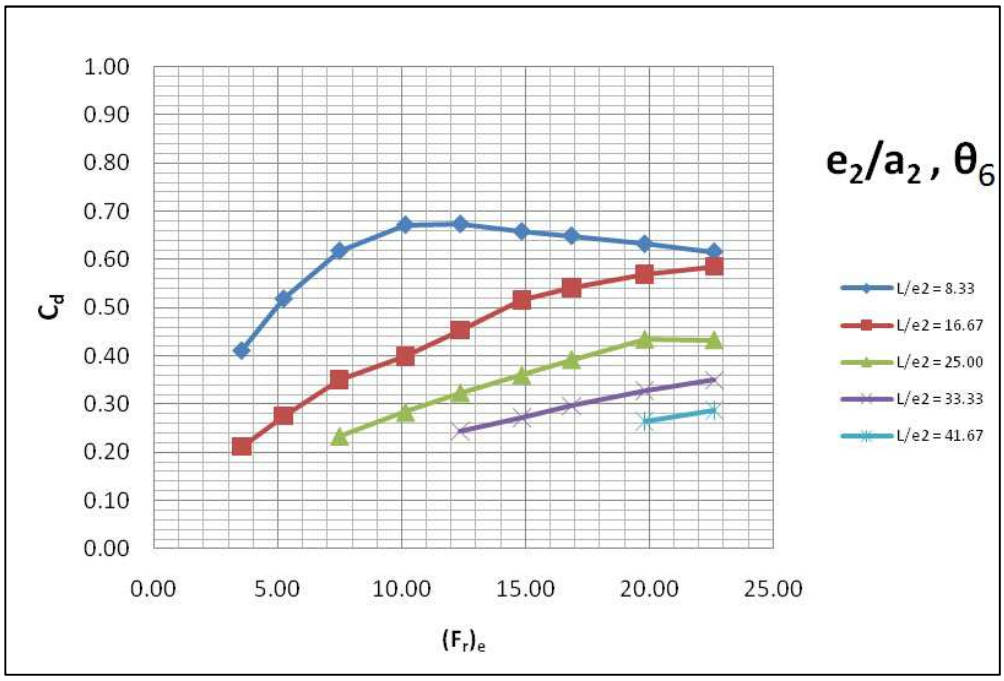


Figure 23 : $C_d$ vs $(Fr)_e$ for $e_2/a_2$ = 0.375 and $\theta_6$ = 27.800° (Şahiner,2012)

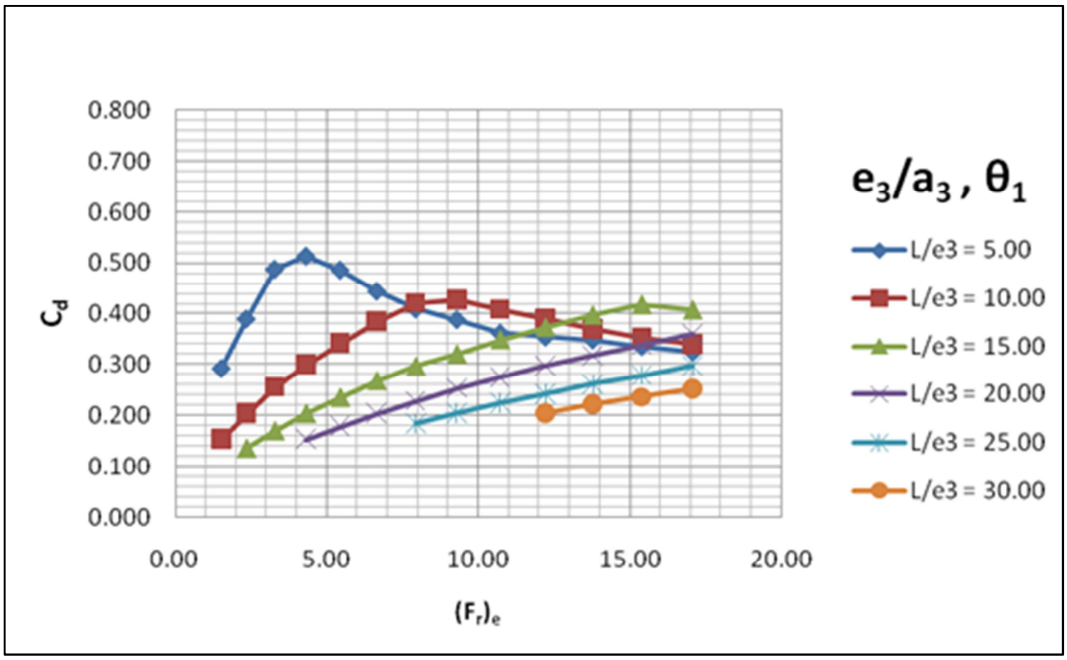


Figure 24 : $C_d$ vs $(Fr)_e$ for $e_3/a_3$ = 0.5 and $\theta_1$ = 14.477° (Yılmaz,2010)

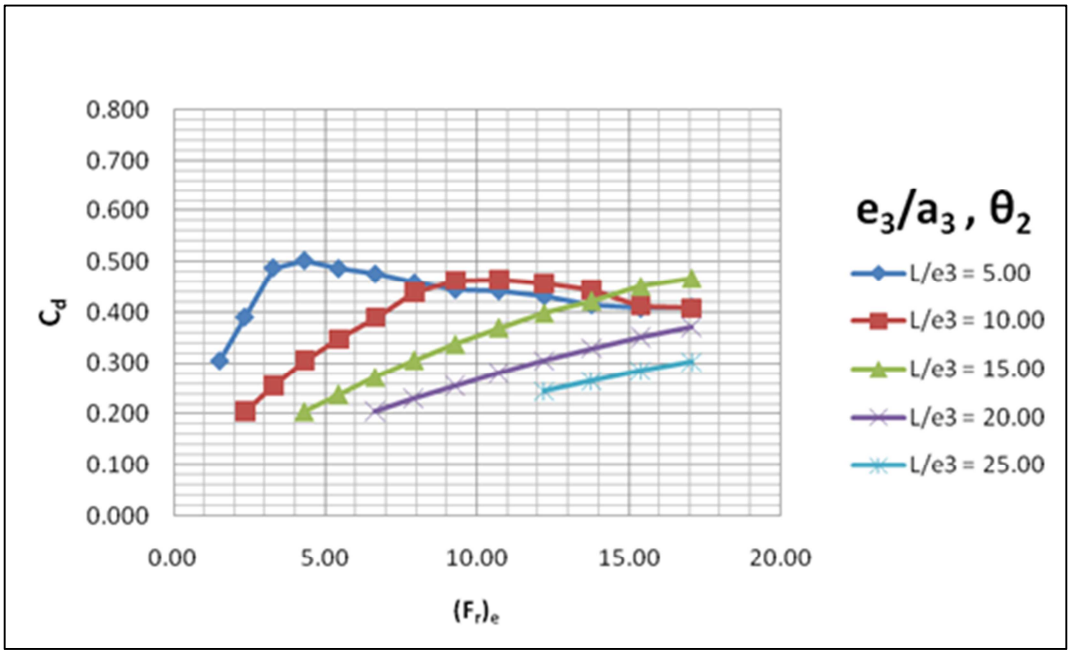


Figure 25 : $C_d$ vs $(Fr)_e$ for $e_3/a_3$ = 0.5 and $\theta_2$ = 9.594° (Yılmaz,2010)

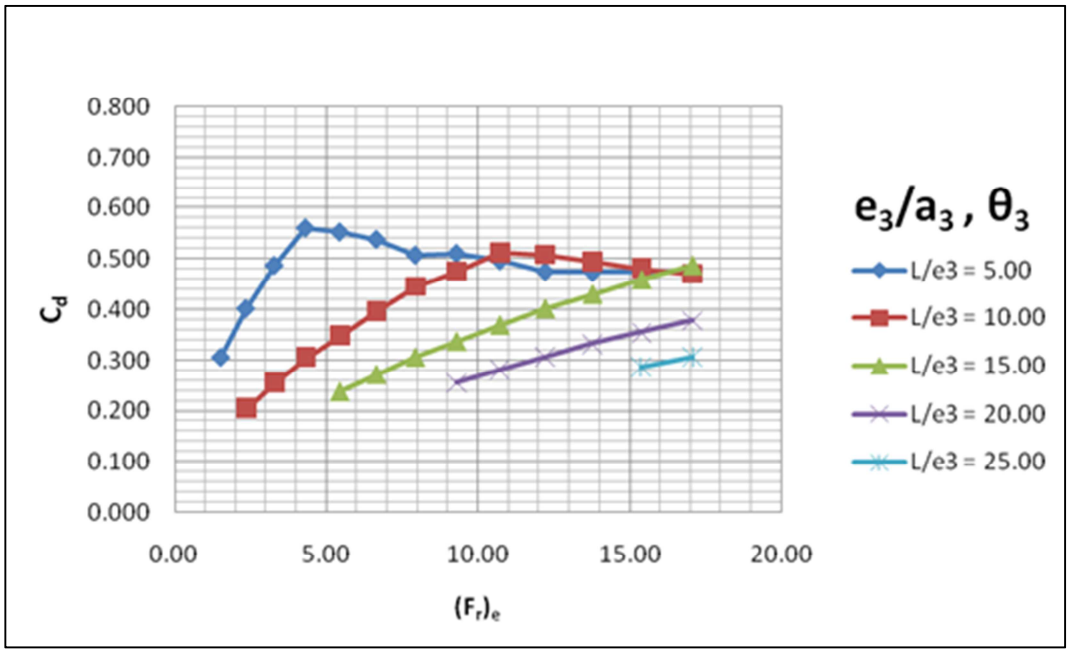


Figure 26 : $C_d$ vs $(Fr)_e$ for $e_3/a_3$ = 0.5 and $\theta_3$ = 4.780° (Yılmaz,2010)

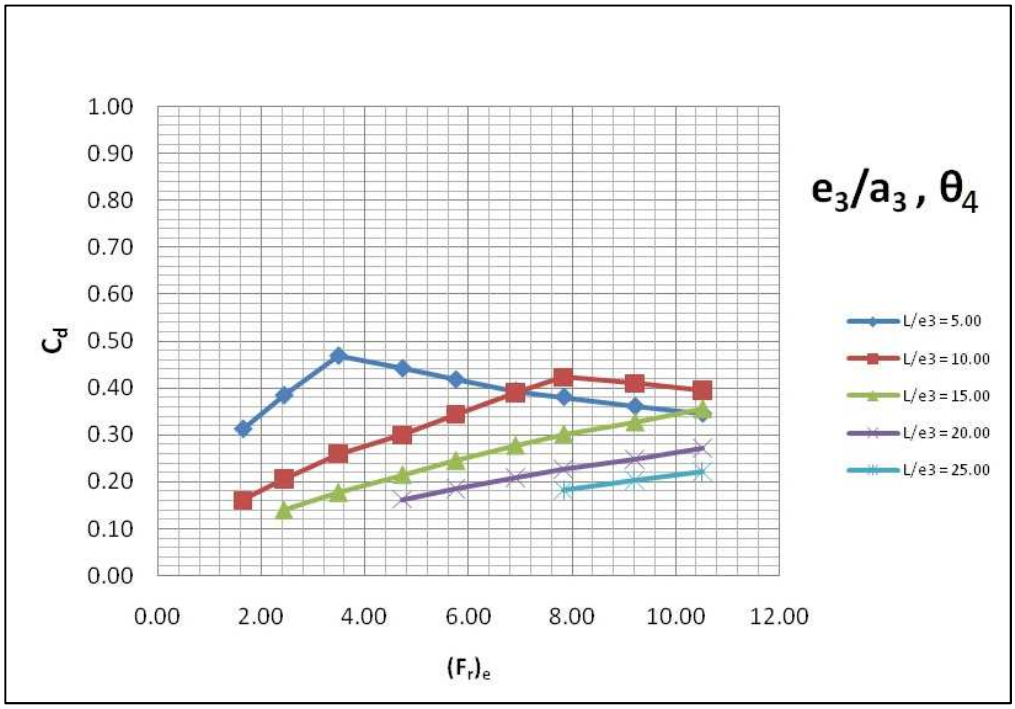


Figure 27 : $C_d$ vs $(Fr)_e$ for $e_3/a_3$ = 0.5 and $\theta_4$ = 37.000° (Şahiner,2012)

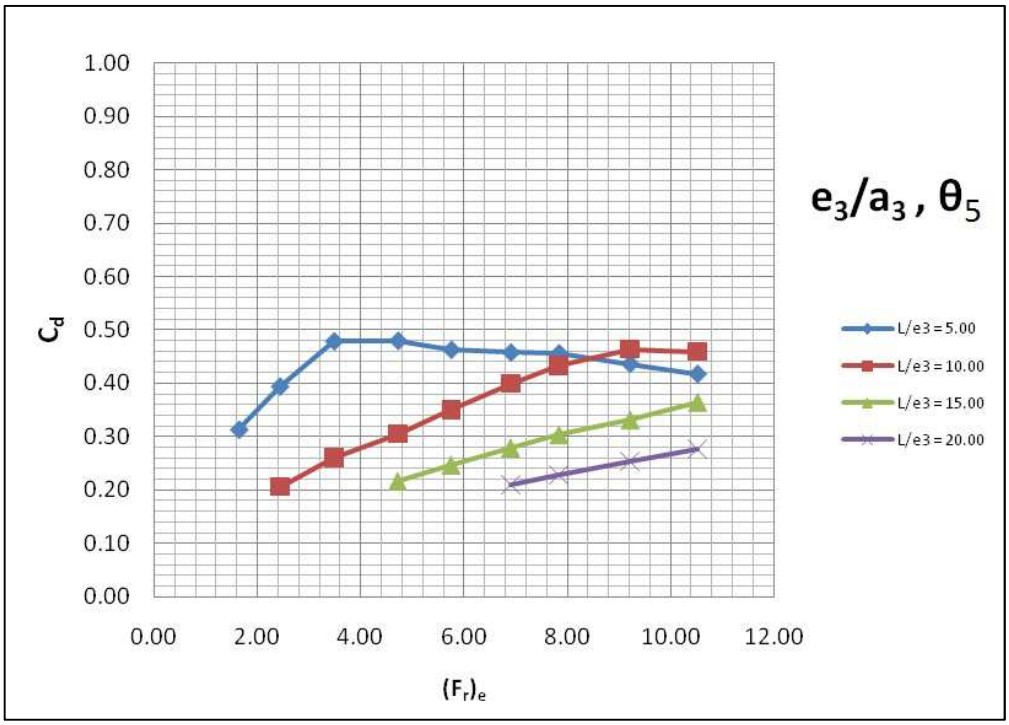


Figure 28 : $C_d$ vs $(Fr)_e$ for $e_3/a_3$ = 0.5 and $\theta_5$ = 32.800°(Şahiner,2012)

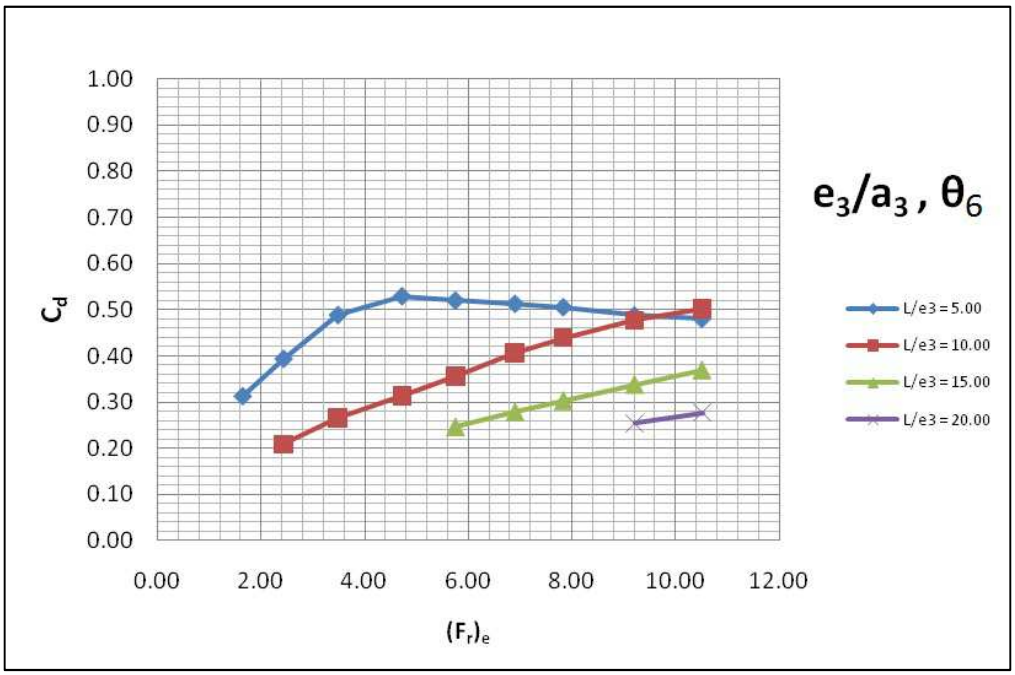


Figure 29 : $C_d$ vs $(Fr)_e$ for $e_3/a_3$ = 0.5 and $\theta_6$ = 27.800°(Şahiner,2012)

Figures 30-47 show the relationship between water capture efficiency, $(q_w)_i$ / $(q_w)_T$, $(Fr)_e$ and $L/e$ for the screens of various $e/a$ and $\theta$. The following conclusions were drawn from these figures;

- For the screens of known $L/e$ and angle of inclination $\theta$, as $(Fr)_e$ increases, water capture efficiency $(q_w)_i$ / $(q_w)_T$ decreases.

- When $L/e$ value becomes higher than about 83, $(q_w)_i$ / $(q_w)_T$ becomes almost independent of $(Fr)_e$ and approaches to 1.0.

- When $(Fr)_e$ and $L/e$ are constant, an increase in rack inclination causes a decrease in $(q_w)_i$ / $(q_w)_T$.

For a Tyrolean weir, when angle of inclination $(\theta)$ , rack opening $(e)$, rack length $(L)$ and total discharge $(q_w)_T$ are given, water capture efficiency $(q_w)_i$ / $(q_w)_T$ and $(q_w)_i$ can be calculated by following the steps given in the chart below.

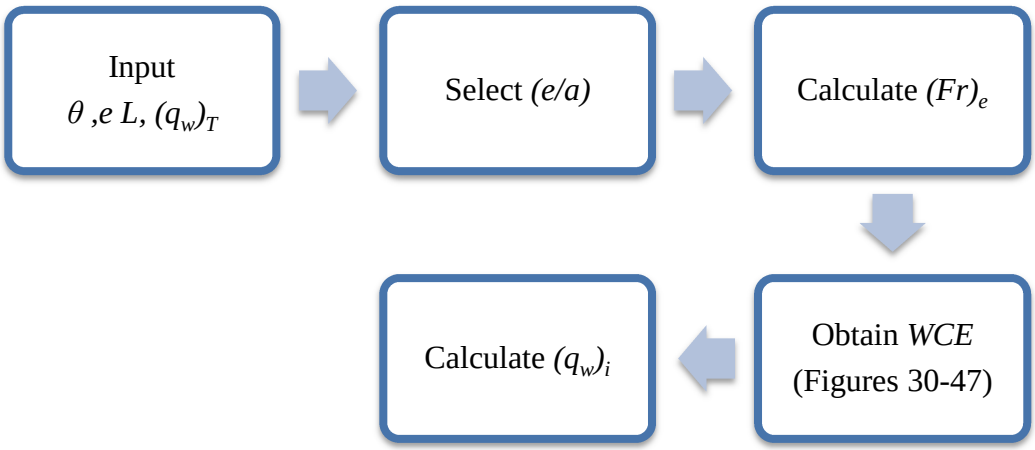

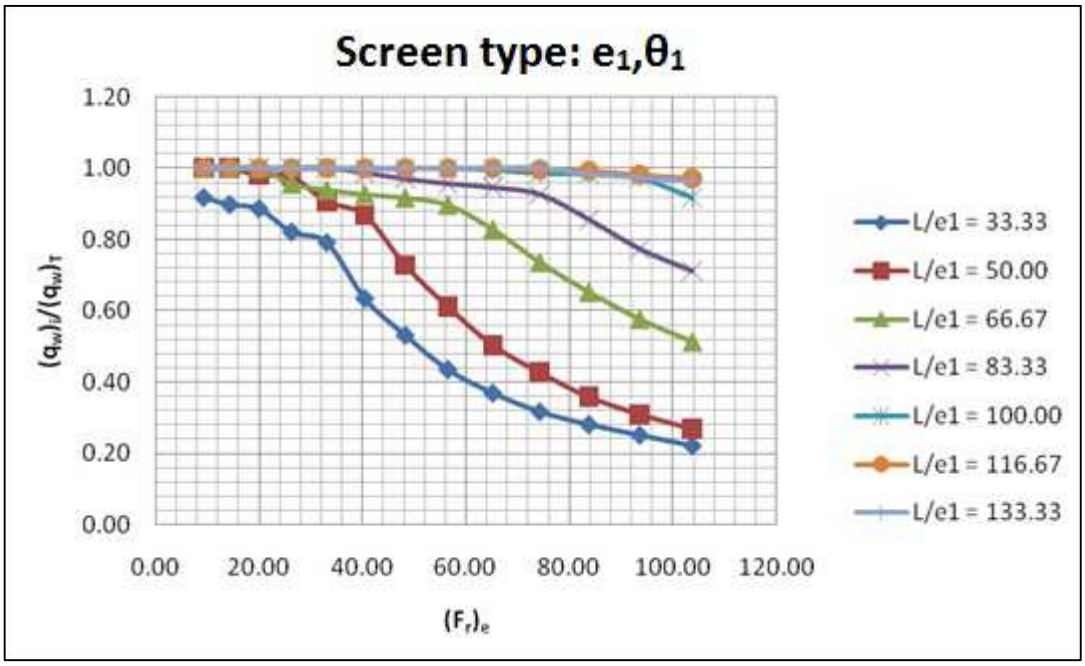


Figure 30 : $(q_w)_i/(q_w)_T$ vs $(Fr)_e$ for $e_1/a_1$ = 0.23 and $\theta_1$ = 14.477° (Yılmaz,2010)

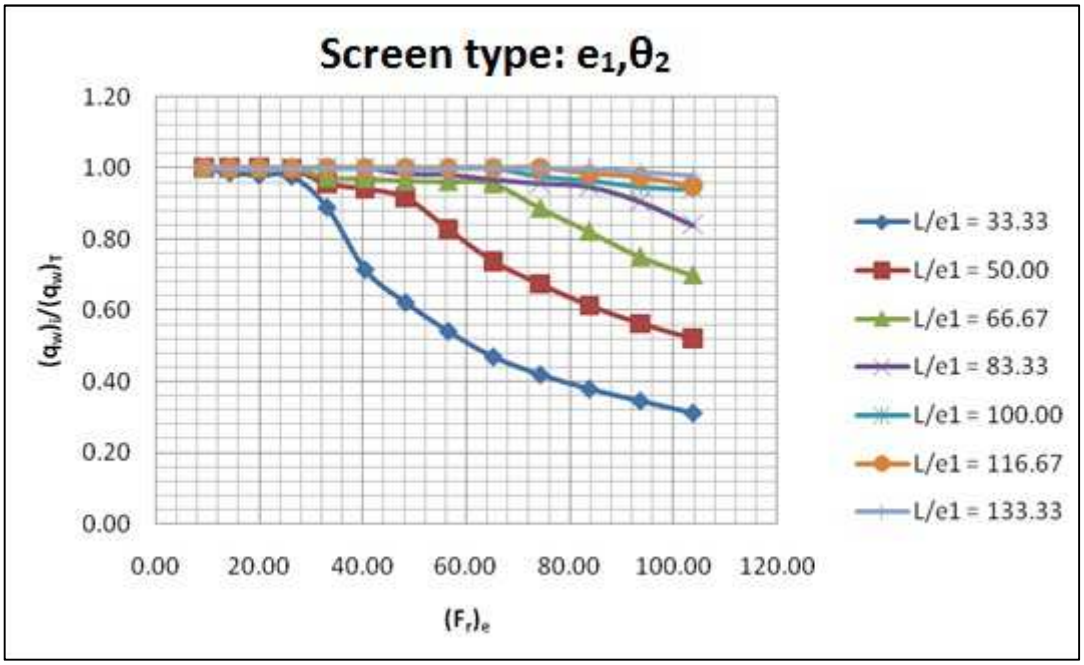


Figure 31 : $(q_w)_i/(q_w)_T$ vs $(Fr)_e$ for $e_1/a_1$ = 0.23 and $\theta_2$ = 9.594° (Yılmaz,2010)

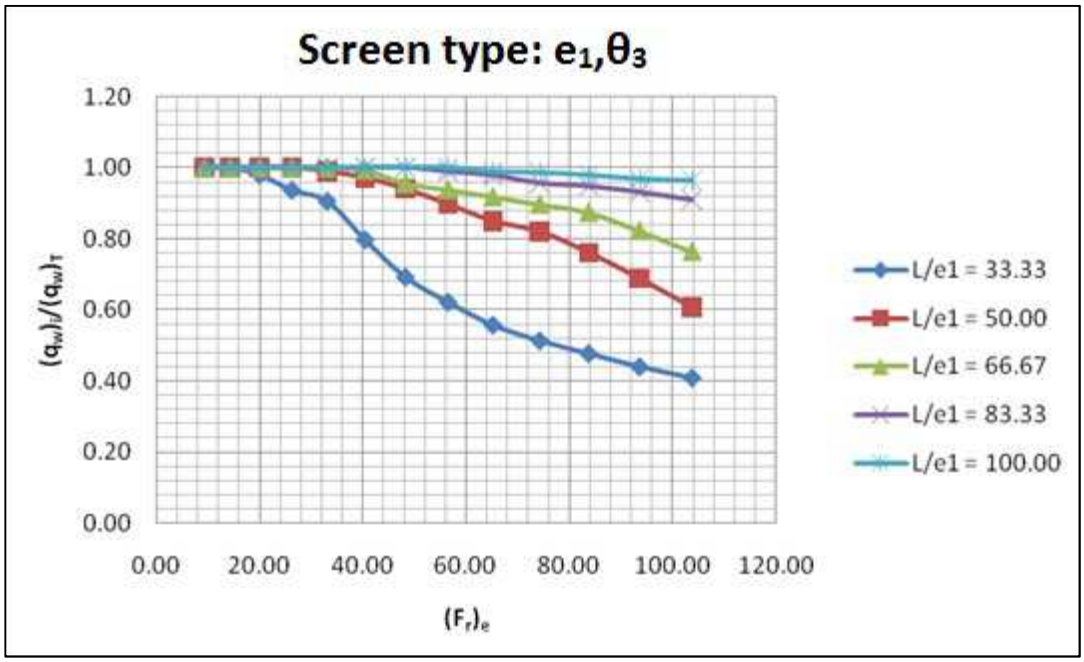


Figure 32 : $(q_w)_i/(q_w)_T$ vs $(Fr)_e$ for $e_1/a_1$ = 0.23 and $\theta_3$ = 4.480° (Yılmaz,2010)

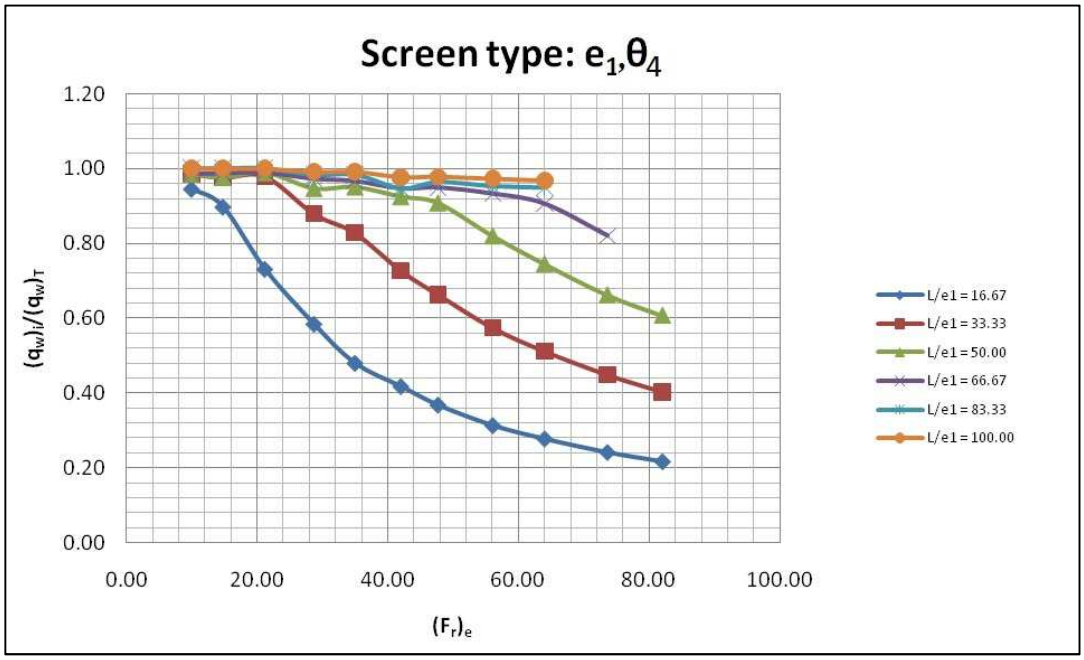


Figure 33 : $(q_w)_i/(q_w)_T$ vs $(Fr)_e$ for $e_1/a_1$ = 0.23 and $\theta_4$ = 37.000°(Şahiner,2012)

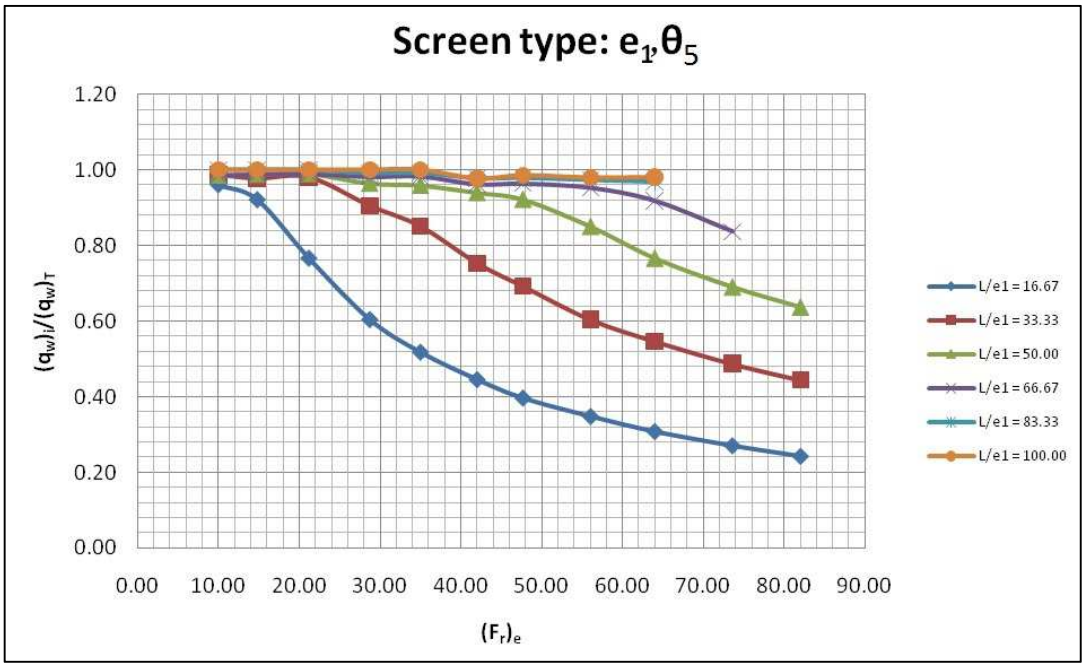


Figure 34 : $(q_w)_i/(q_w)_T$ vs $(Fr)_e$ for $e_1/a_1$ = 0.23 and $\theta_5$ = 32.800°(Şahiner,2012)

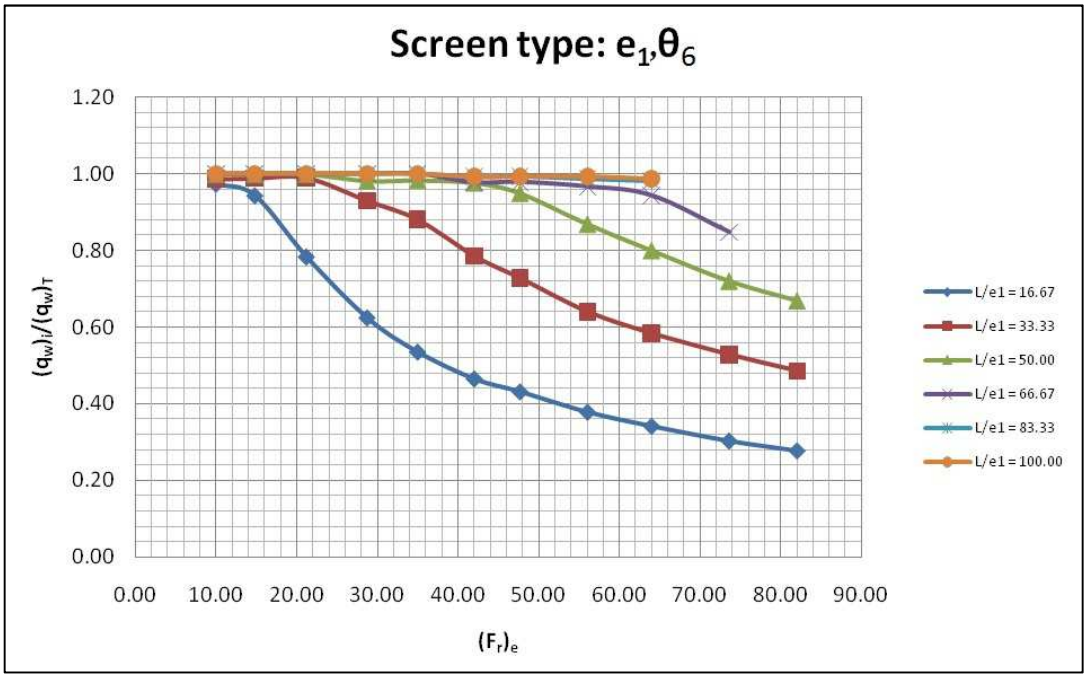


Figure 35 : $(q_w)_i/(q_w)_T$ vs $(Fr)_e$ for $e_1/a_1$ = 0.23 and $\theta_6$ = 27.800°(Şahiner,2012)

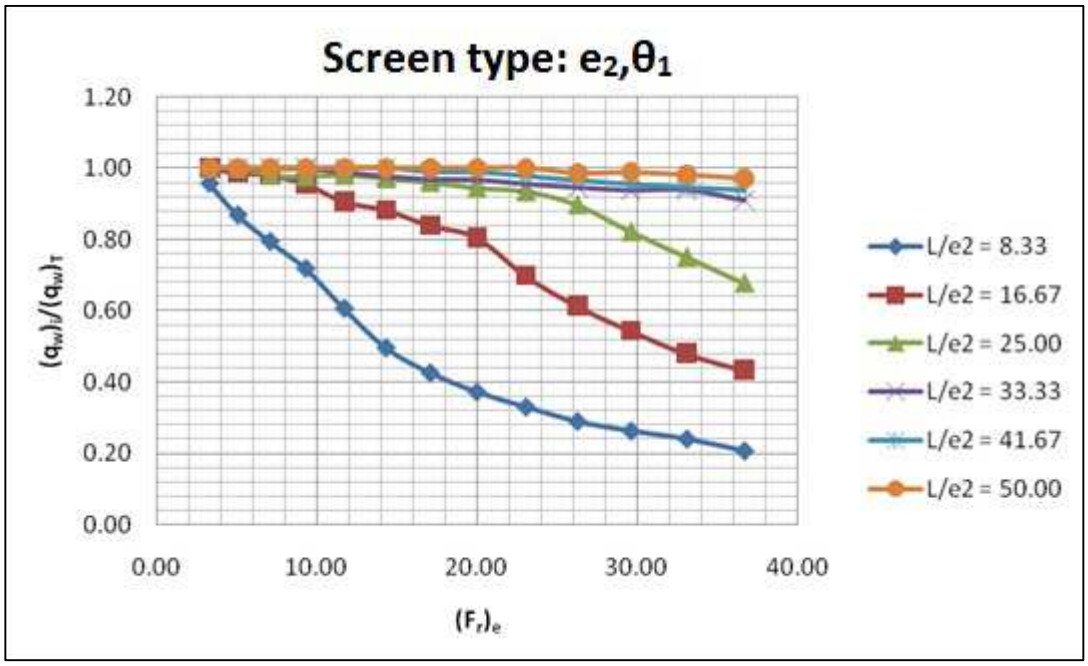


Figure 36 : $(q_w)_i/(q_w)_T$ vs $(Fr)_e$ for $e_2/a_2$ = 0.375 and $\theta_1$ = 14.477° (Yılmaz,2010)

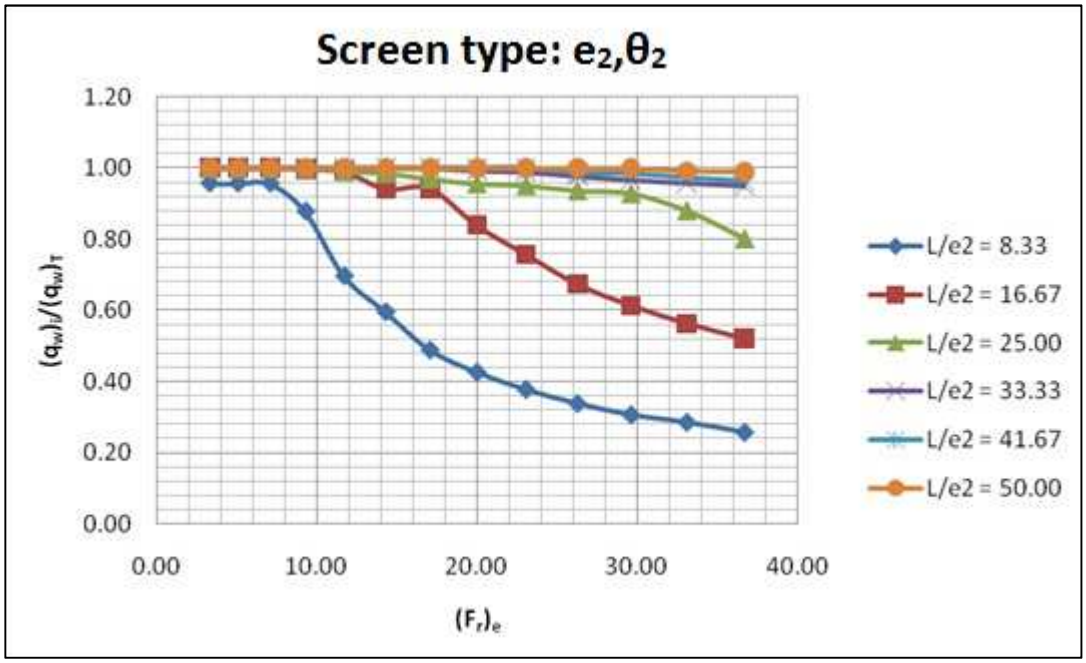


Figure 37 : $(q_w)_i/(q_w)_T$ vs $(Fr)_e$ for $e_2/a_2$ = 0.375 and $\theta_2$ = 9.594° (Yılmaz,2010)

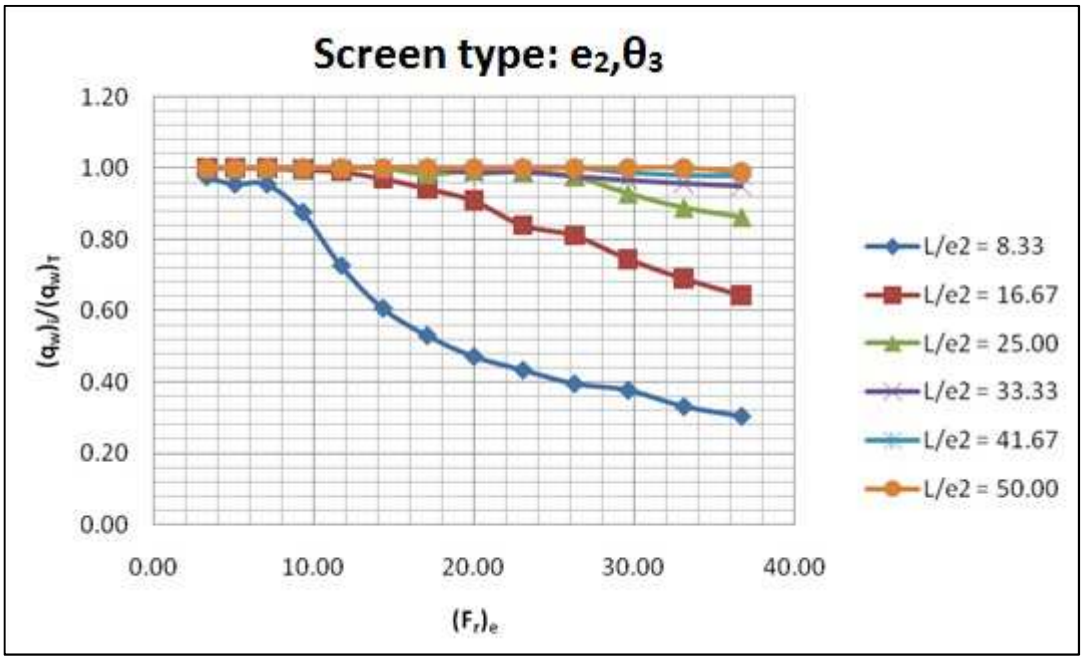


Figure 38 : $(q_w)_i/(q_w)_T$ vs $(Fr)_e$ for $e_2/a_2$ = 0.375 and $\theta_3$ = 4.480° (Yılmaz,2010)

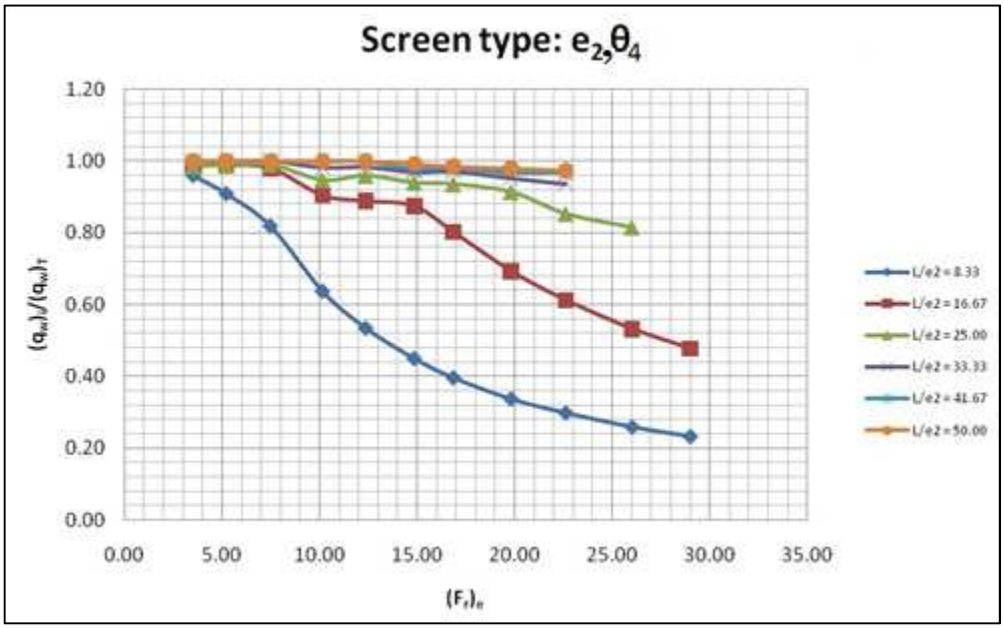


Figure 39 : $(q_w)_i/(q_w)_T$ vs $(Fr)_e$ for $e_2/a_2$ = 0.375 and $\theta_4$ = 37.000°(Şahiner,2012)

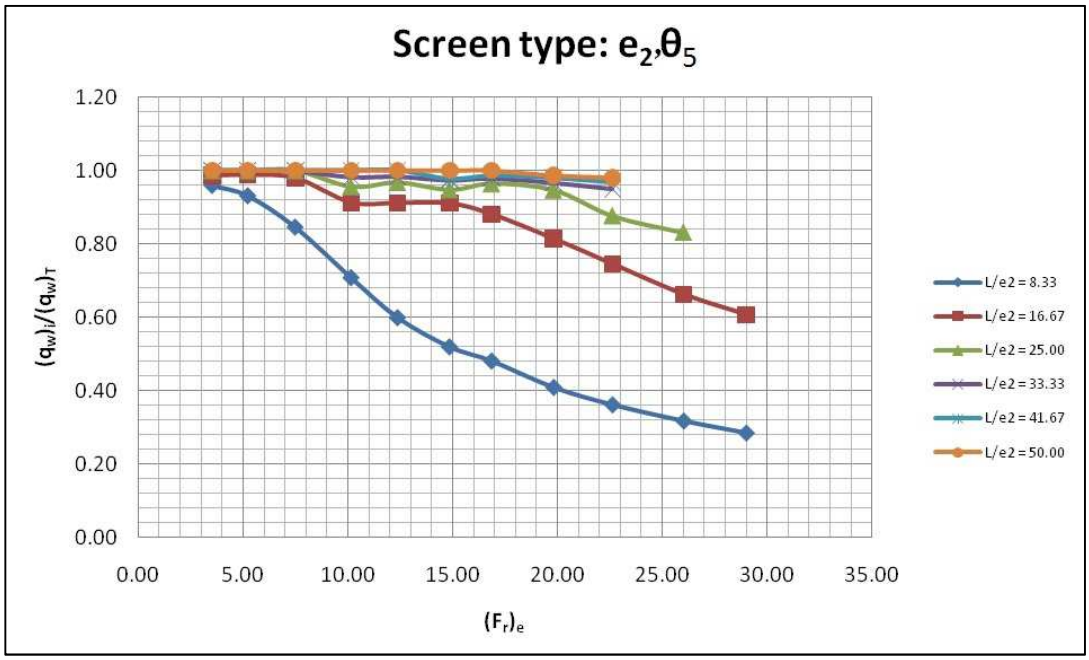


Figure 40 : $(q_w)_i/(q_w)_T$ vs $(Fr)_e$ for $e_2/a_2$ = 0.375 and $\theta_5$ = 32.800°(Şahiner,2012)

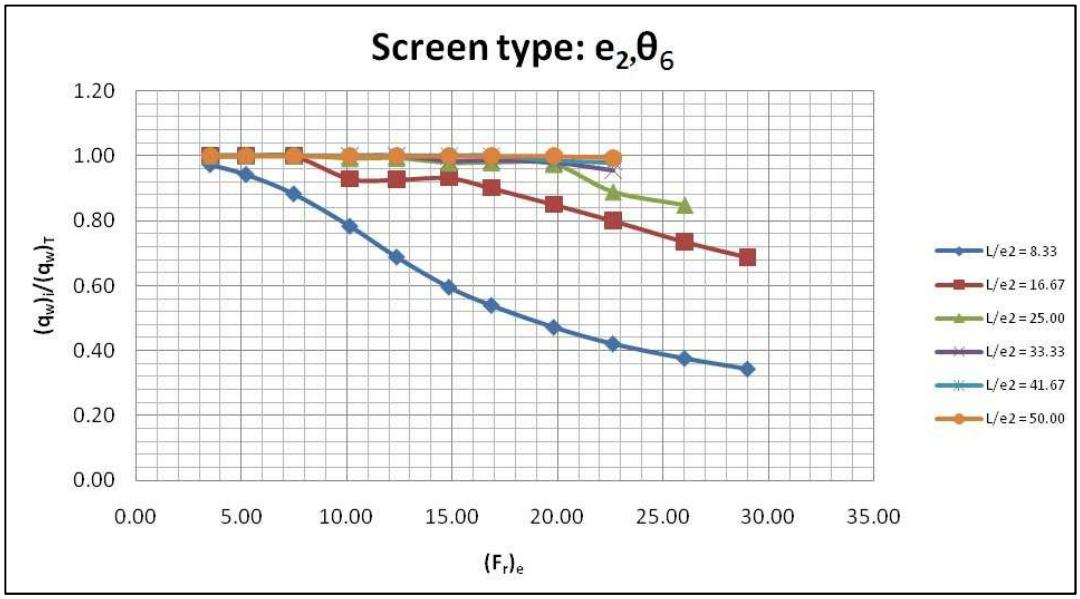


Figure 41 : $(q_w)_i/(q_w)_T$ vs $(Fr)_e$ for $e_2/a_2$ = 0.375 and $\theta_6$ = 27.800°(Şahiner,2012)

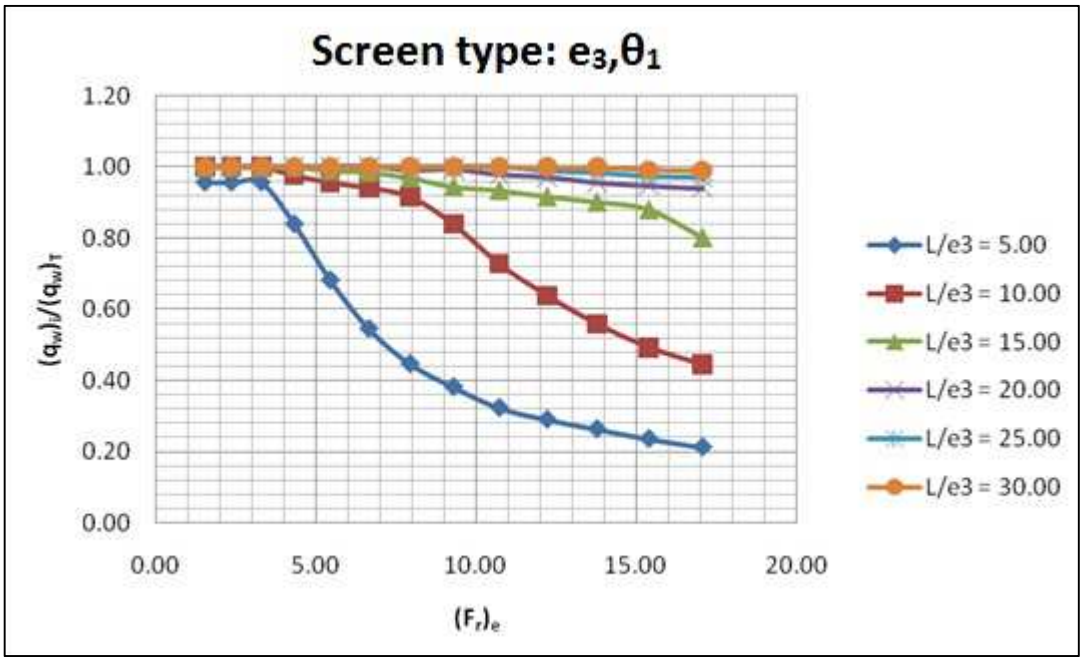


Figure 42 : $(q_w)_i/(q_w)_T$ vs $(Fr)_e$ for $e_3/a_3$ = 0.5 and $\theta_1$ = 14.477° (Yılmaz,2010)

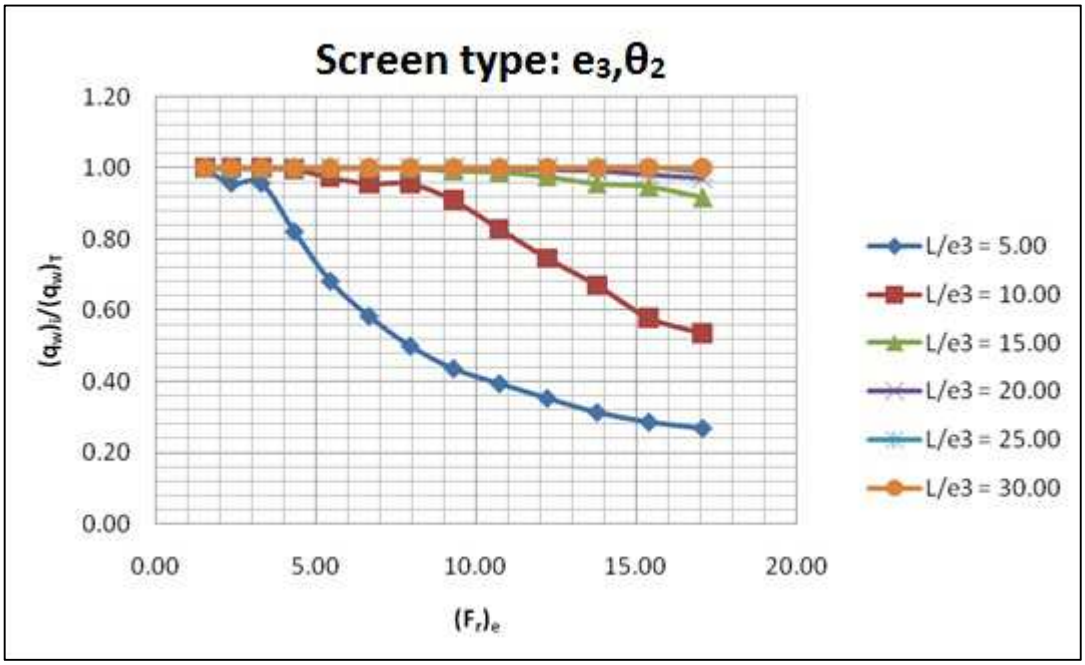


Figure 43 : $(q_w)_i/(q_w)_T$ vs $(Fr)_e$ for $e_3/a_3$ = 0.5 and $\theta_2$ = 9.594° (Yılmaz,2010)

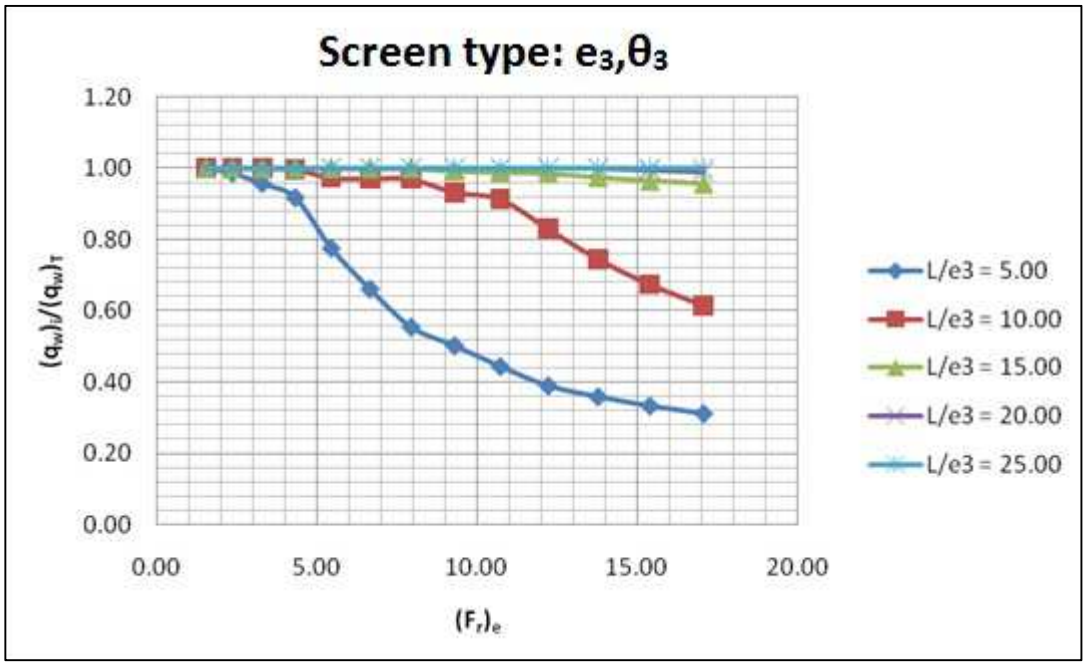


Figure 44 : $(q_w)_i/(q_w)_T$ vs $(Fr)_e$ for $e_3/a_3$ = 0.5 and $\theta_3$ = 4.480° (Yılmaz,2010)

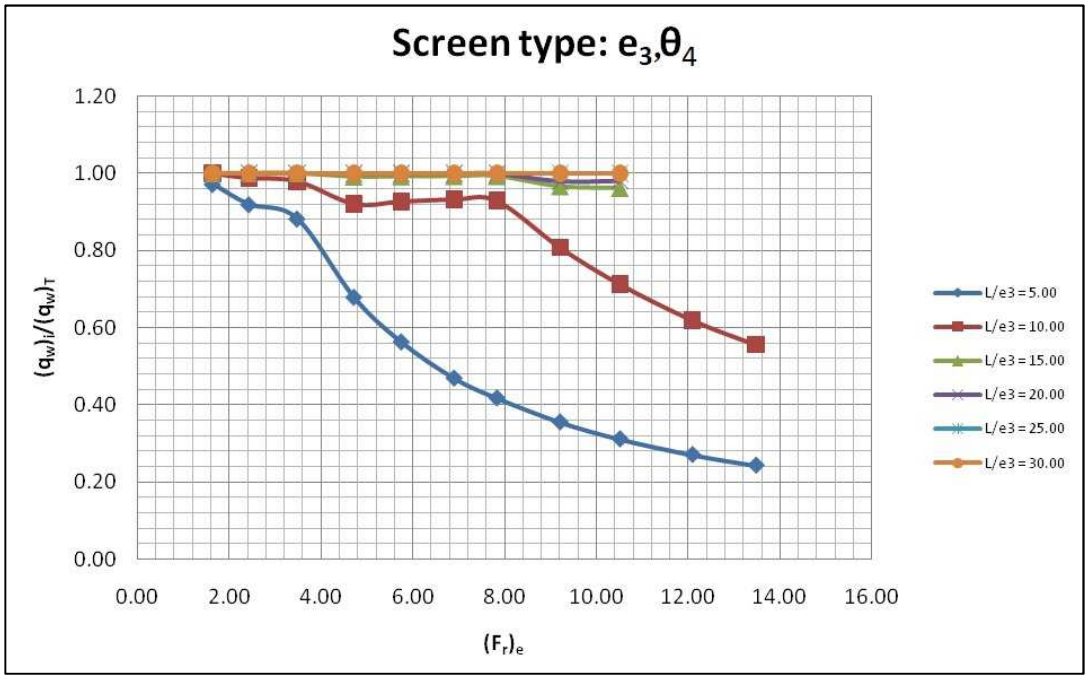


Figure 45 : $(q_w)_i/(q_w)_T$ vs $(Fr)_e$ for $e_3/a_3$ = 0.5 and $\theta_1$ = 37.000°(Şahiner,2012)

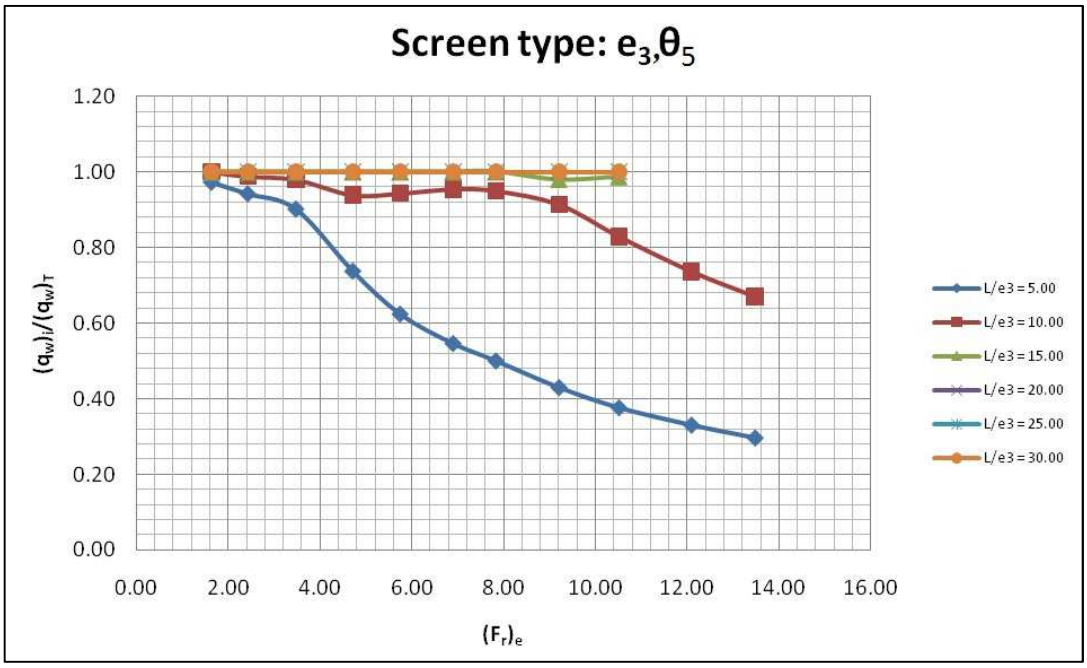


Figure 46 : $(q_w)_i/(q_w)_T$ vs $(Fr)_e$ for $e_3/a_3$ = 0.5 and $\theta_2$ = 32.800°(Şahiner,2012)

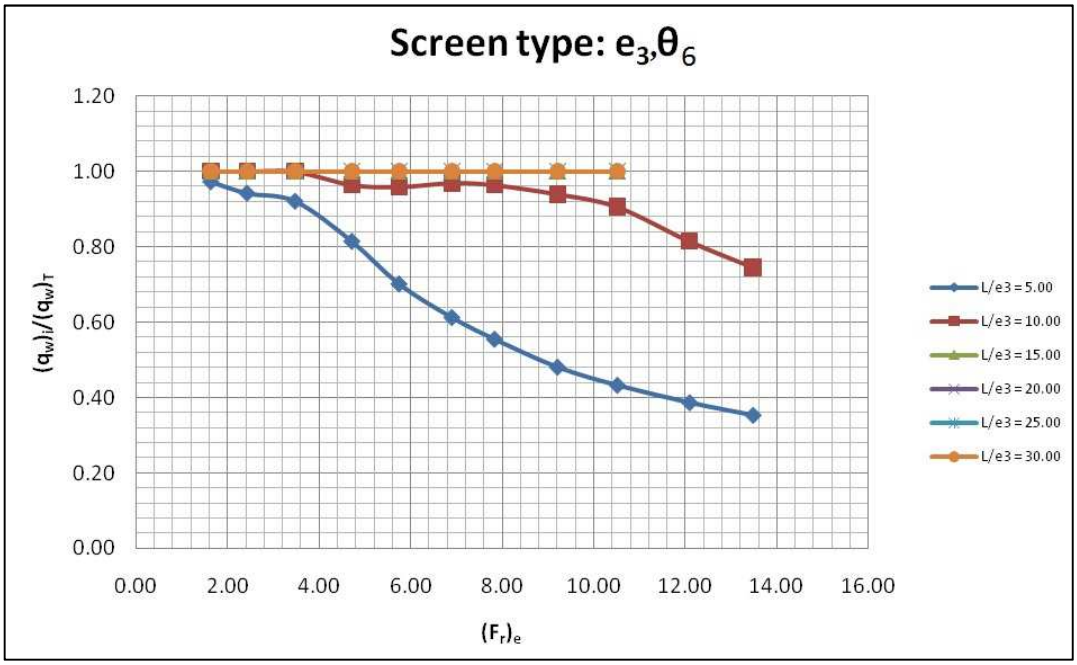


Figure 47 : $(q_w)_i/(q_w)_T$ vs $(Fr)_e$ for $e_3/a_3$ = 0.5 and $\theta_3$ = 27.800°(Şahiner,2012)

Figures 48-50 show the relationship between the dimensionless wetted rack length $L_2/e$ ($L_2$: the minimum required rack length to divert the desired amount of water) and $(Fr)_e$, as a function of $e/a$ and $\theta$. According to these figures the following conclusions can be made.

- Generally $L_2/e$ increases almost linearly with increasing value of $(Fr)_e$ for a given $\theta$.

- Variation of $L_2/e$ with $\theta$ for a given $(Fr)_e$ shows a complex trend.

When the angle of inclination $(\theta)$ , rack opening $(e)$, total incoming discharge $(q_w)_T$ are given, the wetted rack length $(L_2)$ can be calculated by following the steps given below.

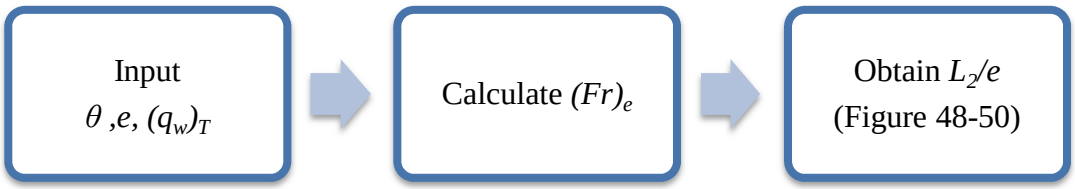

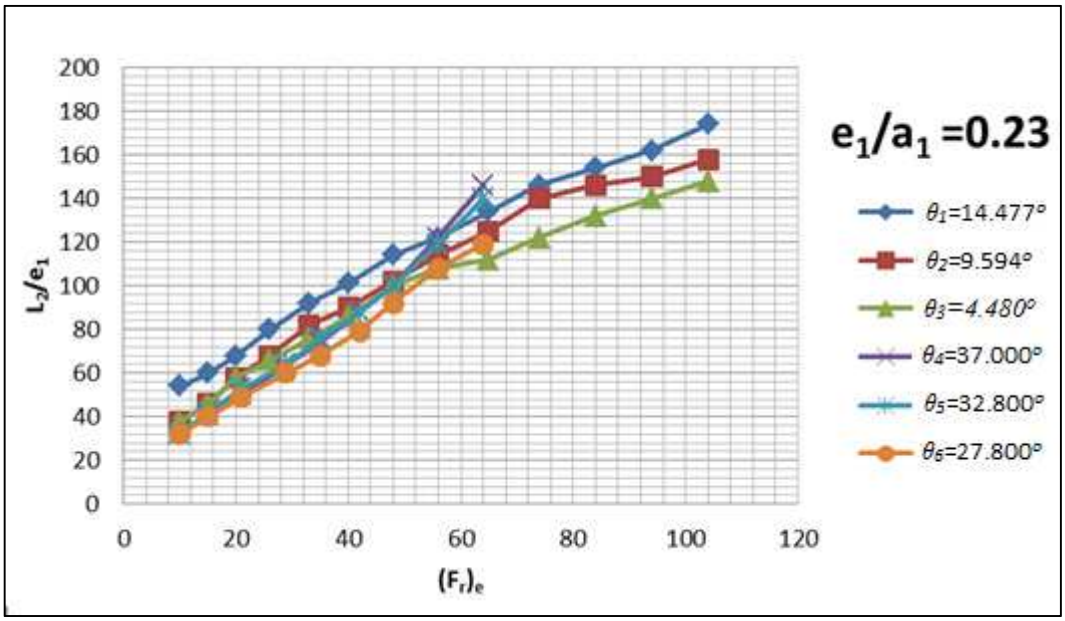


Figure 48 : $L_2/e_1$ vs $(Fr)_e$ for variations of $\theta$ for $e_1/a_1$ = 0.23 (Yılmaz,2010; Şahiner,2012)

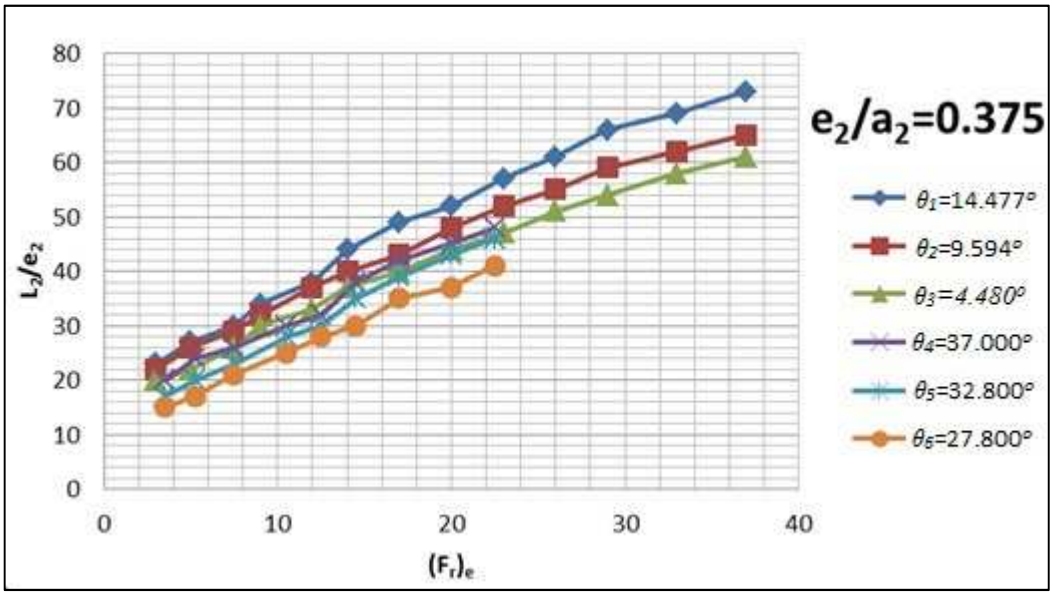


Figure 49 : $L_2/e_1$ vs $(Fr)_e$ for variations of $\theta$ for $e_2/a_2$ = 0.375 (Yılmaz,2010; Şahiner,2012)

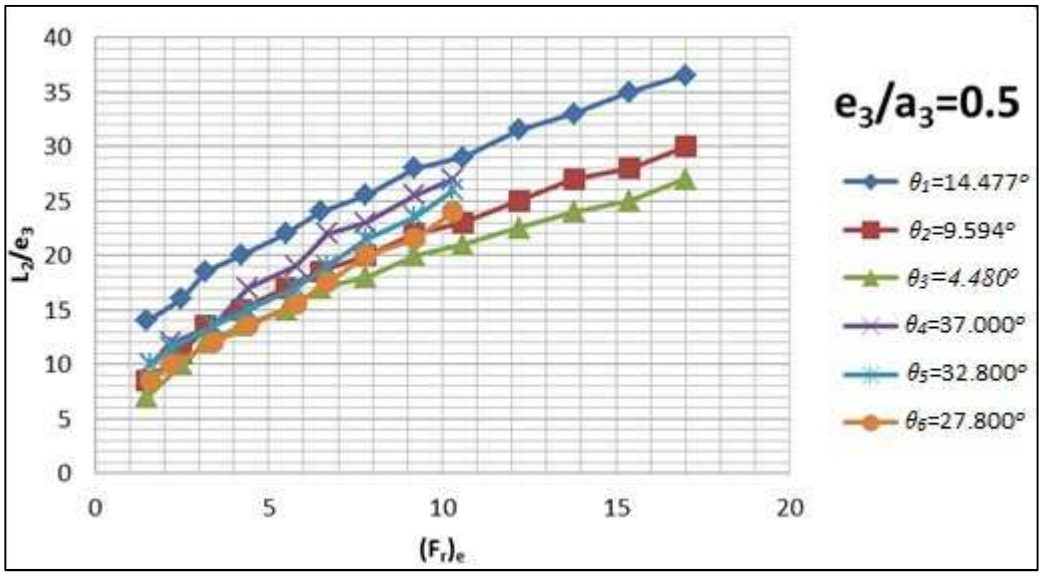


Figure 50 : $L_2/e_1$ vs $(Fr)_e$ for variations of $\theta$ for $e_3/a_3$ = 0.5 (Yılmaz,2010; Şahiner,2012)

# CHAPTER 4

## COMPARISON OF THE METHODS OBTAINED FROM THEORETICAL AND EXPERIMENTAL STUDIES

### 4.1 Introduction

The numerical comparison of the theoretical and experimental solution methods are presented in this chapter. The theoretical solutions can be applied for any design parameters, while the method obtained from experimental studies have limited ranges for various parameters.

A numerical example given below will be solved by using both methods.

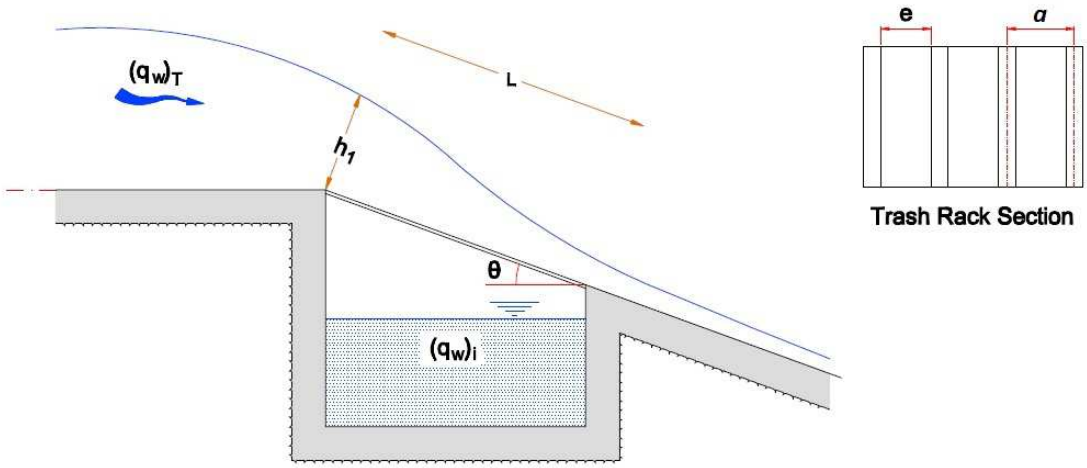


Figure 51 : Sketch for Tyrolean weir design example

$(q_w)_T$=0.50 $m^3$/s/m $L$ = 1.0 m $e$ = 20.0 mm

$h_1$=0.20 m $\theta$ = 32.8$^o$ $a$ = 86.9 mm

Total discharge $(q_w)_T$ of the Tyrolean weir shown in Figure 51 is 0.50 $m^3/s/m$. If the flow depth at the head of the trash rack $(h_1)$ is 0.20 m, the length of the trash rack $(L)$ is 1.0 m, the inclination of the trash rack $(\theta)$ is 32.8° and a and e values of the rack bars are 86.9 mm and 20.0 mm, respectively, calculate the diverted discharge $(q_w)_i$ and the flow depth at the end of the trash rack.

## 4.2 Theoretical Solutions

### 4.2.1 Constant Energy Level Hypothesis

**a) <u>Iterative Solution</u>**

Iterative solution is proceeded by dividing the trash rack into several intervals. In this problem the trash rack divided into 4 equal intervals with 0.25 m length.

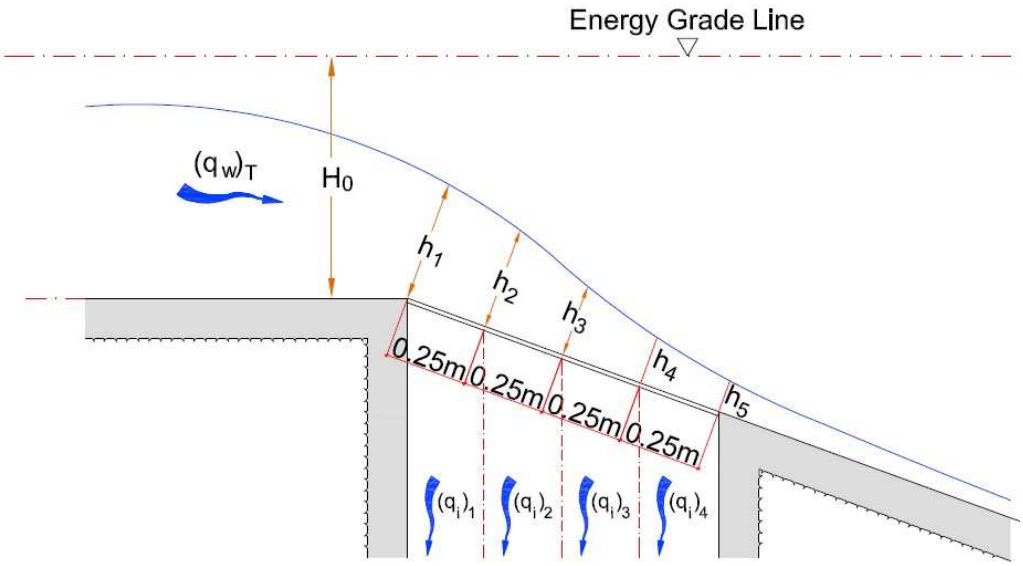


Figure 52 : Constant energy level approach iterative solution sketch

$$(q_w)_T = h_1\sqrt{2g(H_o - h_1\cos\theta)}$$

$$0.5 = 0.20\times\sqrt{2\times 9.81\times(H_o - 0.20\times\cos 32.8)}$$

$$H_o = 0.49m$$

Computation for the first interval

In the first stage, the diverted discharge $(q_w)_{i1}$ in the first 0.25 m interval and the flow depth $h_2$ are computed.

$$(q_w)_{i1} = \lambda\sqrt{h_{ave}}.\Delta x,\ h_{ave} = \frac{h_1 + h_2}{2} \text{ and } \lambda = \psi\mu_s\sqrt{2g\cos\theta}$$

$$\psi = \frac{e}{a} = \frac{20}{86.9} = 0.23$$

$$\mu_s = 0.66\psi^{-0.16}\left(\frac{a}{h_{ave}}\right)^{0.13} = 0.66\times 0.23^{-0.16}\times\left(\frac{0.0869}{h_{ave}}\right)^{0.13} = \frac{0.608}{h_{ave}^{0.13}}$$

First iteration, assume $h_2$=0.15 m

$$h_{ave} = \frac{h_1 + h_2}{2} = \frac{0.20 + 0.15}{2} = 0.175m$$

$$\mu_s = \frac{0.608}{0.175^{0.13}} = 0.763$$

$$\lambda = 0.23\times 0.763\times\sqrt{2\times 9.81\times\cos 32.8} = 0.713$$

$$(q_w)_{i.1} = 0.713\times\sqrt{0.175}\times 0.25 = 0.075m^3/m/s$$

$$(q_w)_1 = (q_w)_T - (q_w)_{i1} = 0.5 - 0.075 = 0.425m^3/m/s$$

$(q_w)_1$ is the remaining discharge that moves towards downstream after the first interval.

The assumption made is to be checked considering that the energy grade line is constant.

$$(q_w)_1 = h_2\sqrt{2g(H_o + \Delta x \sin\theta - h_2\cos\theta)}$$

$$0.425 = h_2\sqrt{2\times 9.81\times(0.49 + 0.25\times\sin 32.8 - h_2\cos 32.8)}$$

$$h_2 = 0.135m \neq 0.15m$$

Second iteration, assume $h_2$ = 0.135 m

$$h_{ave} = \frac{h_1 + h_2}{2} = \frac{0.20 + 0.135}{2} = 0.168m$$

$$\mu_s = \frac{0.443}{0.168^{0.13}} = 0.767$$

$$\lambda = 0.23\times 0.767\times\sqrt{2\times 9.81\times\cos 32.8} = 0.716$$

$$(q_w)_{i1} = 0.716\times\sqrt{0.168}\times 0.25 = 0.073m^3/m/s$$

$$(q_w)_1 = (q_w)_T - (q_w)_{i1} = 0.5 - 0.073 = 0.427m^3/m/s$$

$$(q_w)_1 = h_2\sqrt{2g(H_o + \Delta x \sin\theta - h_2\cos\theta)}$$

$$0.427 = h_2\sqrt{2\times 9.81\times(0.49 + 0.25\times\sin 32.8 - h_2\cos 32.8)}$$

$h_2 = 0.135m$ (assumption is converged)

So, in the first 0.25 m interval 0.073 $m^3$/s/m discharge is diverted and the remaining discharge $(q_w)_1$ 0.427 $m^3$/s/m moves towards downstream. The flow depth $h_2$ was verified as 0.135 m.

Computation for the second interval

First iteration, assume $h_3$=0.120 m,

$$h_{ave} = \frac{h_2 + h_3}{2} = \frac{0.135 + 0.120}{2} = 0.128m$$

$$\mu_s = \frac{0.608}{0.128^{0.13}} = 0.794$$

$$\lambda = 0.23 \times 0.794 \times \sqrt{2 \times 9.81 \times \cos 32.8} = 0.742$$

$$(q_w)_{i2} = 0.742 \times \sqrt{0.128} \times 0.25 = 0.066 m^3/m/s$$

$$(q_w)_2 = (q_w)_1 - (q_w)_{i2} = 0.427 - 0.066 = 0.361 m^3/m/s$$

$$(q_w)_2 = h_3 \sqrt{2g(H_o + 2\Delta x \sin\theta - h_3 \cos\theta)}$$

$$0.361 = h_3 \sqrt{2 \times 9.81 \times (0.49 + 2 \times 0.25 \times \sin 32.8 - h_3 \cos 32.8)}$$

$$h_3 = 0.100 \neq 0.120m$$

By assuming $h_3$=0.100 the same procedure is followed and verification is made. Final values are found as;

$$h_3 = 0.100m$$

$(q_w)_{i2} = 0.064 m^3/s/m$ (diverted discharge in the 2nd interval)

$(q_w)_2 = 0.363 m^3/s/m$ (remaining discharge after the 2nd interval)

The same computations are made for each interval and the outcome is given below.

Computation for the third interval

$h_4 = 0.075m$

$(q_w)_{i3} = 0.058m^3/s/m$ (diverted discharge in the 3rd interval)

$(q_w)_3 = 0.305m^3/s/m$ (remaining discharge after the 3rd interval)

Computation for the forth interval

$h_5 = 0.058m$

$(q_w)_{i4} = 0.052m^3/s/m$ (diverted discharge in the 4th interval)

$(q_w)_{out} = 0.253m^3/s/m$ (remaining discharge after the 4th interval, end of the trash rack)

So water diverted to the collection channel can be summed up,

$(q_w)_i = (q_w)_{i1} + (q_w)_{i2} + (q_w)_{i3} + (q_w)_{i4}$

$(q_w)_i = 0.073 + 0.064 + 0.058 + 0.052 = 0.247m^3/s/m$

Discharge that passes over the trash rack and moves towards downstream is $(q_w)_{out}$=0.253 $m^3$/s/m.

Flow depth at the end of the trash rack $h_5$=0.058m.

**b) Closed Form Solution**

$(q_w)_T = 0.5m^3/s/m$ and $h_1 = 0.20m$

$\lambda = \psi\mu_s\sqrt{2g\cos\theta}$, $\psi = \frac{e}{a} = \frac{20}{86.9} = 0.23$

$$\mu_s = 0.66\psi^{-0.16}\left(\frac{a}{h_1}\right)^{0.13} = 0.66\times 0.23^{-0.16}\times\left(\frac{0.0869}{0.20}\right)^{0.13} = 0.749$$

$$\lambda = 0.23\times 0.749\times.\sqrt{2\times 9.81\times\cos 32.8} = 0.700$$

Flow length over the trash rack is computed as

$$L = 2.561\frac{(q_w)_T}{\lambda\sqrt{h_1}} = 2.561\frac{0.5}{0.700\sqrt{0.20}} = 4.09m > 1m$$

It is seen that, some portion of the incoming discharge is diverted to the collection channel while the remaining discharge flows towards downstream. To determine the diverted discharge $(q_w)_i$, the depth at the end of trash rack $h_2$ is to be calculated.

$$\frac{s^2}{L^2} = 2\frac{h_2}{h_1} - \frac{h_2^{\,2}}{h_1^{\,2}},\ s = 4.09 - 1 = 3.09m$$

$$\frac{3.09^2}{4.09^2} = 2\frac{h_2}{0.20} - \frac{h_2^{\,2}}{0.20^2},\ h_2 = 0.069m$$

After completing calculation of $h_2$

$$(q_w)_i = 1.707(q_w)_T\left[2-\left(1+\frac{h_2}{h_1}\right)\left(\sqrt{2-\frac{h_2}{h_1}}\right)\right]$$

$$(q_w)_i = 1.707(q_w)_T\left[2-\left(1+\frac{0.069}{0.20}\right)\left(\sqrt{2-\frac{0.069}{0.20}}\right)\right]$$

$$(q_w)_i = 0.230m^3/s/m$$

$$(q_w)_{out} = 0.270m^3/s/m$$

### 4.2.2 Constant Energy Head Hypothesis

#### a) Iterative Solution

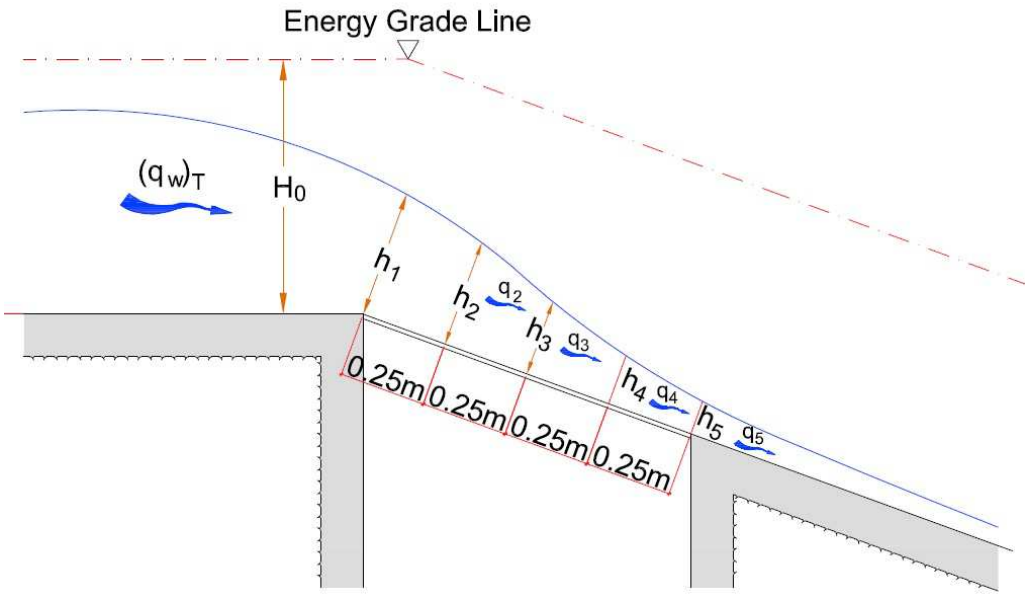


Figure 53 : Constant energy head approach iterative solution sketch

In iterative solution, the depth of the flow in each interval must be computed to determine the flow condition. Calculations are made in two stages. In the first stage, the flow depths and in the second stage, the discharge that passes over each interval will be calculated.

Calculation of $h_2$

$$\Delta x = \frac{H_0}{\mu_s \psi}\left[\phi\left(\frac{h_2}{H_0}\right) - \phi\left(\frac{h_1}{H_0}\right)\right]$$

$$\mu_s = 0.66\psi^{-0.16}\left(\frac{a}{h_1}\right)^{0.13} = 0.66\times 0.23^{-0.16}\times\left(\frac{0.0869}{0.20}\right)^{0.13} = 0.749$$

$$H_o = 0.49m,\ h_1 = 0.20m,\ \psi = \frac{e}{a} = \frac{20}{86.9} = 0.23$$

$$0.25 = \frac{0.49}{0.749 \times 0.23}\left[\phi\left(\frac{h_2}{0.49}\right) - \phi\left(\frac{0.20}{0.49}\right)\right]$$

$\phi$ function can be solved by using the related equation or with the help of Table 1.

$$\phi\left(\frac{0.20}{0.49}\right) = \frac{1}{2} \times \arccos\sqrt{\frac{0.20}{0.49}} - \frac{3}{2} \times \sqrt{\frac{0.20}{0.49} \times \left(1 - \frac{0.20}{0.49}\right)} = -0.300$$

$\phi\left(\frac{h_2}{0.49}\right) = -0.212$, by matching Table 1 or iterating from equations; $\left(\frac{h_2}{0.49}\right) = 0.314$,

$h_2 = 0.154m$

Calculation of $h_3$

$$\Delta x = \frac{H_0}{\mu_s \psi}\left[\phi\left(\frac{h_3}{H_0}\right) - \phi\left(\frac{h_2}{H_0}\right)\right]$$

$$0.25 = \frac{0.49}{0.749 \times 0.23}\left[\phi\left(\frac{h_3}{0.49}\right) - \phi\left(\frac{0.154}{0.49}\right)\right],\ \phi\left(\frac{0.154}{0.49}\right) = -0.212,$$

$$\phi\left(\frac{h_3}{0.49}\right) = -0.123,\ h_3 = 0.121m$$

Calculation of $h_4$

$$\Delta x = \frac{H_0}{\mu_s \psi}\left[\phi\left(\frac{h_4}{H_0}\right) - \phi\left(\frac{h_3}{H_0}\right)\right]$$

$$0.25 = \frac{0.49}{0.749 \times 0.23}\left[\phi\left(\frac{h_4}{0.49}\right) - \phi\left(\frac{0.121}{0.49}\right)\right],\ \phi\left(\frac{0.121}{0.49}\right) = -0.123,$$

$$\phi\left(\frac{h_4}{0.49}\right) = -0.034,\ h_4 = 0.094m$$

Calculation of $h_5$

$$\Delta x = \frac{H_0}{\mu_s \psi}\left[\phi\left(\frac{h_4}{H_0}\right) - \phi\left(\frac{h_3}{H_0}\right)\right]$$

$$0.25 = \frac{0.49}{0.749 \times 0.23}\left[\phi\left(\frac{h_5}{0.49}\right) - \phi\left(\frac{0.094}{0.49}\right)\right],\ \phi\left(\frac{0.094}{0.49}\right) = -0.034$$

$$\phi\left(\frac{h_5}{0.49}\right) = 0.055,\ h_5 = 0.072m$$

Flow depths ($h_1$, $h_2$, $h_3$, $h_4$, $h_5$) are calculated.

In the second step the discharges will be calculated and the flow depth found in the first step will be used to check the flow condition.

Calculation of $q_2$

$$\Delta x = \frac{H_0}{\mu_s \psi}\left[\beta\left(\frac{q_2}{q_{\max}}\right) - \beta\left(\frac{q_1}{q_{\max}}\right)\right]$$

$$q_{\max} = 1.705 \times {H_0}^{3/2} = 1.705 \times 0.49^{3/2} = 0.580 m^3/s/m$$

$\beta$ function can be solved by using the related equation or with the help of Table 1. But to solve $\beta$ function, first the flow condition must be determined.

$$h_{cr} = \sqrt[3]{\frac{{q_1}^2}{g}} = \sqrt[3]{\frac{0.5^2}{9.81}} = 0.294m,\ h_{cr} > h_1 = 0.20m$$, flow is supercritical.

$$\beta\left(\frac{q_1}{q_{\max}}\right)=\frac{1}{2}\times\arccos\left(\frac{1}{\sqrt{3}}\times\sqrt{2\cos\varphi+1}\right)-\frac{\sqrt{2}}{2}\times\sqrt{(2\cos\varphi+1)\times(1-\cos\varphi)}$$

$$\varphi=\frac{1}{3}\times\arccos\left(1-2\times\left(\frac{0.5}{0.580}\right)^2\right)+240^o=279.74^o$$

$\beta\left(\frac{q_1}{q_{\max}}\right)=-0.327,\quad \beta\left(\frac{q_2}{q_{\max}}\right)=-0.237,$ by matching Table 1 or iterating from equations.

$$\frac{q_2}{q_{\max}}=0.720m^3/s/m\,,q_2=0.417m^3/s/m$$

Calculation of $q_3$

$$\Delta x=\frac{H_0}{\mu_s\psi}\left[\beta\left(\frac{q_3}{q_{\max}}\right)-\beta\left(\frac{q_2}{q_{\max}}\right)\right]$$

$h_{cr}=\sqrt[3]{\frac{{q_2}^2}{g}}=\sqrt[3]{\frac{0.417^2}{9.81}}=0.261m,\ h_{cr}>h_2=0.154m$, flow is supercritical.

$$\varphi=\frac{1}{3}\times\arccos\left(1-2\times\left(\frac{0.417}{0.580}\right)^2\right)+240^o=270.64^o$$

$\beta\left(\frac{q_2}{q_{\max}}\right)=-0.237,\quad \beta\left(\frac{q_3}{q_{\max}}\right)=-0.148,$ by matching Table 1 or iterating from equations.

$$\frac{q_3}{q_{\max}}=0.592m^3/s/m\,,q_3=0.343m^3/s/m$$

Calculation of $q_4$

$$\Delta x = \frac{H_0}{\mu_s \psi}\left[\beta\left(\frac{q_4}{q_{\max}}\right) - \beta\left(\frac{q_3}{q_{\max}}\right)\right]$$

$h_{cr} = \sqrt[3]{\frac{q_3^{\,2}}{g}} = \sqrt[3]{\frac{0.343^2}{9.81}} = 0.229m,\ h_{cr} > h_3 = 0.121m$, flow is supercritical.

$$\varphi = \frac{1}{3} \times \arccos\left(1 - 2 \times \left(\frac{0.343}{0.580}\right)^2\right) + 240^o = 264.18^o$$

$\beta\left(\frac{q_3}{q_{\max}}\right) = -0.148,\quad \beta\left(\frac{q_4}{q_{\max}}\right) = -0.060,$ by matching Table 1 or iterating from equations.

$\frac{q_4}{q_{\max}} = 0.482 m^3/s/m$, $q_4 = 0.279 m^3/s/m$

Calculation of $q_5$

$$\Delta x = \frac{H_0}{\mu_s \psi}\left[\beta\left(\frac{q_5}{q_{\max}}\right) - \beta\left(\frac{q_4}{q_{\max}}\right)\right]$$

$h_{cr} = \sqrt[3]{\frac{q_4^{\,2}}{g}} = \sqrt[3]{\frac{0.279^2}{9.81}} = 0.199m,\ h_{cr} > h_4 = 0.094m$, flow is supercritical.

$$\varphi = \frac{1}{3} \times \arccos\left(1 - 2 \times \left(\frac{0.279}{0.580}\right)^2\right) + 240^o = 259.16^o$$

$\beta\left(\frac{q_4}{q_{\max}}\right) = -0.060, \quad \beta\left(\frac{q_5}{q_{\max}}\right) = 0.029,$ by matching Table 1 or iterating from equations.

$$\frac{q_5}{q_{\max}} = 0.382 m^3/s/m \, , q_5 = 0.221 m^3/s/m$$

$q_5$ is the amount of discharge that passes over the trash rack and moves towards downstream. By subtracting $q_5$ from the total discharge, the diverted discharge $(q_w)_i$ can be calculated.

$$(q_w)_i = (q_w)_T - q_5 = 0.5 - 0.221 = 0.279 m^3/s/m$$

**b) Closed Form Solution**

Closed form solution is not recommended for most cases because $C_c$ coefficient is selected as 0.497 for horizontal trash rack and 0.435 for the trash rack of inclination 0.2. This situation prevents obtaining exact results. Closed form solution of constant energy head approach is recommended only when horizontal trash rack is designed.

$$\frac{x}{H_0} = \frac{1}{C_c \mu_s}\left(\frac{h_1}{H_0}\sqrt{1-\frac{h_1}{H_0}} - \frac{h}{H_0}\sqrt{1-\frac{h}{H_0}}\right)$$

Inclination of trash rack is $32.8^o$ so $C_c$ is accepted as 0.435.

First the distance where the flow depth becomes zero must be determined. If it is less than the total length of the trash rack, it means that the total discharge is diverted to the collection channel. Otherwise, by taking $x$ as the full length of the trash rack, $h_2$ (flow depth at the end of the trash rack) is to be computed.

$$(q_w)_{out} = h_2\sqrt{2g(H_0 - h_2)}$$

So first h=0,

$$\frac{x}{0.49}=\frac{1}{0.435\times 0.749}\left(\frac{0.20}{0.49}\sqrt{1-\frac{0.20}{0.49}}-\frac{0}{0.49}\sqrt{1-\frac{0}{0.49}}\right)$$

$x$=0.471m

The flow length over the trash rack is 0.471 m and all incoming discharge is diverted into the collection channel.

$$(q_w)_i = 0.50 m^3/s/m$$

As mentioned above due to inaccurate value of $C_c$, exact results may not be obtained. Therefore, the closed form solution of constant energy head approach is not recommended unless the trash rack is horizontal.

### 4.2.3 Experimental Solution

Experimental solution is performed with the help of figures which are obtained as a result of the experiments given in Chapter 3.

Numerical examples are given below in order to show how to use the figures to design a Tyrolean weir. According to the given parameters two different approaches will be applied.

**1st Solution**

Given parameters:

$\theta$ = 32.8° , $e$ =2.0 cm ( $e/a$ = 0.23)

$L$ = 100 cm ( $L/e$ = 50.00 ) , and $(q_w)_T$ = 0.5 $m^2$/s

Determine $(q_w)_i$ and $L_2$

a) $Fr_e = (q_w)_T / (e^3 g)^{1/2} = 0.5 / ((0.02)^3 \times 9.81)^{1/2} = 56.44$

From Fig. 16 for $Fr_e = 56.44$ and $L/e = 50.00 \longrightarrow C_d = 0.60$

$e = 2.0$ cm , $e/a = 0.23 \longrightarrow a = 8.69$ cm

$\psi = 0.23$

For $(q_w)_T = 0.5$ m$^2$/s $\longrightarrow h_c = ( (q_w)_T^2 / g )^{1/3}$

$h_c = 0.294$ m

$H_c = 3/2\ h_c = 0.441$ m

$(q_w)_i = C_d \psi (2gH_c)^{1/2} = 0.60 \times 0.23 \times (2 \times 9.81 \times 0.441)^{1/2}$

$(q_w)_i = 0.41$ m$^2$/s

b) $Fr_e = (q_w)_T / (e^3 g)^{1/2} = 0.5 / ((0.02)^3 \times 9.81)^{1/2} = 56.44$

From Fig. 34 for $Fr_e = 56.44$ and $L/e = 50.00 \longrightarrow (q_w)_i / (q_w)_T = 0.84$

$(q_w)_i = 0.42$ m$^2$/s

c) From Figure 48 for $(Fr)_e = 56.44$ and $\theta = 32.8°$

$L_2/e = 120 \longrightarrow L_2 = 0{,}02 \times 120 = 2.40$ m

**2nd Solution**

Given parameters:

$\theta = 32.8°$ , $(q_w)_T = 0.50$ m$^2$/s , $(q_w)_i = 0.35$ m$^2$/s

Determine $e$ and $L$

a) Select $L/e = 50$ and $e/a = 0.23$

From Fig. 34 , for $(q_w)_i / (q_w)_T = 0.70 \longrightarrow (Fr)_e = 72$

$72 = (q_w)_T / (e^3 g)^{1/2} \longrightarrow e^3 = (0{,}50)^2 / 72^2 \times 9{,}81 \longrightarrow e = 0.017$ m

$L/e = 50 \longrightarrow L = 0.85$ m

$e/a = 0.23 \longrightarrow a = 0.074$

If $L/e = 33.33$ is selected;

From Fig. 34 $\longrightarrow$ for $(q_w)_i / (q_w)_T = 0.70 \longrightarrow (Fr)_e = 46$

$e^3 = (0.50)^2 / (46)^2 \times 9{,}81 \longrightarrow e = 0{,}023$ m

$L/e = 33.33 \longrightarrow L = 0.764$m

By using the same inputs the design of a Tyrolean weir is completed with 4 different theoretical and 1 experimental method. Comparison of the results of these methods are presented in Table 2. “Constant energy head closed form solution” is recommended for only horizontal trash racks. Because of this reason results of this method is not given in comparisons. The method based on the experimental results gives much larger value for the diverted discharge than those of the theoretical methods. The required rack length to divert the total incoming discharge obtained from the experimental method is less than those of the theoretical methods.

Table 2: Summary of the results of the theoretical and experimental solutions (1/2)

| INPUTS | | | | | |
|---|---|---|---|---|---|
| $(q_w)_T$= 0.5 $m^3/s/m$ | L= 1.00m | e= 20.0mm | *a*= 86.9mm | $h_1$= 0.20m | θ= 32.8° |

| COMPARISONS | | | |
|---|---|---|---|
| **Solution Method** | **$(q_w)_i$ (diverted discharge)** | **$(q_w)_i/(q_w)_T$** | **$L_2$ (required rack length to divert total discharge)** |
| Constant Energy Level Iterative Solution | 0.247 $m^3/s/m$ | 49.48% | 2.950m |
| Constant Energy Level Closed Form Solution | 0.230 $m^3/s/m$ | 46.00% | 4.090m |
| Constant Energy Head Iterative Solution | 0.279 $m^3/s/m$ | 55.73% | 2.900m |
| Experimental Solution | 0.410 $m^3/s/m$ | 82.00% | 2.400m |

In order to offer diversity, another set of inputs are used to design a Tyrolean weir with the same methods. Comparison of the results of these methods are presented in Table 3. As expected, the method based on the experimental results gives larger value for the diverted discharge and shorter value for the rack length (except the constant energy level iterative solution) than those of the theoretical methods.

Table 3: Summary of the results of the theoretical and experimental solutions (2/2)

| INPUTS | | | | | |
|---|---|---|---|---|---|
| $(q_w)_T$= 0.6 $m^3/s/m$ | L= 1.00m | e= 20.0mm | *a*= 86.9mm | $h_1$= 0.45m | θ= 14.477° |

| COMPARISONS | | | |
|---|---|---|---|
| **Solution Method** | **$(q_w)_i$ (diverted discharge)** | **$(q_w)_i/(q_w)_T$** | **$L_2$ (required rack length to divert total discharge)** |
| Constant Energy Level Iterative Solution | 0.307 $m^3/s/m$ | 51.16% | 2.760m |
| Constant Energy Level Closed Form Solution | 0.320 m3/s/m | 53.37% | 3.350m |
| Constant Energy Head Iterative Solution | 0.307 m3/s/m | 63.11% | 3.400m |
| Experimental Solution | 0.352 $m^3/s/m$ | 58.67% | 2.760m |

### 4.2.4 Applications of Theoretical Solutions

Iterative solutions of constant energy level and constant energy head approaches need a lot of effort in terms of calculation. To simplify the solution methods and provide a reliable design guide for designers, each method is formulized with the

help of Microsoft Excel. Interface of the excel table and working principle is given in the appendix.

In this part, summary of the results of the theoretical solutions for various input data are given in tabular forms (Table 4-7). In each table one variable is changed while keeping all the other values constant.

From the tables it can be concluded that "constant energy level iterative solution" and "constant energy head iterative solution" give very similar results for $(q_w)_i$ with varying $\theta$, $L$, $e$ and $h$. The both method, yield increasing $(q_w)_i$ values with increasing $L$, $e$, and $h_1$. Whereas, $(q_w)_i$ values slightly decrease with increasing $\theta$ in "constant energy level iterative solution" method while the reverse situation is observed in the values of $(q_w)_i$ in "constant energy head iterative solution" method. The "constant energy level closed form solution" yields slightly lower $(q_w)_i$ values than those of other two methods discussed above as a function of varying $\theta$, $L$, e and $h_1$.

Table 4: Diverted discharge results for different angle of inclinations $(\theta)$

| **INPUTS** | | | | | | |
|---|---|---|---|---|---|---|
| **$(q_w)_T$=** 1.500 $m^3/s/m$ | **L=** 2.00 | **e=** 20.00mm | ***a*=** 40.00mm | **$h_1$=** 0.45m | | |
| | | | | | | |
| **COMPARISONS** | | | | | | |
| **Solution Method** | **$(q_w)_i$ (diverted discharge)** | | | | | |
| | **$\theta=20^o$** | **$\theta=24^o$** | **$\theta=27^o$** | **$\theta=30^o$** | **$\theta=32^o$** | **$\theta=37^o$** |
| Constant Energy Level Iterative Solution | 1.124 | 1.106 | 1.091 | 1.076 | 1.064 | 1.034 |
| Constant Energy Level Closed Form Solution | 1.005 | 0.995 | 0.987 | 0.977 | 0.970 | 0.950 |
| Constant Energy Head Iterative Solution | 1.121 | 1.129 | 1.129 | 1.133 | 1.133 | 1.142 |

Table 5: Diverted discharge results for different rack lengths *(L)*

| INPUTS | | | | | | |
|---|---|---|---|---|---|---|
| $(q_w)_T$= 1.500 $m^3/s/m$ | $\theta$= $30^o$ | **e**= 20.00mm | ***a***= 40.00mm | $h_1$= 0.45m | | |
| | | | | | | |
| **COMPARISONS** | | | | | | |
| **Solution Method** | **$(q_w)_i$ (diverted discharge)** | | | | | |
| | **L=1.5m** | **L=2.0m** | **L=2.5m** | **L=3.0m** | **L=3.5m** | **L=4.0m** |
| Constant Energy Level Iterative Solution | 0.866 | 1.076 | 1.250 | 1.389 | 1.488 | 1.500 |
| Constant Energy Level Closed Form Solution | 0.791 | 0.977 | 1.132 | 1.259 | 1.359 | 1.431 |
| Constant Energy Head Iterative Solution | 0.934 | 1.133 | 1.288 | 1.401 | 1.471 | 1.500 |

Table 6: Diverted discharge results for different clearance distances between bars *(e)*

| INPUTS | | | | | | |
|---|---|---|---|---|---|---|
| $(q_w)_T$= 1.500 $m^3/s/m$ | **L**= 2.00 | $\theta$= $30^o$ | ***a***= 40.00mm | $h_1$= 0.45m | | |
| | | | | | | |
| **COMPARISONS** | | | | | | |
| **Solution Method** | **$(q_w)_i$ (diverted discharge)** | | | | | |
| | **e=15mm** | **e=18mm** | **e=20mm** | **e=24mm** | **e=27mm** | **e=30mm** |
| Constant Energy Level Iterative Solution | 0.887 | 1.004 | 1.076 | 1.203 | 1.286 | 1.359 |
| Constant Energy Level Closed Form Solution | 0.820 | 0.918 | 0.977 | 1.083 | 1.153 | 1.215 |
| Constant Energy Head Iterative Solution | 0.965 | 1.070 | 1.133 | 1.240 | 1.308 | 1.364 |

Table 7: Diverted discharge results for different flow depths just upstream of the Tyrolean screen

| INPUTS | | | | | | |
|---|---|---|---|---|---|---|
| $(q_w)_T$= 1.500 $m^3/s/m$ | **L**= 2.00 | **e**= 20.00mm | ***a***= 40.00mm | $\theta$= 30 | | |
| | | | | | | |
| **COMPARISONS** | | | | | | |
| **Solution Method** | **$(q_w)_i$ (diverted discharge)** | | | | | |
| | **$h_1$=0.20m** | **$h_1$=0.25m** | **$h_1$=0.30m** | **$h_1$=0.35m** | **$h_1$=0.40m** | **$h_1$=0.45m** |
| Constant Energy Level Iterative Solution | 0.918 | 0.969 | 1.008 | 1.037 | 1.059 | 1.076 |
| Constant Energy Level Closed Form Solution | 0.784 | 0.836 | 0.878 | 0.915 | 0.948 | 0.977 |
| Constant Energy Head Iterative Solution | 0.950 | 1.009 | 1.051 | 1.086 | 1.113 | 1.133 |

# CHAPTER 5

## CURRENT SITUATION OF SOME TYROLEAN WEIRS IN TURKEY

In previous chapters, design of a Tyrolean weir with theoretical methods and experimental method is explained by presenting approaches and showing various examples and comparisons. In this chapter, current situations of some Tyrolean weirs already constructed will be discussed. Discussion will be made by examining design and operation of some of the Tyrolean weirs in operation in Turkey. The same design parameters of these Tyrolean weirs will be used in the theoretical and experimental methods and the results will be compared.

### 5.1 Arpa Weir and HEPP

Arpa weir is operated in Borçka, Artvin, located north-eastern part of Turkey. The project area is highly mountainous and sediment carried through water is a threat to the water intake structure. Due to this reason Tyrolean weir is selected for water intake (Figure 54). The design parameters are as given in Table 8.

Table 8: Design parameters of Arpa Weir and HEPP

| Arpa Weir and HEPP | |
|---|---|
| $(q_w)_i$= | 1.15 $m^3$/s/m |
| $L$= | 5.2 m |
| $e$= | 50 mm |
| $a$= | 80 mm |
| $h_1$= | 0.44 m |
| $\theta$ = | $16^o$ |

The water diverted from the stream by the trash racks first is taken into the settling basin before it is leaded to the transmission channel. By a spillway constructed on the edge of the settling basin the excess water is discharged into the stream. So, the settling basin is able to discharge excessive water. For this reason, the designer selected a trash rack which is longer than expected.

Figure 54 : General layout of Arpa Weir and HEPP

The design parameters of Arpa Weir and HEPP were used in the theoretical calculation methods explained in previous chapters. The experimental method is not applicable because the inputs are beyond the limits of the design charts.

The rack length is calculated for each method and the results are given in Table 9.

Table 9: Calculated rack lengths for Arpa Weir and HEPP

| **Solution Method** | **L ( required length to divert the design discharge of 1.15 $m^3$/s/m)** |
|---|---|
| Constant Energy Level Iterative Solution | 1.98m |
| Constant Energy Level Closed Form Solution | 2.85m |
| Constant Energy Head Iterative Solution | 2.50m |
| Constant Energy Head Closed Form Solution | 1.16m |

For Arpa Weir and HEPP project, a trash rack with 5.2 m length and 10 m width was designed. According to the theoretical solution results, it is clearly seen that the rack length is over estimated. This over estimation does not cause any problem, on the contrary, it helps to regulate the system.

To record the flow conditions there are two gauging stations ( one upstream and one downstream of the weir). Considering these records, it is found out that the design discharge is diverted and the facility is operated perfectly.

**Maintenance and Operation**

The project is constructed on a mountain region and does not have a reservoir. Sediments and rocks carried with water are deposited on the upstream side of the weir. In long term, this deposition of sediment will block the entrance of the weir and will have to be removed.

Operation of the facility directly depends on safe operation of the trash rack. However, the trash rack is exposed to various environmental effects. In figure Figure 55 current situation of the trash rack is shown. As seen, there are plants deposited around the trash rack. This may cause plugging of the trash rack and affect healthy operation of the system.

Several visits per year to the site are necessary for inspection, cleaning and minor repairs of these problems. Overall, maintenance is easy to carry out due to the use of local labor and materials.

Figure 55 : Trash rack of Arpa Weir and HEPP

## 5.2 Kale Weir and HEPP

Kale Weir is located in Rize, Turkey (Figure 56). The design parameters are as given in Table 10.

Table 10: Design parameters of Kale Weir and HEPP

| Kale Weir and HEPP | |
|---|---|
| $(q_w)_i$= | 0.151 $m^3$/s/m |
| $L$= | 1.3 m |
| $e$= | 50 mm |
| $a$= | 80 mm |
| $h_1$= | 0.11 m |
| $\theta$ = | $20^o$ |

Figure 56 : General layout of Kale Weir and HEPP

Design parameters of Kale Weir and HEPP are used in the theoretical calculations. The rack length is calculated for each method and the results are presented in Table 11.

Table 11: Calculated rack lengths for Kale Weir and HEPP

| **Solution Method** | **L ( required length to divert the design discharge of 0.151 $m^3$/s/m)** |
|---|---|
| Constant Energy Level Iterative Solution | 0.44m |
| Constant Energy Level Closed Form Solution | 0.55m |
| Constant Energy Head Iterative Solution | 0.50m |
| Constant Energy Head Closed Form Solution | 0.25m |

For Kale Weir and HEPP project, a trash rack with 1.3 m length and 35 m width was designed. In Figure 57 it can be seen that, half of the trash rack is quite enough to divert the required discharge.

**Maintenance and Operation**

Quality of the construction has high importance in terms of hydraulic behavior of the system. As seen in Figure 57, water leaps towards downstream and splashes over the trash rack. This is a quite important problem. Regarding the performance of the trash rack. The reason of this undesired situation may be the mistakes made on the installation of the trash rack.

Figure 57 : Trash rack of Kale Weir and HEPP

# CHAPTER 6

## CONCLUSIONS AND FURTHER RECOMMENDATIONS

In this study, theoretical and experimental solution methods of Tyrolean weirs were investigated. Theoretical methods were given in two perspectives which named as “constant energy level approach” and “constant energy head approach”. Also, outcomes of two experimental studies, completed in Hydraulics Laboratory of Middle East Technical University, were presented as an experimental solution. By presenting numerical examples for both theoretical and experimental solutions, the outcomes of these methods were compared with each other. Moreover, to simplify the calculations, formulization of the theoretical methods is completed with Microsoft Excel. Current situation of two Tyrolean weirs under operation were examined and presented with the possible problems they are faced.

The following conclusions can be drawn from this study:

1) Each method described in this study can be used in the design of Tyrolean weir.

2) The outcome of the theoretical solutions, except constant energy head approach closed form solution, show similar results.

3) Constant energy head approach closed form solution is recommended only for horizontal racks.

4) Experimental methods are valid only for the ranges of the variables tested in the experiments.

5) Maintenance and quality of the construction has high importance on the performance of the trash racks.

Recommendations for future studies are as follows;

Although improvement of the theoretical solutions seems limited, the experimental solutions can be advanced by conducting similar experiments with new variables and building general design charts according to the outcomes of these tests.

Although these solutions give an idea about the design of Tyrolean weirs, design of a suitable Tyrolean weir is directly related to an experimental model study.

## REFERENCES


Ahmad, Z. & Mittal M. K. (2006). *Recent Advances in the Design of Trench Weir*. Himalayan Small Hydropower Summit. Dehradun, India: pp. 72-84.

Andaroodi, M. (2005). Standardization of Civil Engineering Works of Small Hydropower Plants. *École Polytechnique Federale De Lausanne*, Switzerland.

Brunella, S., Hager, W.H. & Minor, H.E. (2003). Hydraulics of Bottom Intake. *Journal of Hydraulic Engineering*. *ASCE 0733-9429*.

Drobir, H., Kienberger, V. & Krouzecky, N. (1999). *The Wetted Rack Length of the Tyrolean Weir*. Proceedings XXVIII IAHR congress, IAHR.

Çeçen, K. (1962). *Vahşi Derelerden Su Alma*. İTÜ Yayınevi.

Kamanbedast, A. A. & Bejestan, M. S. (2008). Effects of Slope and Area Opening on the Discharge Ratio in Bottom Intake Structures. *Journal of Applies Sciences, ISSN 1812-5654.*

Noseda, G. (1955). *Operation and Design of Bottom Intake Racks*. 6th International Association of Hydraulic Research Congress, La Haye,C17, 1–11.

Özcan, Ç. (1999). *Tirol Tipi Bağlamalarin Hidrolik Hesabi ile ilgili irdelemeler*. Gazi Üniversitesi İnşaat Mühendisliği Bölümü Yüksek Lisans Tezi, Ankara, Turkey.

Şahiner, H. (2012). *Hydraulic Characteristics of Tyrolean Weirs Having Steel Racks and Circular-Perforated Entry*. Thesis Submitted in Partial Fulfillment of The

Requirements for the Degree of Master of Science in the Department of Civil Engineering The Middle East Technical University, Ankara,Turkey.

Yılmaz, N.A. (2010). *Hydraulic Characteristics of Tyrolean Weirs*. Thesis Submitted in Partial Fulfillment of the Requirements for the Degree of Master of Science in the Department of Civil Engineering The Middle East Technical University, Ankara, Turkey.

# APPENDIX A

## INTERFACE AND WORKING PRINCIPLE OF THEORETICAL SOLUTION PROGRAM

Calculation of the theoretical methods are formulized with the help of Microsoft Excel with macro functions and presented below.

Total incoming discharge $(q_w)_T$, length of trash rack *(L)*, clearance distance between the rack bars *(e)*, distance between the center of the rack bars *(a)*, flow depth at the head of the trash rack $(h_1)$ and inclination angle of the rack $(\theta)$ are the required parameters for excel table.

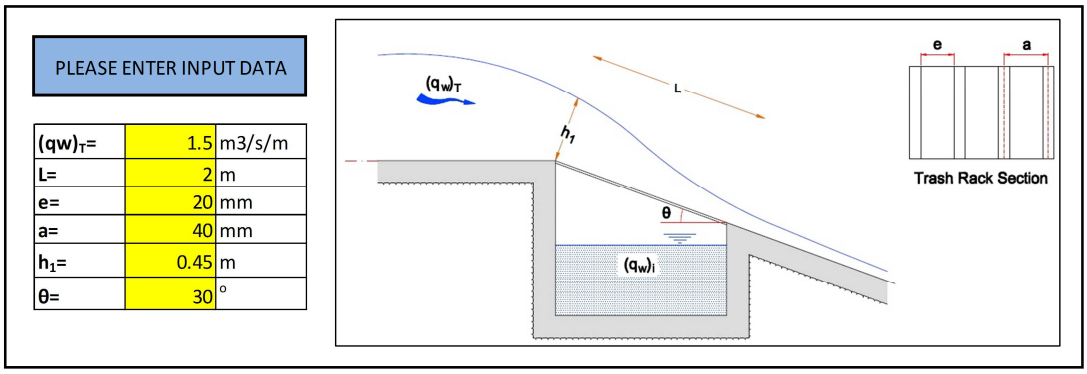


Figure 58 : Interface of excel table

Each approach is given on the following pages and by following the numbered steps the solution is completed.

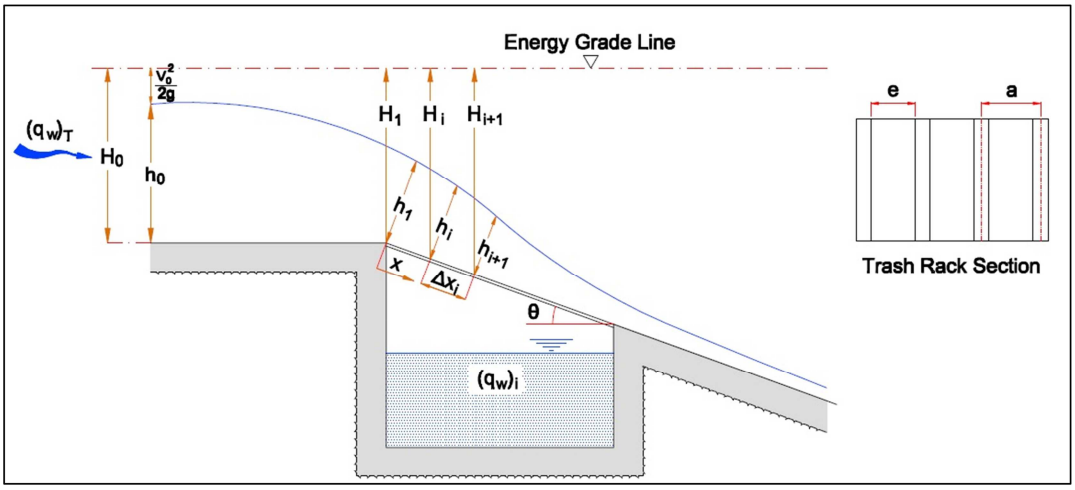


| $H_0$= | 0.96 | m |
|---|---|---|

Compute $H_0$ 1

Iterations

| $h_2$ = | 0.264 |
|---|---|

| $h_{ave}$ | $\mu_s$ | λ | $(qw)_{i1}$ |
|---|---|---|---|
| 0.357 | 0.555 | 1.143 | 0.342 |

Compute $h_2$ 2

| $h_3$ = | 0.172 |
|---|---|

| $h_{ave}$ | $\mu_s$ | λ | $(qw)_{i2}$ |
|---|---|---|---|
| 0.218 | 0.591 | 1.219 | 0.285 |

Compute $h_3$ 3

| $h_4$ = | 0.112 |
|---|---|

| $h_{ave}$ | $\mu_s$ | λ | $(qw)_{i3}$ |
|---|---|---|---|
| 0.142 | 0.625 | 1.289 | 0.243 |

Compute $h_4$ 4

| $h_5$ = | 0.070 |
|---|---|

| $h_{ave}$ | $\mu_s$ | λ | $(qw)_{i4}$ |
|---|---|---|---|
| 0.091 | 0.663 | 1.366 | 0.206 |

Compute $h_5$ 5

| | | |
|---|---|---|
| Total diverted discharge into the collection channel $(q_w)_i$ | **1.076** | m3/m/s |
| Total discharge that passes towards downstream $(q_w)_{out}$ | **0.424** | m3/m/s |

Figure 59 : Constant energy level iterative solution interface

Click “Compute $H_0$”, “Compute $h_2$”, “Compute $h_3$”, “Compute $h_4$”, “Compute $h_5$” respectively.

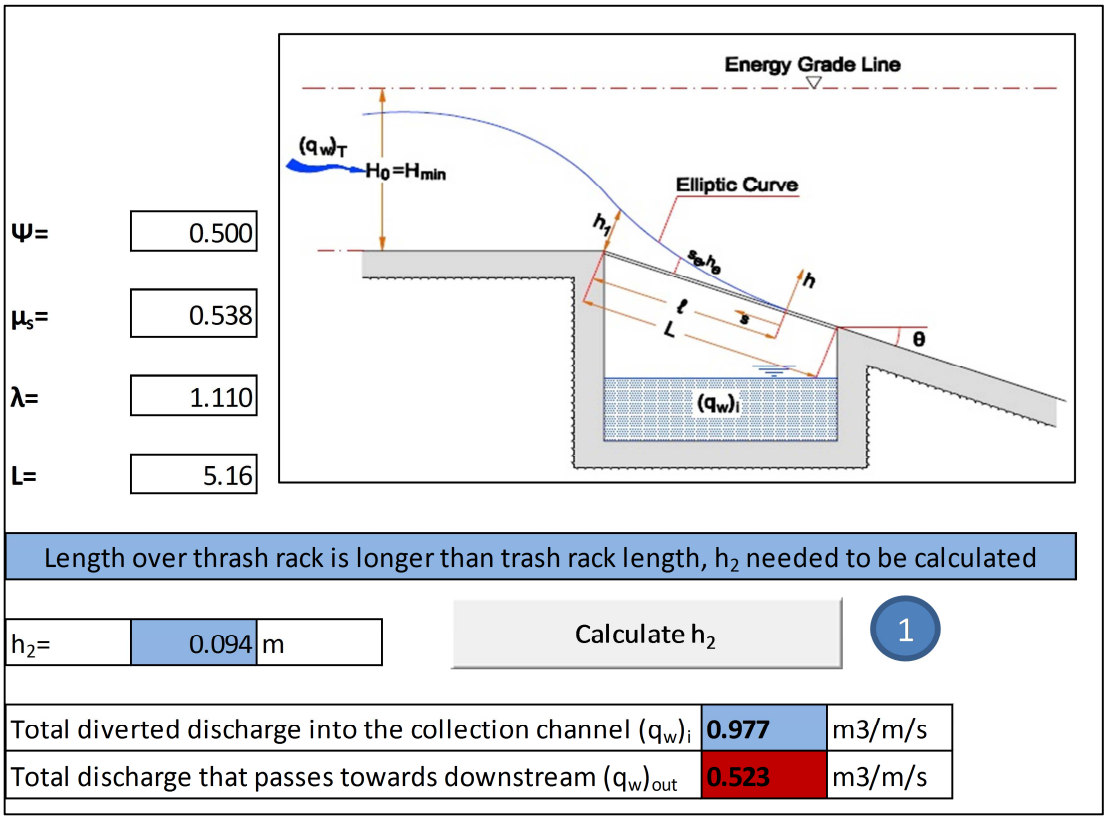


Figure 60 : Constant energy level closed form solution interface

Click “Calculate $h_2$” only.

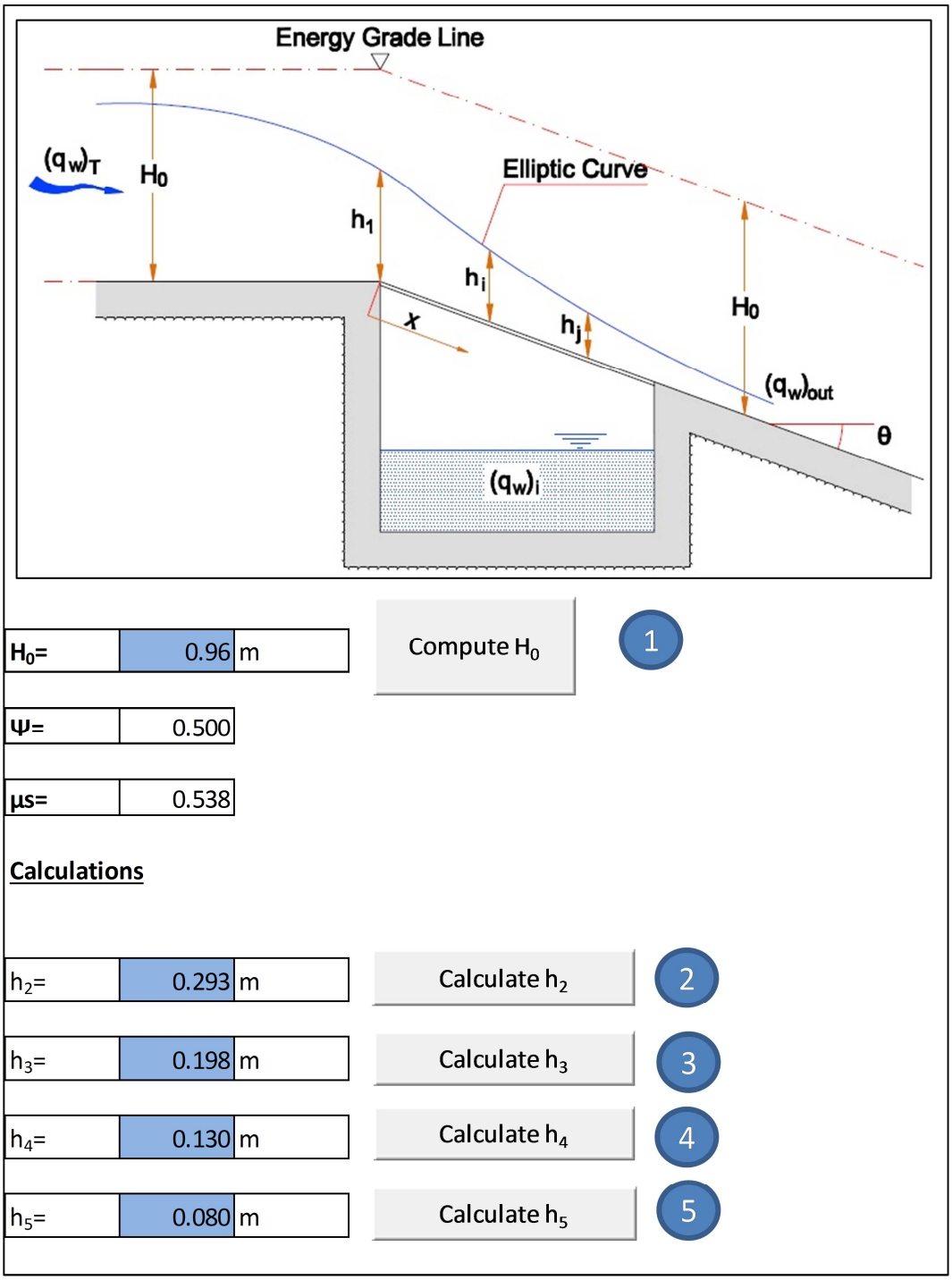


Figure 61 : Constant energy head iterative solution interface (1/2)

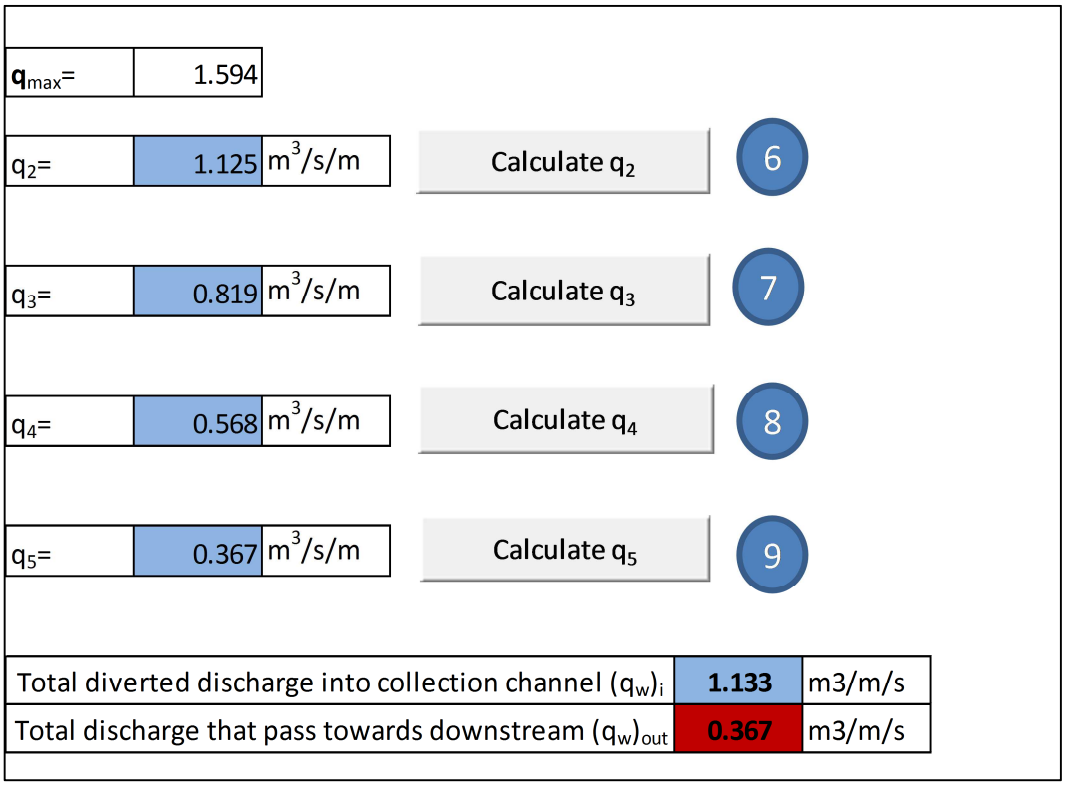


Figure 62 : Constant energy head iterative solution interface (2/2)

Click "Compute $H_0$", "Compute $h_2$", "Compute $h_3$", "Compute $h_4$", "Compute $h_5$", "Calculate $q_2$", "Calculate $q_3$", "Calculate $q_4$", "Calculate $q_5$" respectively.

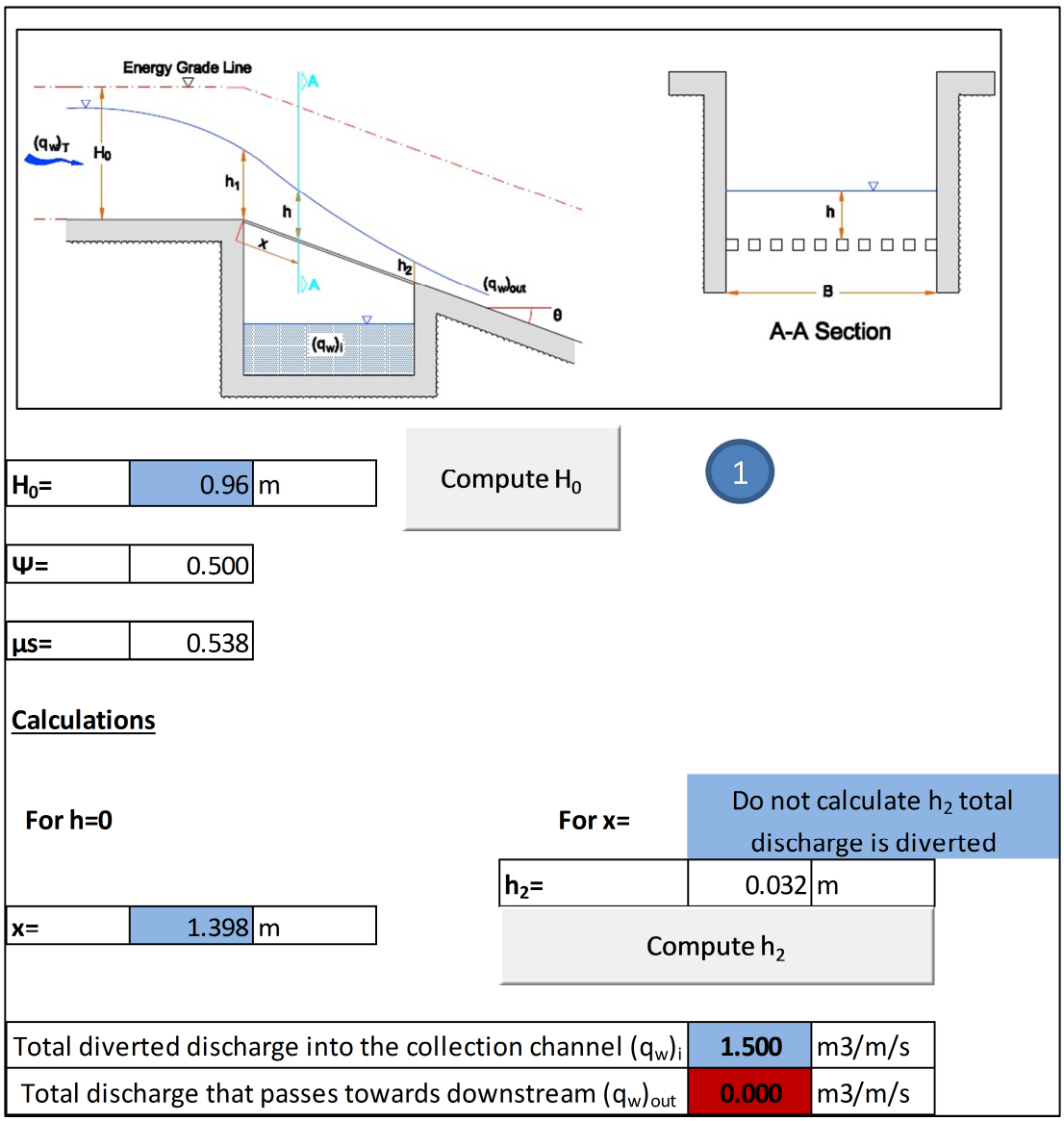


Figure 63 : Constant energy head closed form solution interface

Click "Compute $H_0$", if $x$ is larger than $L$, click "Compute $h_2$". Otherwise, total discharge is diverted.

| Solution Method | Diverted Discharge $(q_w)_i$ | $(q_w)_i/(q_w)_T$ |
|---|---|---|
| Constant Energy Level Iterative Solution | 1.062 $m^3/s/m$ | 70.8% |
| Constant Energy Level Closed Form Solution | 0.977 $m^3/s/m$ | 65.1% |
| Costant Energy Head Iterative Solution | 1.133 $m^3/s/m$ | 75.5% |
| Costant Energy Head Closed Form Solution | 1.500 $m^3/s/m$ | 100.0% |

Figure 64 : Summary and comparison of the theoretical solutions

On the last page of the excel table summary and comparison of the theoretical solutions are given.